Identification and characterisation of novel marker proteins involved in X-linked muscular dystrophy

Submitted to National University of Ireland Maynooth for the degree of

Doctor of Philosophy.

NUI MAYNOOTH

Ollscoil na hÉireann Má Nuad

Caroline Lewis, B.Sc

July 2010

Head of Department

Professor Kay Ohlendieck,
Department of Biology,
NUI Maynooth,
Co. Kildare

Supervisor

Professor Kay Ohlendieck,
Department of Biology,
NUI Maynooth,
Co. Kildare

Publications (peer reviewed)

Lewis C. and Ohlendieck K. 2010. Proteomic profiling of naturally protected extraocular muscles from the dystrophin-deficient mdx mouse. *Biochem Biophys Res Commun*; 396(4): 1024-1029

Lewis C. Jockusch, H. and Ohlendieck K. 2010. Proteomic profiling of the dystrophin-deficient mdx heart reveals drastically altered levels of key metabolic and contractile proteins. *J Biomed Biotechnol*; Volume 2010, article ID 648501, 20 pages

Lewis C. and Ohlendieck K. 2010. Mass spectrometric identification of dystrophin isoform Dp427 by on-membrane digestion of sarcolemma from skeletal muscle. *Anal Biochem.* Volume 404; 197-203

Review (peer reviewed)

Lewis C. Carberry, S. and Ohlendieck K. 2009. Proteomic profiling of X-linked muscular dystrophy. *J Muscle Res Cell Motil*.;30(7-8):267-9. Review

Conferences and Presentations

Poster presentation

Life Sciences 2007, 8-12 July 2007 , SECC, Glasgow, UK.

Poster number: PC524.

Title: Optimisation of 2-D gel electrophoretic separation of dystrophic cardiac muscle

Internal seminars presented to peers in NUI maynooth

2007 Identification and characterisation of novel biomarkers of dystrophic tissue

2008 Identification and characterisation of novel biomarkers of dystrophic tissue

Table of Contents

List of Figures

List of Tables

Acknowledgements

Firstly, I would like to thank my supervisor, Prof. Kay Ohlendieck, who has seen me through to the end. Thank you for enabling me to get publications during my time. You passed your love of research on to all of us and I hope you get a chance to return and work on the bench.

Thank you to all my colleagues past and present. Phil for getting me started, Kathy and Joan for showing me most everything else, Pam for teaching me not to be scared of DIGE and Edel and Lisa for providing me with the best laughs ever, everyday and to all of you who never let me give up when I was having yet another one of "those" days.

To all the other labs usually KKs who lent chemicals when we occasionally forgot to order items...again and again.

The technicians in NUIM, the best team anywhere; Michelle a most helpful and organized person, Joe for fixing things and endless listening when equipment was down. All the help I received from Caroline for keeping the mass spec going as best she could and to Ica for help with confocal microscopy.

To university policy makers, who made it possible for me as a mature student to complete a degree, something I never thought possible. To the college also for the John Hume scholarship –a wonderful incentive to do well.

IRCSET, without whom I never could have considered a Ph.D.

To Joe and Karen from Muscular Dystrophy Ireland, and all the other families I have met over the years, who remind me that what I am doing is so important.

A huge thank you to my immensely supportive family. How proud they have always been, and supportive of all my choices. My mother and father, how can I ever thank you for all you have done for me. I have amazing parents who always make me feel special and encourage me to do the right thing. I know they would give up and do anything for me so I am glad I have pushed myself this far. To my mother in-law for minding my most precious bundle in those early days when I needed to return to the bench. In addition, to John, Mary, Noreen, Ian and my parents for all the financial support, hours of babysitting, dinners, collecting from crèche and all the effort of helping me bring up your grandchild, including buying shoes, clothes, toys and books when I was too busy and she really needed them…! Thank you to the rest of my family who seem to have understood that a PhD takes over your life and I look forward to visiting everyone and catching up.

To my closest friend, Henry, thank you for the support and fantastic cooking over the years...Keep running!

Thank you to all my LLL friends who helped me feel good about myself through those very tough times of trying to be a working mother and who never let me give up on a bad day.

My darling husband, what can I say, we did it. Together we have achieved more than we thought ourselves capable. You are here, in my life, out of choice. That is what makes this remarkable. You have given me strength to carry on, provided answers to my problems and offered support when I had to do it for myself. You have powerful inner belief and you believed in me. I feel so small sometimes when I think of you only because you are my hero, my love, my life. Thank you for being you.

To my most emotional thank you, to my amazing little girl, who doesn't understand why life is so hard. I could so easily have given up a long time ago because I wanted to spend all my time with you. I need you to know I did the best I could. I think you found this PhD the hardest; the travelling, the late nights, the seven days a week working. I needed to finish this for myself, to prove that I could graduate with the highest award academically and to help me appreciate that mothering will be the greatest success I can ever achieve.

I hope some day I can empower you to achieve your goals.

Declaration

This thesis has not been submitted in whole or part to this or any other university for any degree, and is the original work of the author except where stated.

Signed _____

Date _____

Abbreviations

1D	One dimensional
2D	Two-dimensional
2D-GE	Two-dimensional gel electrophoresis
Ab	Antibody
ADP	Adenosine diphosphate
AK1	Adenylate kinase
AMC	Actin membrane cytoskeleton
AT	Amino terminal
ATP	Adenosine triphosphate
BMD	Becker muscular dystrophy
Ca^{2+}	Calcium
CF	Confocal
CMD	Congential muscular dystrophy
CMXRos	Chloromethyl-X-Rosamine
CR	Cysteine-rich
CSQ	Calsequestrin
CT	Carboxyl terminal
cvHSP	Cardiovascular heat shock protein
Cy	Cyanine
CYT	Cytosol
DAGC	Dystrophin-associated glycoprotein complex
DAPI	Diamidino-phenylindole
Des	Desmin
DG	Dystroglycan
DGC	Dystrophin-glycoprotein complex
DHPR	Dihydropyridine receptor

DIGE	Difference in-gel electrophoresis
DMD	Duchenne muscular dystrophy
DTT	Dithiothreitol
DYB	Dystrobrevin
ECM	Extracellular matrix
EOM	Extraocular muscle
ES	Extracellular space
ESI-MS	Electrospray ionisation mass spectrometry
FABP	Fatty acid binding-protein
fmol	Femtomole
Gt	Goat
HCl	Hydrochloric acid
Hsp	Heat shock protein
ID	Identification
IDH	Isocitrate dehydrogenase
IEF	Isoelectric focusing
IF	Intermediate filament
IPG	Immobilized pH gradient
LAM	Laminin
LC-MS	Liquid chromatography mass spectrometry
LGMD	Limb-girdle muscular dystrophy
LV	Left ventricular
m/z	Mass/charge
MDX	Murine X chromosome linked
MHC	Myosin heavy chain
MLC	Myosin light chain
mRNA	messenger Ribonucleic acid
MS	Mass spectrometry
Ms	Mouse

MT	Mitochondria
NADH	Nicotinamide adenine dinucleotide
NAG	N-acetylglucosamine
NC	Novocastra
NCX	Sodium/calcium exchanger
NDK	Nucleoside diphosphate kinase
ng	Nanogram
NIH	National Institutes of Health
OCT	Optimum cutting temperature
PAGE	Polyacrylamide gel electrophoresis
p*I*	Isoelectric point
PPD	p-Phenylenediamine
Pro	Prohibitin
PTM	Post-translational modifications
PVP	Polyvinylpyrrolidone
Rb	Rabbit
Rt	Rat
RuBPS	Ruthenium (II) tris-bathophenantroline disulfonate
RyR	Ryanodine receptor
SC	Santa Cruz
SDH	Succinate dehydrogenase
SDS	Sodium dodecyl sulphate
SERCA	Sarcoplasmic endoplasmic reticulum calcium ATPase
SG	Sarcoglycan
SGN	Stressgen
SL	Sarcolemma
SR	Sarcoplasmic reticulum
SS	Sarcospan
SYN	Syntrophin

Tp	Troponin
TpC	Troponin C
TR	Triad junction
TT	Transverse tubules
VCP	Valosin-containing protein
VDAC	Voltage-dependent anion-selective channel
WB	Western blotting
WGA	Wheat germ agglutinin
XLDCM	X-linked dilated cardiomyopathy
α-DG	alpha-Dystroglycan
β-DG	beta-Dystroglycan

Abstract

Progressive X-linked muscular dystrophy represents the most commonly inherited neuromuscular disorder in humans. Although the primary abnormality lies with the loss of dystrophin and reduction of its associated glycoprotein complex, secondary alterations in metabolic pathways, cellular signalling and ion homeostasis regulation cause fibre degeneration leading to severe muscle weakness. Skeletal muscle deteriorates to the extent that sufferers are wheelchair bound by early adulthood and severe diaphragm degeneration can lead to respiratory failure. Therapy in this area has lengthened life-span but at a more advanced stage of the disease, most Duchenne muscular dystrophy patients suffer cardiomyopathic complications.

The purpose of this study was to carry out proteomic profiling on differentially affected dystrophic tissues. Differences in protein concentration levels of the severely affected cardiac muscle and the naturally protected extraocular muscle were used to explore pathogenesis of the disease.

A mass spectrometry-based approach combined with the highly sensitive difference in-gel electrophoresis technique was used to reveal changes and identify novel biomarkers in the dystrophic tissues. Following the pathogenesis of the disease the naturally protected tissue displayed only moderate changes in protein concentration expression. With a replacement of dystrophin with its homologue utrophin, restoration of β-dystroglycan was observed along with an increased concentration in heat shock proteins. While the severely affected cardiac muscle exhibited drastic decreases in the expression levels of many proteins involved in energy metabolism including adenylate kinase and many ATP synthase isoforms. Reduced concentrations were also observed in numerous contractile proteins and intermediate filament proteins. With the loss of these structural elements, a drastic increase in stress proteins was observed within dystrophic myofibrils compared to normal fibres.

This thesis has successfully identified novel biomarkers that may be used to determine suitability of new treatments or therapies of muscular dystrophy.

1 Introduction

Muscle is the most abundant tissue in the body. It is the effector organ of the nervous system resulting in the transformation of potential energy into contractile force. The four main muscle types divide into two groups: those that we control voluntarily, skeletal muscle for mobility and posture, and those under control of the central nervous system namely the smooth muscle, heart and myoepithelial cells of glands. In this study, we looked at a subtype of skeletal muscle, the striated extraocular muscle and also at the cardiac muscle of a murine animal model.

1.1 Contractile muscle structure

A muscle is made up of many muscle fibres. A single muscle fibre is composed of bundles of myofibrils. The striated muscle pattern of skeletal muscle comes from the alignment of thick and thin filaments. This regular lattice pattern makes up the sarcomeres within the myofibril (Huxley and Niedergerke, 1954). The sarcomere structure consists of the thick filament located in the centre and surrounded by six thin filaments (see Figure 1-1). The overlap of these thick and thin filaments is visualized as a darkly stained area known as the A-band lying in the centre of each sarcomere. The centre has a narrow M-line where proteins link together the thick filaments of myosin chains. Also contained in the A-band is the presence of the H-zone where there is an absence of thin actin filaments. The end of each sarcomere is marked by the Z-line where a section of proteins anchor the thin filaments. Either side of the Z-line is the lightly stained due to the absence of any thick filaments and contains only thin filaments and is known as the I-band (Sjostrom and Squire, 1977) . It was proved in the 1950s that the lengths of these thick and thin filaments did not change during contraction of the muscle; therefore it was thought that contractile force was developed between the overlapping sections. With the development of electron microscopy the source of force was elucidated. The projecting myosin heads in the A-band provide the force with which

muscle contracts. The projections form cross-bridges with the actin of the thin filament and shorten the sarcomere by causing the thin filaments to slide over the thick filaments (Huxley, 2004).

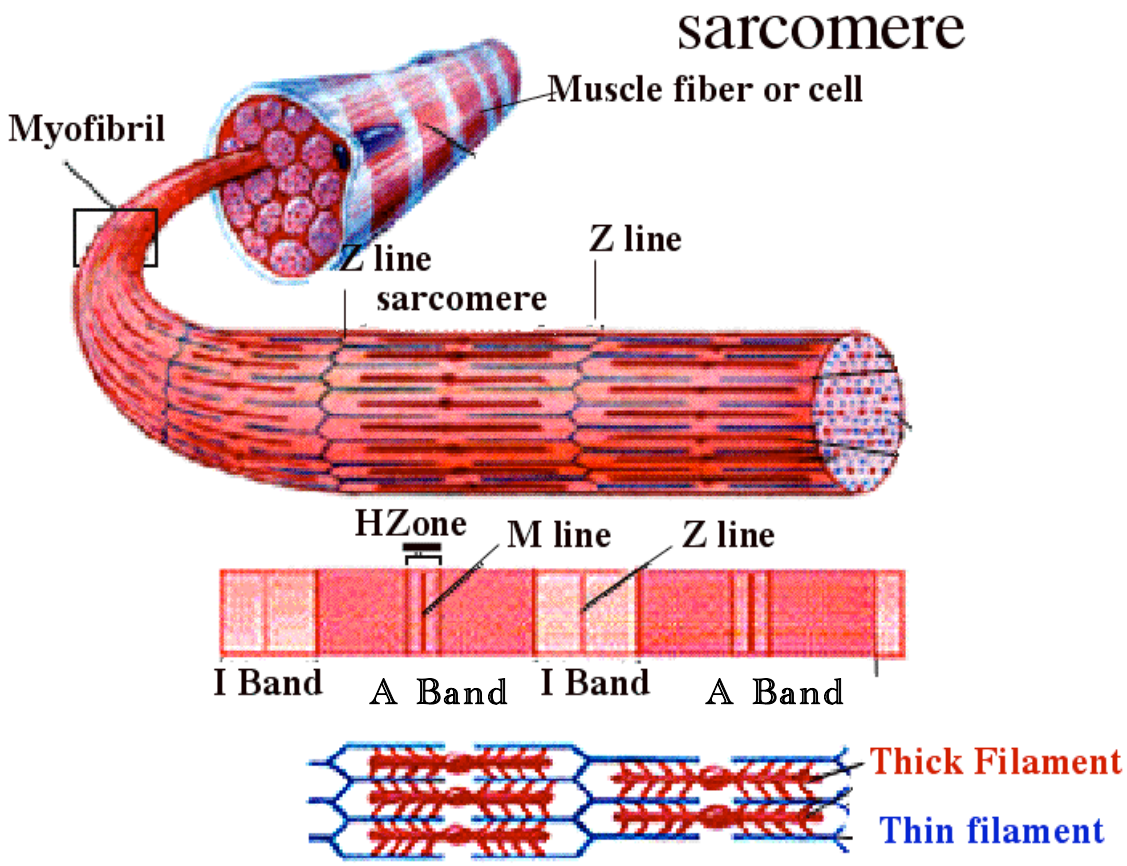

Figure 1-1 Contractile muscle structure

Contractile elements make up the repeating sarcomeres, which align to form the myofibrils. The thick filaments of the A band are composed of intertwined myosin chains surrounded by the thin actin filaments. (image taken from ucl.ac.uk)

1.2 Sliding filament mechanism

Contraction of the muscle involves two types of filaments. Thick filaments consist of myosin and myosin heads and thin filaments consist of actin, tropomyosin and troponin (Tp). Calcium released from the potential activated sarcoplasmic reticulum (SR), binds Troponin C (TpC), causing tropomyosin to expose an actin binding site. This eliminates the inhibition of actin to bind to myosin. A TpT/TpI interaction with tropomyosin alters the conformation of contractile actin and allows a myosin head to interact with actin

initiating a cross bridge (Rayment et al., 1993). Two globular heads linked by a coil make up the myosin head. ATP binds the cleft between the heads. It is hypothesised that the energy is gained by (i) myosin binding actin, (ii) that the cleft opens releasing the hydrolysed phosphate from ATP and that (iii) the cleft closes providing a conformational change, creating a 'powerstroke' that pulls on the thin filament (Veigel et al., 1999). ADP is then released and ATP binds again, causing the head to release actin, bringing the myosin head back to its original position and becoming energized again. In the presence of calcium, this cycle causes continued shortening of the muscle fibres by interaction of many myosin head/actin cross bridges. Either side of the M-line the cross bridges lie in opposite directions, each side is oriented with the arm end toward the M-line and the head pointing away. The thick and thin filaments do not change length but the H zone and I band shorten and the degree of shortening corresponds with the level of contraction (Reedy, 2000) (*see* Figure 1-2*)*.

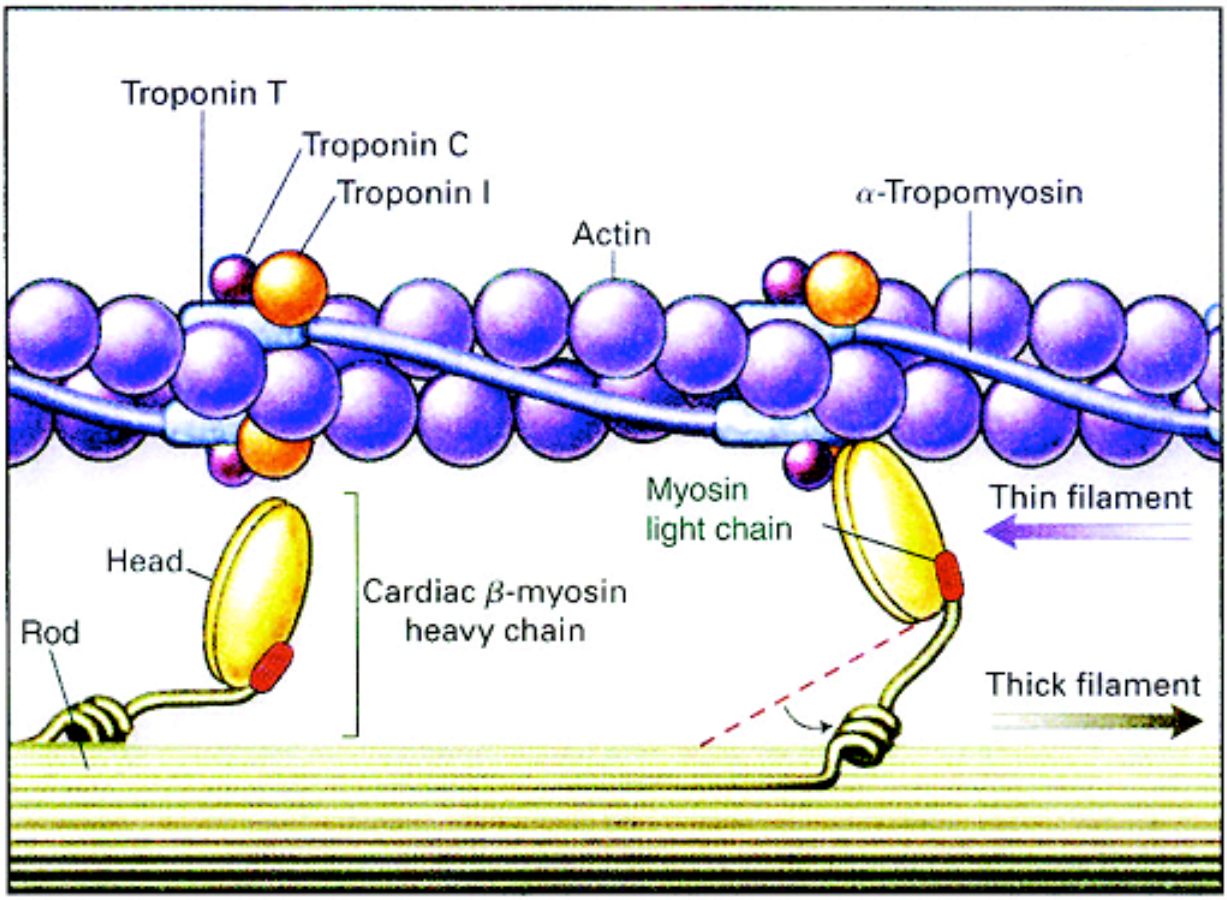

Figure 1-2 Sliding filament theory

A conformational change occurs to tropomyosin following the binding of calcium to troponin C. A actin binding site is exposed and the myosin head forms a crossbridge. The thin filament slides over the thick filament causing muscle shortening. (image from edoc.hu-berlin.de)

1.3 Skeletal muscle excitation-contraction coupling

Before a muscle can contract a series of action potentials along a nerve must occur to cause the release of calcium from the stores within the myofibril. An action potential above a sufficient threshold travels along the axon of a motor neuron. Waves of activation of voltage-gated channels transmit the potential until it reaches the axon terminal where it activates calcium voltage gated channels. The calcium released in the end-plate causes acetycholine transmitter molecules to be released from the terminal into the synaptic cleft, which in turn bind acetycholine receptors along the post synaptic

junction (Farley and Miles, 1977). The potential is then carried along the muscle surface membrane where voltage dependent channels are activated, causing sodium ions to flux out of the muscle and potassium ions move into the sarcoplasm. The sodium ions amplify the potential along the sarcolemma and it is carried down into invaginations known as transverse tubules (T-tubules). These invaginations lie between the termini of sarcoplasmic reticulum (SR) (Cooke, 1986). Depolarization of the T-tubules is sensed by the α_{1s}-dihydropyridine receptor (DHPR). A conformational change then allows the II-III loop domain of the DHPR to physically interact with the ryanodine receptor (RyR) on the SR (Tanabe et al., 1990). Transient opening of skeletal muscle, RyR1 allows calcium storage bodies from the lumen of the SR to release calcium along a steep gradient into the cytosol (Meissner and Lu, 1995). The increase in cytosolic calcium causes conformational changes to tropomyosin that allows the interaction of the myosin head with actin (Cooke, 1986).

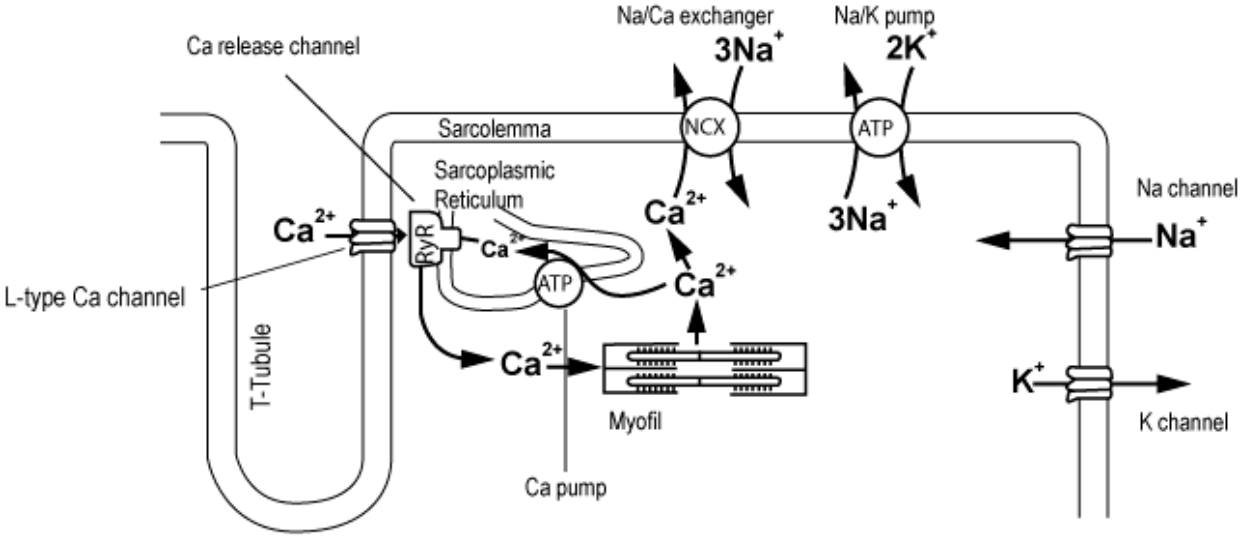

Figure 1-3 Voltage-gated action potential

An impulse activates voltage-gated channels along the sarcolemma and into transverse tubules (t-tubules). Calcium activates the L-type channel, which physically interacts with the ryanodine receptor (RyR) of the sarcoplasmic reticulum (SR). Storage bodies within the SR release calcium, which in turn can interact with the contractile elements of the myofibril. www.sim-bio.org

1.4 The cardiac action potential

Cardiac cells are branched and adjacent cell membranes are intertwined at areas known as intercalated discs (ID). The ID contains gap junctions, which allow the transfer of ions from one cell to another. This allows an action potential to travel from one muscle cell to another causing an electrochemical syncytium, whereby all the heart cells can act as one. Cardiac cells do not carry potential down nerves and across neuromuscular junctions. Instead, a regular impulse is generated spontaneously in the sinoatrial node and transmitted through specialized pacemaker cells known as Purkinje fibres. As the atria contract the action potential is carried through the intercalated discs throughout the myocardium, a second threshold is overcome in the atrioventricular node and this causes the contraction of the ventricles (Shih, 1994).

1.5 Cardiac excitation-contraction mechanism

In cardiac muscle, the contraction of myofibrils is activated by the influx of calcium ions into the muscle, but there are a number of differences to the mechanisms used by skeletal muscle. In cardiac muscle the DHPR complex does not couple directly with the SR release channel, instead the cardiac specific α_{1C}-DHPR allows a small amount of calcium to enter the cytosol via a calcium gradient. This calcium influx causes the cardiac isoform of the ryanodine receptor, RyR2, to open and release large amounts of calcium from the SR (Wasserstrom, 1998). The calcium released then activates neighbouring RyR and thus amplifies the signal. This is known as ‘the calcium induced calcium release mechanism’ and is thought to be the dominant pathway in cardiac muscle. When the calcium concentration increases sufficiently, calcium then binds TpC within the sarcomere, which induces sliding of the filaments and shortening of the sarcomere (Bers, 2000).

The re-uptake of calcium must occur for the muscle to relax. The calcium concentration must decrease so that dissociation occurs from troponin. Calcium is removed from the cytosol by calcium buffering systems. Re-uptake of free cytosolic calcium occurs by various binding moieties including, the cardiac sarcoplasmic reticulum Ca^{2+} ATPase 2 (SERCA2) pumping calcium back into the lumen of the SR and the cardiac isoform sodium/calcium exchanger (NCX) returning free calcium to mitochondria and extruding it across the sarcolemma membrane (Bassani et al., 1994). Bers (2000) showed that in rabbit ventricular myocytes, SERCA2 removes 70% of the calcium and the NCX 28% from the cytosol, they demonstrated that two calcium ions were removed per ATP molecule using SERCA2 and the NCX indirectly removes one calcium ion per ATP. This is therefore an energy expensive mechanism and it is thought a vast number of these pumps line the SR and that the number of pumps equals the number of calcium ions released from a single twitch.

1.6 Dystrophin

Contractile muscle force is reduced in damaged cells. The cytoskeleton of a cell is composed of actin filaments that provide a structural network below the membrane. Repeated muscle contraction damages membranes not supported by a cytoskeletal network (Lovering and De Deyne, 2004). Dystrophin binds actin filaments in the structural network to the extracellular matrix thus anchoring the glycoprotein complex in the membrane of a myofibre. The loss of the dystrophin protein causes reorganisation of the membrane. The membrane attempts to replace the missing proteins by substitution with ion pores. Calcium ions from muscle contraction cause further damage to a dystrophic cell.

Genetic alterations in the dystrophin gene lead to the dystrophic phenotype in muscle. The dystrophin 14kb mRNA codes for a 427kDa protein (Hoffman et al., 1987). Dystrophin contains four domains; the amino terminal whose sequence has been conserved from cytoskeletal actin binding proteins and binds cortical actin in myofibrils.

The “rod domain” which contains 24 helical repeats and four hinge domains, which give it a flexible characteristic (Koenig et al., 1988; Koenig and Kunkel, 1990). Both these domains make up 14% coverage of the whole dystrophin protein. The third domain is a cysteine-rich domain which binds β-dystroglycan and α-dystrobrevin (Rentschler et al., 1999). Finally, a carboxyl terminal domain is a unique sequence to the dystrophin protein. Utrophin, is an autosomal protein with similar homology to the dystrophin protein. Both actin binding proteins, bind dystrophin-associated proteins dystrobrevin and syntrophin (Tinsley et al., 1992) (*see* Figure 1-4). Three full-length dystrophin proteins are transcribed by three alternative promoters and are Dp427 (B), Dp427 (M) and Dp427 (P) and found in the brain, muscle and Purkinje cells respectively. They differ in their amino terminal end sequences (Boyce et al., 1991; Gorecki et al., 1992; Yaffe et al., 1992). Four internal promoters produce truncated isoforms of dystrophin. These transcribe Dp260, a 260kDa protein found in the retina, Dp140 located in the brain, Dp116 transcribed in Schwann cells and Dp71 transcribed ubiquitously throughout non-muscle cells. These isoforms each have a unique amino terminal end and all contain the conserved region of the carboxyl domain of full-length dystrophin (Byers et al., 1993; D'Souza et al., 1995; Lidov et al., 1995).

Dystrophin localizes to the sarcolemma on the cytoplasmic side of the membrane (Zubrzycka-Gaarn et al., 1988). It interacts within the sub-sarcolemmal cytoskeleton, the costameres, of myofibrils via its actin binding domain and the cysteine-rich domain links the extracellular dystroglycan complex via ß-dystroglycan (Campbell, 1995). Dystrophic muscle becomes weak, with sarcolemmal disruptions and costameric reorganization.

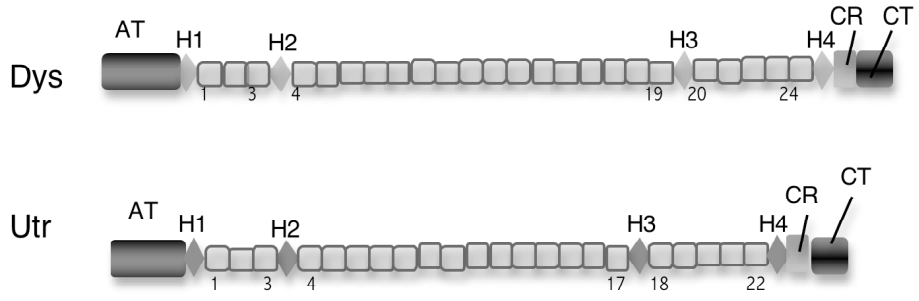

Figure 1-4 Dystrophin and Utrophin domain structures

Shown is a diagram comparing the domain regions and similarity of murine dystrophin and utrophin. Utrophin lacks modules of the rod domain corresponding to helical repeats 15 to 19 in dystrophin. The structures contain an amino terminal (AT) domain, four hinge regions (H1-H4) within the rod domain of up to 24 helical repeats, a cysteine-rich (CT) domain and finally a carboxyl terminal (CT) domain.

1.7 Dystrophinopathies

Genetic alterations in dystrophin and various dystrophin-associated proteins are responsible for a number of neuromuscular disorders (*see* Figure 1-5). The effect is seen through many different muscle types although the end-stage phenotype is usually caused by secondary effects due to mechanical stresses exacerbated by altered ion handling brought about by abnormal excitation-contraction coupling, sarcolemmal fragility, muscle weakness and necrosis (Carlson and Makiejus, 1990; Weller et al., 1990; Williams and Bloch, 1999). The primary disorder is due to the absence of dystrophin and subsequently the loss of various dystroglycan proteins anchored by the dystrophin protein.

Dystrophin is the largest gene in the human genome, consisting of 14 kilobases encoding a 3,685 amino acid protein (Koenig et al., 1988). Due to its large size 30-40% of the genetic alterations are spontaneous, most of these being deletions with about a third being point mutations (Den Dunnen et al., 1989). Being on chromosome Xp21 it is an X-linked disease, with about 1:3500 males being affected worldwide. The onset of difficulties in walking begins around 1-5 years of age, with weakness in limbs leading to

loss of ambulation by teenage years. Enlargement of the limbs occurs due to the infiltration of adipose and connective tissue. Serious cardiac implications emerge by late teenage years and respiratory and or cardiac failure represents a significant number of deaths from Duchenne muscular dystrophy (DMD) occurring during the second decade (Emery, 2002).

A partial absence of dystrophin leads to the milder Becker muscular dystrophy (BMD). The onset of the disease is later, with moderate weakness in adults. Walking is affected by the mid teens with cardiac problems beginning by 20 years of age. Patients can survive through to 40 and 50 years old (Monaco et al., 1988).

X-linked dilated cardiomyopathy muscular dystrophy is an abnormality on the same gene as DMD. However, it involves the promoter on the 5' end of the gene that produces the cardiac specific dystrophin protein. Little or no skeletal muscle disease is observed during this disease with males suffering cardiac failure in their 20's (Towbin et al., 1993).

Other muscular dystrophies have been recorded due to loss of dystrophin-associated proteins. Sarcoglycanopathies are due to the loss of proteins from the tetrameric sarcoglycan complex leading to a range of limb-girdle muscular dystrophies (LGMD). These are progressive skeletal muscle diseases affecting shoulder and pelvic girdle muscles. Different types of LGMD are linked to absence in each of the different sarcoglycan isoforms with some of the disorders associated with cardiac involvement (Lim et al., 1995; Jung et al., 1996). Sarcospan deficiency has shown no human myopathy.

Laminin, the protein that interacts with the dystrophin-glycoprotein complex (DGC) via α-dystroglycan, proves to be the protein in deficiency in congenital muscular dystrophy. Children display weakness at birth and although is it not a progressive disease, children usually cannot walk (Minetti et al., 1996).

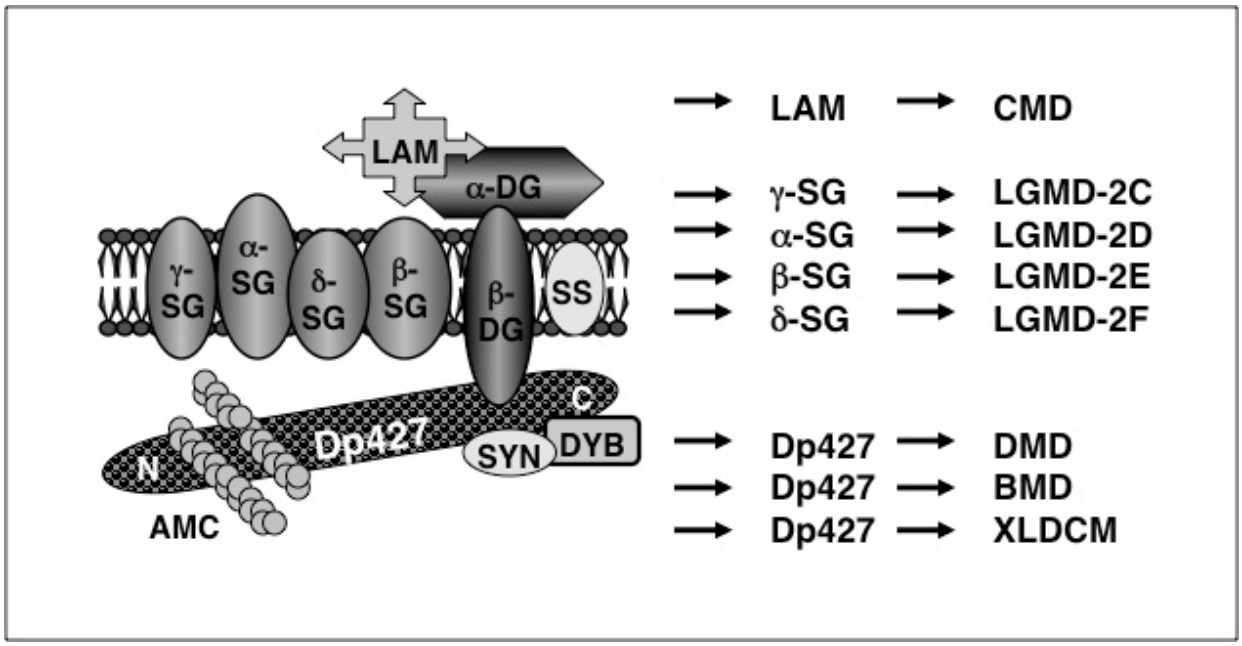

Figure 1-5 Synopsis of neuromuscular disorders with primary abnormalities in the dystrophin-glycoprotein complex.

Shown are a diagrammatic presentation of the dystrophin-associated protein complex and a list of muscle proteins with a genetic defect in muscular disorders. Genetic alterations in laminin (LAM), γ-sarcoglycan (γ-SG), α-SG, β-SG or δ-SG are associated with congenital muscular dystrophy (CMD) and subtypes 2C, 2D, 2E and 2F of limb-girdle muscular dystrophy (LGMD), respectively. Primary defects in the Dp427 isoform of dystrophin in the actin membrane cytoskeleton (AMC) cause severe Duchenne muscular dystrophy (DMD), benign Becker muscular dystrophy (BMD) and X-linked dilated cardiomyopathy (XLDCM). The Dp427 isoform of dystrophin also binds syntrophin (SYN) and dystrobrevin (DYB) proteins, mutations in which have no known neuromuscular disorders.

1.8 Dystroglycan complex

The dystrophin-associated glycoprotein complex (DAGC) is made up of three complexes. The dystroglycan complex which serves to link the extracellular matrix to the cytoplasm, the sarcoglycan complex which stabilizes the DAGC within the sarcolemma and the dystrophin-containing complex which links the complex to actin in myofibrils. The DAGC complex was identified after dystrophin was separated using wheat germ agglutinin chromatography (Campbell and Kahl, 1989). It was shown that dystrophin was tightly associated to a glycoprotein complex in the sarcolemma. An

overview of the structure of this DAGC is diagrammatically represented in Figure 1-6.

The largest of these proteins, the 156kDa protein α-dystroglycan (αDG) was found in the extracellular matrix and it bound to laminin via a calcium dependency (Ibraghimov-Beskrovnaya et al., 1992; Hohenester et al., 1999). It also had a physical interaction with the 43kDa protein β-dystroglycan (βDG) (Rentschler et al., 1999). The carboxyl terminus of the transmembrane protein, βDG is located on the cytoplasmic side of the sarcolemma and the 15 C-terminal amino acids of this domain bind directly to dystrophins' cysteine-rich domain (Jung et al., 1995). Calveolin-3, another transmembrane protein, competes with dystrophin for the βDG binding site in non-contractile muscle (Sotgia et al., 2000).

Five proteins were identified in the syntrophin family, the α-syntrophin, β_1- and β_2 – syntrophins and the γ_1- and γ_2- syntrophins (Adams et al., 1993; Ahn et al., 1994; Ahn et al., 1996; Piluso et al., 2000). They are found distributed differently in muscle, and dystrophin and dystrobrevin contain syntrophin-binding sites (Newey et al., 2000).

Two genes encode the dystrobrevin family, transcribing α- and β-dystrobrevin. These cytoplasmic proteins bind syntrophin and dystrophin via the carboxyl end (Albrecht and Froehner, 2002). The dystrobrevins have a number of similarities to dystrophin. Namely, a carboxyl terminus of similar homology to the dystrophin protein and also has a number of promoters like dystrophin that produce full-length isoforms proteins (Wagner et al., 1993). Alpha-dystrobrevin binds dystrophin in the cytoplasm whereas β-dystrobrevin is found in non-muscle tissues (Blake et al., 1999; Loh et al., 2000).

The sarcoglycan complex comprises four transmembrane glycoproteins and the sarcospan protein (Crosbie et al., 1997; Lim and Campbell, 1998). The α-sarcoglycan protein is found in skeletal and cardiac muscle, whereas other sarcoglycans can be found in smooth muscle (Barresi et al., 2000). The sarcospan protein is tightly linked to this complex of proteins, which is anchored by the DGC in the sarcolemma. The DGC complex appears to be maintained with the loss of sarcospan, as shown with sarcospan knockout mice, therefore appears not essential in maintaining the integrity of the membrane (Duclos et al., 1998; Lebakken et al., 2000).

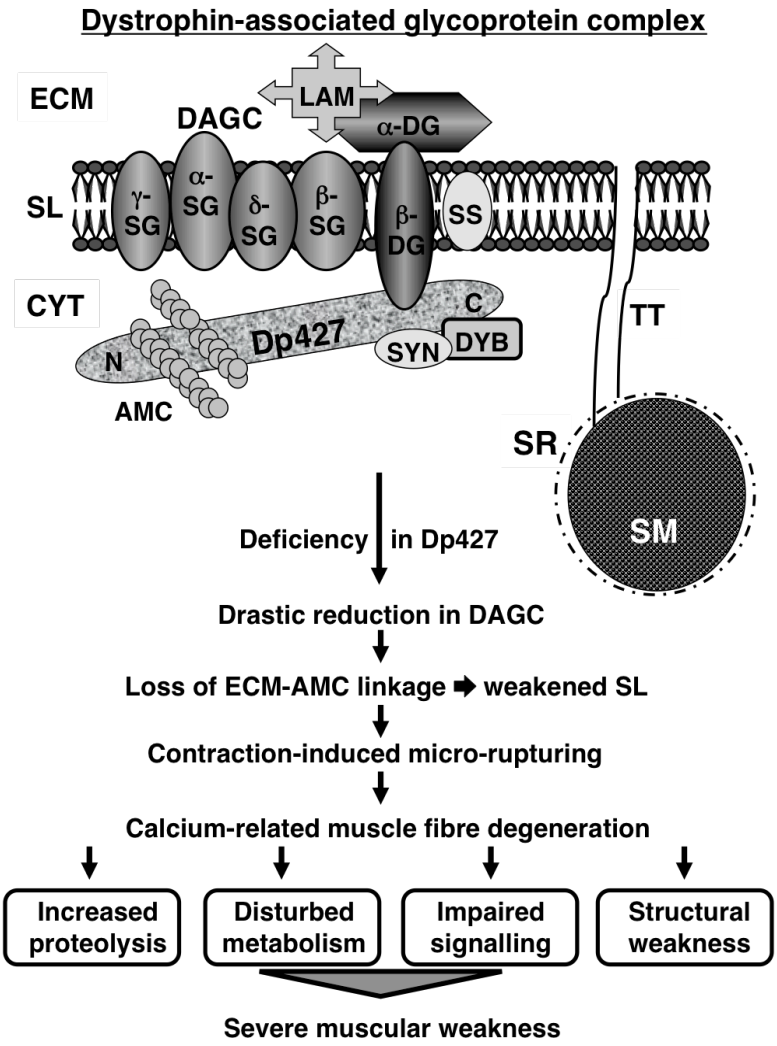

Figure 1-6 Overview of the structure of the dystrophin-glycoprotein complex form skeletal muscle and its involvement in the molecular pathogenesis of X-linked muscular dystrophy.
Shown is a diagram of the supramolecular dystrophin complex of the sarcolemma (SL) that links the actin membrane cytoskeleton (AMC) of the cytosol (CYT) to the extracellular matrix (ECM) component laminin (LAM). The full-length dystrophin isoform Dp427 binds directly to syntrophins (SYN), dystrobrevins (DYB) and the integral glycoprotein β-dystroglycan (β–DG), which in turn interacts with the extracellular laminin-binding protein α-dystroglycan (α-DG). Other Dp427-associated proteins are represented by sarcospan (SS) and the sarcoglycans (α/β/γ/δ-SG). Shown also located within the muscle cell is an invagination of the sarcolemma, the transverse tubule (TT) leading to the sarcomere (SM) containing the contractile elements, which is surrounded by the sarcoplasmic reticulum. Deficiency of Dp427 in muscle fibres from Duchenne muscular dystrophy (DMD) patients and its animal model, the dystrophic mdx mouse, cause a drastic reduction in the dystrophin-associated glycoprotein complex (DAGC). Loss of the linkage between the ECM and AMC results in a weakened SL membrane system, triggering various cellular abnormalities and finally severe muscular degeneration

1.9 Animal model of Duchene muscular dystrophy

The murine X chromosome-linked (*MDX*) mouse model is internationally recognized as a suitable model for the study of DMD/BMD. Absence of the 427kDa protein dystrophin affects muscle and non-muscle tissue. This defect causes muscular dystrophies to varying effect in different muscles, with the diaphragm being most severely affected (Stedman et al., 1991). The DMD^{mdx} mouse has a mutation on exon 23 of the dystrophin gene (Xp21) causing an absence in the Dp427 protein-Dystrophin. A single base pair change in the exon from cysteine to thymine creates a termination codon. This point mutation in the dystrophin gene results in a truncated protein of only 115kDa in length, which may attach to the extracellular dystroglycan complex conferring some membrane stability but with two-thirds of the rod and terminal domain missing, it would be unable to bind to the intracellular actin cytoskeleton. The *MDX* mouse does express four shorter isoforms containing the C-terminal end. These isoforms are expressed in non-muscle tissues and these various tissues show less severe pathologies of the dystrophy; this could possibly be explained by the production of these dystrophin isoforms. This may explain the milder pathology in the *MDX* mouse compared with DMD patients (Sicinski et al., 1989).

The MDX^{3cv} mouse, a strain lacking the four shorter isoforms does not show more severe abnormalities than *MDX* mice in skeletal muscle as the isoforms are produced in non-muscle tissue. Shorter isoforms of the dystrophin protein can be produced from the Xp21 gene, and the MDX^{3cv} model mouse, deficient in dystrophin, has an additional point mutation on exon 65, which removes the isoforms Dp260, Dp140, D116 and Dp71. The proteins of 260, 140 and 116 are produced in the retina, brain and Schwann cells, respectively, and the 71kDa protein expressed in most tissues except skeletal (Cox et al., 1993; Rafael et al., 1999).

Utrophin, a similar protein with significant gene homology to dystrophin has been shown to be up-regulated in *MDX* strains of mice (Blake et al., 2002). An autosomal protein may be expressed in all tissues and is therefore not subject to the X-linked mutation. Although down-regulated after birth, utrophin is thought to compensate for the

absence of dystrophin as it is up-regulated three fold in the *MDX* extraocular muscle and found in the sarcolemma of regenerating muscles. The extraocular muscles of the *MDX* mouse appear free from the pathology of Duchenne muscular dystrophy, even though they are a skeletal muscle lacking in dystrophin (Porter et al., 1998). Therefore, utrophin is thought to play a compensatory role in *MDX* and *MDX*^{3cv}mouse models, replacing dystrophin to some extent in skeletal muscles and rescuing the dystrophic mouse. Utrophin knockout mice, *utr/mdx* and *utr/mdx*^{3cv} show more severe pathology to DMD than their single knockout counterparts, although it appears that the shorter isoforms produced in *MDX* rescue the non-muscle tissue only but the *utr/mdx*^{3cv} mice lack utrophin and all isoforms of dystrophin do not live past 20 weeks of age (Deconinck et al., 1997; Rafael et al., 1999).

1.10 Proteomics

The word 'Proteome' comes from two words '*prote*in' and 'gen*ome*'. Proteomics is the study of the entire protein complement from one organism. This includes all the modifications made to any number of proteins. Translation of the nucleotide sequence has been shown not to match fully the proteins produced (Anderson and Seilhamer, 1997). This is because the proteome is subject to environmental influences and can act to apply post-translational modifications (PTM) to adapt to changing situations. Therefore, proteomics can be a useful tool in describing the changing expression of proteins in an organism subject to disease. Regardless of the starting material used there are a number of techniques which must be optimized. These include sample preparation, separation, imaging and characterization.

1.10.1 Sample preparation

This first step in the study of the proteome requires the solubilisation of the sample proteins. The sample should be homogenized into a suitable lysis buffer. The buffer must be capable of reducing bonds and usually contains protease inhibitors to inhibit

the inherent proteases in the sample (Rabilloud, 1996). Any modifications introduced, via salts or temperature can influence spot pattern during two-dimensional (2D) gel electrophoresis and therefore need to be kept to a minimum. There is no standard lysis buffer suitable for all tissue solubilisation and each sample should be optimized to its most suitable reducing buffer. Disruption of protein-protein interactions can be caused by a combination of reductants and detergents. Reducing agents such as dithiothreitol (DTT) break disulphide bridges. Chaotropic reagents like urea and thiourea disrupt hydrogen and hydrophobic bonds (Rabilloud, 1998). Other additions commonly used are detergents and ampholytes, which disrupt membranes and other hydrophobic bonds and further inhibit reformation of bonds by maintaining pH levels and scavenging cyanate artifacts produced by carbamylation of urea.

1.10.2 2D gel electrophoresis

Two-dimensional electrophoresis allows separation and subsequent identification of proteins in a sample. The technique can be optimised to separate out a single protein, which can be excised from a gel and characterised using mass spectrometry. The technique was first described by O'Farrell (1975) where he separated an *Escherichia coli* sample. O'Farrell proved by reproducibility that proteins migrate to the same spot on a gel based on their pH and molecular mass.

The first dimension is known as isoelectric focusing (IEF) and proteins are separated based on their pH. The sample is applied to a gel adhered to a plastic strip. The strip has a gradient in the form of carrier ampholytes, across a specified pH range, embedded in the gel. The first dimensional strips are rehydrated in a buffer similar to the lysis buffer of the sample. The solubilised sample may be mixed with the rehydration buffer at this point and be taken up across the gel strip in a passive manner, known as 'in-gel' rehydration. Alternatively, the samples may be applied post-rehydration in two ways. Firstly, the sample may be placed in a plastic cup and 'cup-loaded' onto the strip actively, under a current. Secondly, the sample can be introduced to the strip via a paper bridge and, again, allow the current to attract the proteins. Proteins carry a charge, which is dependent on the pH of their surroundings. When an

electric field is applied, proteins with a negative charge will move towards the anode becoming less charged as it reaches its p*I*. Likewise, positively charged proteins will move toward the cathode under an applied current. The p*I* of a protein is reached when the charge is zero at a specific pH. This allows the charged proteins in the sample to find their respective p*I*, or isoelectric point, when a charge is applied to the gel.

Sodium dodecyl sulphate polyacrylamide gel electrophoresis (SDS-PAGE) separates proteins based on their molecular mass; this is carried out subsequent to isoelectric focusing. The focused strip is placed along the top of a slab gel composed of an SDS/acrylamide mixture. The proteins must be coated in SDS to give them an overall negative charge. Sodium dodecyl sulphate is a detergent and therefore contains hydrophobic domains. In solution, the SDS and proteins form complexes. The SDS masks the charge of the protein, but applies a negative charge itself. The degree of separation in the gel now depends on the size and therefore the molecular mass of each individual protein. Prior to SDS-PAGE, the proteins on the strip can be equilibrated with DTT to reduce any reformed disulphide bonds in the proteins. The strip is then equilibrated with iodoacetamide to react with any residual DTT and to alkylate thiol groups on proteins, preventing their reoxidation. The buffer system most commonly used is the Tris-glycine method described by Laemmli (1970). A front is formed between the negatively charged chloride ions from the Tris-HCl, and glycine, which moves more slowly. The high pH of the Tris buffer allows minimal protein aggregation, which helps the proteins enter the gel and travel through the pores of the polyacrylamide matrix. The larger proteins become retarded by the pore size and become retained, while smaller proteins migrate towards the anode within the buffer front. A tracking dye of bromophenol blue, a small molecule, migrates along with the buffer front and indicates when separation is complete. Gels can then be fixed and stained to visualise proteins.

1.10.3 Western blotting

Blotting was first described in 1975 (Southern) when DNA was transferred to a nitrocellulose membrane. Subsequently, Towbin and colleagues (1979) described a method for transferring protein from SDS-PAGE gels. Ten percent polyacrylamide mini gels are used for separation of proteins up to approx 200kDa. For detection of larger proteins 3% (v/v) gels or gradient 3-10% (v/v) gels are used. As in 2D gel electrophoresis, bromophenol blue indicates when separation is complete and gels can be fixed and stained. Alternatively, proteins can be electrophoretically transferred from the gel matrix to nitrocellulose membrane. The proteins can now be probed with specific antibodies. Non-specific sites are blocked with excess milk protein after transfer, masking all available sites on the nitrocellulose membrane. A secondary antibody labelled with a conjugate binds the protein specific primary antibody and levels of fluorescence or colour change can then be quantified to show differences between samples.

1.11 Difference in-gel electrophoresis

Difference in-gel electrophoresis (DIGE) is a modification of 2D SDS-PAGE whereby comparisons of samples can be analysed together on a single gel. Analysing biological samples within a gel removes variation found from conducting technical replicates. Two protein samples are labelled with cyanine dyes, combined, separated on a gel and subsequently imaged using fluorescence software (see Figure 1-7). The cyanine dyes used in DIGE have a number of criteria that must be met to ensure reproducibility: (i) the dyes must match the charge of the amino acid they are replacing, (ii) the difference dyes must have a similar charge to each other and (iii) the dyes must have distinct fluorescent spectra (Unlu et al., 1997). Originally, a Cy2 dye was used but was shown to alter the proteins mass proportionally greater than the other two cyanine (Cy) dyes. It is now commonplace to use only cyanine dyes Cy3 and Cy5. The exception where the three-dye system is used applies when analysis of complex human samples is required, and the third dye, Cy2, is used for normalisation. In this instance the pooled sample is

labelled with the Cy2 dye, leaving differences in expression in sample groups to be anaylzed using the structurally similar alternative dyes (Tonge et al., 2001). The dyes contain a reactive N-hydroxy succinimidyl ester bound to fluorescence cyanine and fluoresce at different wavelengths, Cy3 at λ=550nm and Cy5 λ=650nm due to slightly different structures. The dyes themselves are hydrophobic and could cause proteins to precipitate prior to entering the gel. To overcome this, minimum labelling is preformed at 1-2% of total lysine content (Unlu et al., 1997). CyDyes can detect down to the nanogram level making them the most sensitive dyes available.

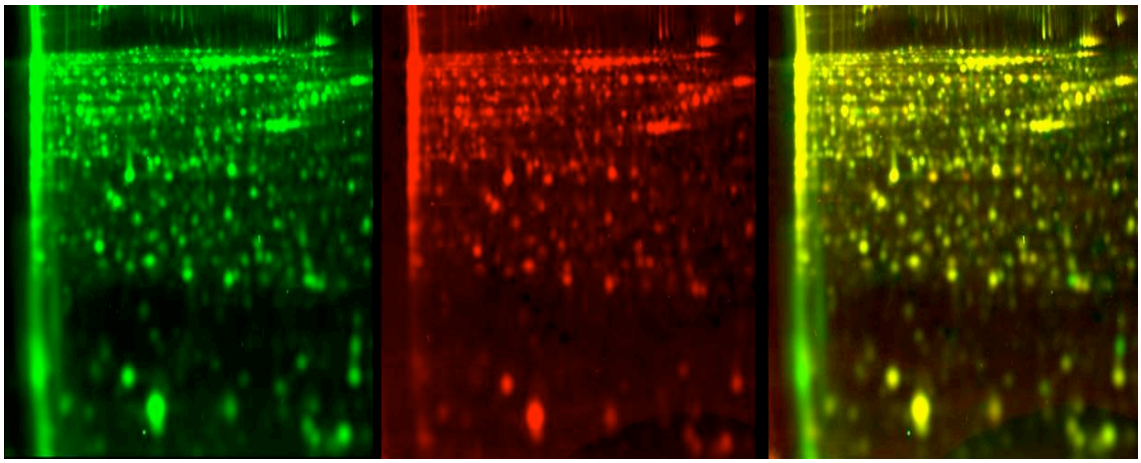

Figure 1-7 DIGE image of separated cardiac muscle
Shown is a single gel with labelled Cy3, Cy5 and overlay images of 2D gel electrophoresis separation of combined normal and dystrophic cardiac muscle.

1.12 Visualisation

There are a number of post separation visualisation methods. A method may be chosen for its sensitivity, downstream processing or because it is cheap and convenient. Coomassie staining provides a simple and cheap method of staining. Neuhoff and colleagues (1985) originally described how Coomassie brilliant blue binds to proteins, via basic amino acids, in a hydrophobic manner. This hydrophobicity has been further sensitised by the addition of ammonium sulfate so that this mass spectrometry-compatible method can detect down to 100ng of protein per spot. Another

commonly used stain in the laboratory is silver staining. Many methods have been described for this more sensitive stain. Detection down to 1ng of protein may be possible, but silver staining has a very limited dynamic range. This becomes an issue when separating complex tissue samples. Negative staining occurs on abundant protein making quantification difficult. Silver nitrate binds proteins and then the silver ions become reduced to metallic silver upon the addition of formaldehyde (Rabilloud et al., 1994). If gluteraldehyde is removed from the assay the excised stained proteins can be used for future mass spectrometry analysis, but this removes some of the sensitivity of silver binding. Fluorescent labelling has shown to be a quantifiable, sensitive and have a large dynamic range and can be utilised usually at more expense. The use of ruthenium as in the SYPRO ruby dye is mass spectrometry compatible but requires the use of fluorescent scanners.

1.13 Identification

Following on from a quantitative comparative proteomic study, the workflow moves to identification of the individual proteins. Two-dimensional electrophoresis can highlight changes between groups of samples and subsequent analysis using mass spectrometry can provide the amino acid sequences of peptides, which can be used to identify a protein from a database. Samples must be digested before being applied to an analyser. This can be carried out by in-gel digestion or by electroblotting and digestion on a membrane.

1.13.1 In-gel digestion

Rosenfeld and colleagues (1992) first described the extraction of proteins from an SDS-PAGE gel. As the protein is encased within polyacrylamide, the gel must be dehydrated first, to allow the uptake of the trypsin enzyme during the reswelling process. The proteins are then digested within the gel and the peptides can be extracted and analysed. Shevchenko and colleagues (1996) described a method of

successfully sequencing proteins from a silver stained polyacrylamide gel without chemical modifications from the silver. Other stains like Coomassie and Ruthenium (II) tris bathophenantroline disulfonate (RuBPS), bind the protein via hydrophobic methods and are easily removed before digestion.

1.13.2 Digestion on nitrocellulose

In situ digestion with trypsin from a nitrocellulose membrane was described by Aebersold (1987). This method overcame problems encountered with Edman degradation as all amino acids within a sequence of peptides could be cleaved. Trypsin degrades specifically at arginine and lysine residues. The trypsin digestion generates independent sequence information that can be searched in a protein database. Analysing samples run from a 1D SDS-PAGE gel overcomes some of the limitations of 2D proteomics.

Proteins are transferred to the membrane via electrostatic interactions and hydrophobic binding. The membrane-bound proteins can be directly trypsinated, reducing the loss of peptides, as proteins need not be precipitated. Also, mass spectrometric identifications have less missed cleavages and better coverage (Luque-Garcia et al., 2006).

1.13.3 Electrospray ionisation mass spectrometry

Electrospray ionisation mass spectrometry (ESI-MS) is the formation of small droplets of sample, which ionise, evaporate and pass through a vacuum to an analyser. Samples in a formic acid/acetonitrile solution flows into the chamber at 1μL/min. An electric field is applied to the tip of the needle and this charges the solvent. The emerging drop divides into a fine spray of droplets due to repulsion of charges. Residual charge on the drop attracts it to the end wall of the chamber. The temperature of the nitrogen gas flowing through the chamber slows the evaporation of the solvent off the droplets. The size of the droplets decreases as the solvent evaporates. The Rayleigh limit is reached when the surface tension exceeds the charge of the droplet, causing it to de-form and produce daughter droplets. This continues until the droplets

are small enough that the ions can travel through the nitrogen gas vacuum chamber and be passed onto the analyser (Yamashita and Fenn, 1984; Fenn et al., 1989).

1.14 Student's t*-test*

Throughout this project, the Student's *t*-test is used to calculate significant difference of protein expression between normal tissue and an aged-matched diseased tissue. An unpaired Student's *t*-test is used to test the significance of the difference between two sample means where data collected is random or independent of one another. By choosing a probability value of 0.05 within the test, we can say that our data is good enough to support a conclusion with 95% confidence. This is acceptable when working with biological samples. W.S. Gosset went under the pen name of 'Student' while working for Guinness Brewery, Dublin and he designed the test to monitor the quality of batches of Guinness stout being produced.

1.15 Aims of proposed project

Duchenne muscular dystrophy is the most frequently inherited neuromuscular disorder of childhood. The disintegration of the dystrophin-associated glycoprotein complex triggers the initial pathology of muscular dystrophy. Secondary modifications leading to alterations in membrane stability, cellular signalling and the regulation of ion homeostasis cause the further cellular damage of end-stage fibre degeneration. This X-linked muscle disease is extremely progressive with skeletal muscle weakening to the extent that patients are wheelchair bound by their second decade and degeneration of diaphragm muscles lead to respiratory failure. Physiotherapy and early respiratory care intervention has greatly improved the life expectancy of affected boys, but at an advanced stage of the disease, most Duchenne patients are suffering cardiac failure.

Although Duchenne muscular dystrophy is extremely progressive, not all muscles are affected in the same way. While limb skeletal muscles are severely weakened, subtypes of skeletal muscle, namely laryngeal, extraocular and distal muscles are usually spared in Duchenne sufferers.

The purpose of this study was to carry out proteomic profiling on differentially distressed dystrophic muscles. The pathobiochemical steps causing a progressive decline in dystrophin-deficient cardiac muscle are not well understood. Therefore, we carried out a fluorescence difference in-gel electrophoresis, mass spectrometry, immunoblotting, confocal microscopy, one-dimensional gel electrophoresis and 'on-membrane' digestion between normal and dystrophic tissues of the heart and naturally protected extraocular muscles in order to establish the global protein expression pattern.

Mass spectrometry combined with highly sensitive difference in-gel electrophoresis was used to elucidate changes and identify novel biomarkers in dystrophic tissue and antibody probing was used to study the fate of specific groups of proteins. We applied one-dimensional electrophoresis and 'on-membrane' digestion to observe the fate of full-length dystrophin isoform and other proteins, (large complexes, membrane-associated and low-abundant proteins) which are normally excluded from conventional two-dimensional gel electrophoresis.

2 Materials and methods

2.1 Materials

2.1.1 General reagents

General reagents and chemicals were purchased from Sigma Chemical Company (Dorset, UK) and were of reagent/electrophoresis grade, unless stated otherwise. Distilled H_2O was purified using a Millipore Milli-Q apparatus to obtain milli-Q water 18MΩ. Protease inhibitors were from Roche Diagnostics (Mannheim, Germany). All other chemicals used were of analytical grade and purchased from Sigma Chemical Company, Dorset, UK.

2.1.2 1D and 2D gel electrophoresis

For gel electrophoretic protein separation, analytical grade chemicals and materials; Immobilized pH gradient (IPG) strips of pH 4- 7 24cm and pH 6-11 18cm; IPG buffer were purchased from Amersham Biosciences/GE Healthcare (Little Chalfont, Buckinghamshire, UK), and protein molecular mass markers were purchased from Biorad Laboratories (Hemel-Hempstead, Hertfordshire, UK). Ultrapure Protogel acrylamide stock and 4x Protogel Resolving Buffer stock solutions were obtained from National Diagnostics (Atlanta, GA, USA).

2.1.3 Protein staining

The reversible membrane stain MemCode was purchased from Thermo Fisher Scientific (Waltham, MA, USA). CyDye DIGE fluor minimal dyes Cy3 and Cy5 were

purchased from Amersham Biosciences/GE Healthcare (Little Chalfont, Buckinghamshire, UK). 2D silver stain II kit was from Cosmo Bio Company, (Japan). Coomassie Brilliant Blue G-250 was from Perbio Science, (Northumberland,UK).

2.1.4 Mass spectrometry

Sequencing grade-modified trypsin was purchased from Promega (Madison, WI, USA). LC-MS Chromasolv water and formic acid were obtained from Fluka (Milwaukee, WI, USA).

2.1.5 Western blotting

Chemiluminescence substrate was obtained from Roche Diagnostics (Mannheim, Germany). Nitrocellulose transfer membrane was purchased from Carl Stuart (Whitestown, Dublin 24, Ireland). All secondary antibodies were purchased from Chemicon International (Temecula, CA, USA). Table 2-1 lists the antibodies used in this study including ordering details.

Table 2-1 Antibodies

List of antibodies used for this project including company and catalogue number, antibody specificity, host species, dilutions used for both primary and secondary antibodies and its application. Species= Host species; 1^0= primary; 2^0= secondary; pAb= polyclonal antibody; mAb= monoclonal antibody; WB= Western blotting; CF= Confocal microscopy; NC= Novocastra; SGN= Stressgen; SC= Santa Cruz

Antibody	Company	Catalogue #	Ab specificty	Immunogen	1^0 dilution	Species	2^0 dilution	Use
αBCrys	NC	NCL-a-BCrys	pAb	Bovine	1:250	Ms	1:1000	WB
Adenylate kinase	abcam	ab54824	mAb	Human	1:1000	Ms	1:1000	WB
ATP synthase	abcam	ab14730	mAb	Human	1:500	Ms	1:1000	WB
βDystroglycan	NC	NCL-b-DG	pAb	Human	1:50	Ms	1:1000	CF
βDystroglycan	NC	NCL-b-DG	pAb	Human	1:100	Ms	1:500	WB
Calsequestrin	ABR	MA3 913	pAb	Rabbit	1:1000	Rb	1:2000	WB
cvHSP	HyTest	PCV60	mAb	Rabbit	1:250	Rb	1:1000	WB
Desmin	ABR	OMA1-06002	mAb	Chicken	1:100	Ms	1:1000	CF
Desmin	ABR	OMA1-06002	mAb	Chicken	1:250	Ms	1:1000	WB
DJ1 protein	abcam	ab76241	pAb	Human	1:1000	Rb	1:1000	WB
Dystrophin Dp427	NC	NCL-DYS2	mAb	Human	1:10	Ms	1:100	CF

Dystrophin Dp427	NC	NCL-DYS2	mAb	Human	1:50	Ms	1:100	WB
Fatty acid binding protein FABP3	abcam	ab16915	mAb	Human	1:100	Ms	1:500	WB
HSP25	SGN	SPA-801	pAb	Human	1:500	Ms	1:1000	WB
HSP60	SGN	SPA-807	pAb	Human	1:500	Ms	1:1000	WB
HSP90	SGN	SPA-835	mAb	Human	1:1000	Rt	1:2000	WB
Isocitrate dehydrogenase	abcam	ab36329	pAb	Porcine	1:500	Rb	1:1000	WB
Laminin	Sigma	L-9393	pAb	Mouse	1:1000	Rb	1:1000	WB
Myosin heavy chain	Sigma	MF20	mAb	Chicken	1:100	Ms	1:1000	CF
Myosin heavy chain slow/cardiac	Sigma	M8421	mAb	Human	1:500	Ms	1:1000	WB
Prohibitin	abcam	ab28172	pAb	Human	1:100	Rb	1:1000	CF
Prohibitin	abcam	ab28172	pAb	Human	1:500	Rb	1:1000	WB
SERCA1	ABR	MA3 912	mAb	Rabbit	1:1000	Ms	1:2000	WB
Succinate dehydrogenase	SC	sc-27992	pAb	Human	1:50	Gt	1:1000	CF
Succinate dehydrogenase	SC	sc-27992	pAb	Human	1:100	Gt	1:1000	WB
Utrophin Up395	SC	sc-15377	pAb	Human	1:100	Rb	1:250	WB
VDAC1	abcam	ab14734	mAb	Human	1:1000	Ms	1:1000	WB

2.1.6 Immunofluorescence microscopy

Superfrost Plus positively-charged microscope slides were purchased from Menzel Glaesser (Braunschweig, Germany). Optimum cutting temperature (OCT) compound was from Sakura Finetek Europe B.V (Zoeterwoude, Netherlands) and p-phenylenediamine (PPD)-glycerol was purchased from Citifluor Ltd. (London, UK). Molecular Probes MitoTracker Red CMXRos dye was obtained from BioSciences Ltd., Dun Laoghaire, Ireland. The DNA binding dye diamidino-phenyindole (DAPI) was obtained from Sigma Chemical Company (Dorset, UK). Fluorescent secondary antibodies Alexa fluor 594 goat anti-rabbit IgG, Alexa fluor 594 goat anti-mouse IgG and Alexa fluor 488 mouse anti-goat IgG were from Molecular Probes (Eugene, Oregon, USA).

2.2 Methods

2.2.1 Dystrophic MDX animal model

Tissue from C57 control mice and age-matched dystrophic *MDX* mice were obtained through the Bioresource Unit of NUI Maynooth and the Animal House of the Bielefeld University, Germany. Animals were kept under standard conditions and all procedures were performed in accordance with German and Irish guidelines on the use of animals for scientific experiments. Ethics approval for the project was granted from NUI Maynooth Biomedical (& Life) Sciences Research Ethics Sub Committee. Mice were killed by cervical dislocation and snap frozen. As previously demonstrated by immunoblotting, the MDX mouse cohort used in this study lacks the 427 kDa isoform of dystrophin (Lohan et al., 2005) .

2.2.2 Preparation of total crude muscle extracts

For the proteomic profiling of crude muscle extracts, three normal and three age-matched dystrophic hearts, diaphragm or extraocular muscle (n=2 per pool) were separately prepared by washing with distilled water to remove excess blood. Using appropriate safety equipment; coat, facemask and cryo-gloves tissue was frozen in liquid nitrogen. Subsequent to tissue freezing and excess nitrogen evaporating off, grinding using a mortar and pestle pulverized muscle tissue. Ground muscle was solubilised in lysis buffer with the ratio 100 mg wet weight to 1ml lysis buffer consisting of 9.5M urea, 2% (w/v) CHAPS, 0.8% (v/v) IPG buffer pH3-10, 1% (w/v) DTT and protease inhibitors for cardiac samples and 7M urea, 2M thiourea, 4% (w/v) CHAPS, 2% (v/v) IPG buffer pH4-7, 2% (w/v) DTT and protease inhibitors (Doran et al., 2006b). Samples for DIGE analysis were placed in buffer containing only urea, CHAPS and a protease inhibitor cocktail. Samples were gently rocked for 30 min, suspensions were

centrifuged at 4 ^{0}C for 20 min at 20,000*g* and protein concentration was determined using the Bradford assay system (Bradford, 1976).

2.2.3 Fluorescence difference in-gel electrophoretic analysis

Potential differences in the expression pattern of the soluble proteome from normal and MDX muscle were analysed using the fluorescent difference in-gel electrophoretic DIGE technique (Viswanathan et al., 2006), as recommended by Karp and Lilley (2005). The fluorescent dyes Cy3 and Cy5 were reconstituted as a stock solution of 1mM in fresh dimethylformamide, then diluted to a 0.2mM solution prior to use. Labelling was performed with 200pmols of Cy3 fluor dye per 25μg protein. An internal pooled standard of every sample was prepared with the Cy5 fluor. Labelled samples were then vortexed and incubated for 30 min on ice in the dark. The reaction was quenched with 10mM lysine on ice for 10 min. For isoelectric focusing, pH 6-11 IPG strips were rehydrated for 12h in rehydration buffer (8M Urea, 0.5% (w/v) CHAPS, 0.2% (w/v) DTT and 0.2% (v/v) ampholytes) with the addition of 1.2% (v/v) DeStreak rehydration solution (Amersham Biosciences/GE Healthcare, Little Chalfont, Buckinghamshire, UK). Sample and equal volumes of lysis buffer (9.5M Urea, 2% (w/v) CHAPS, 2% (w/v) DTT and 1.6% (v/v) ampholytes) were added by anodic cup loading. For pH4-7 focusing, IPG strips were in-gel rehydrated with sample and equal volumes of 2x lysis buffer made up in rehydration buffer. The strips were run on an Amersham IPGphor IEF system with the following running conditions: 3500V for 21.3h, a 3500 to 8000V gradient over 10min, and 8000V for 2h. For first dimension separation in the pH 6-11 range the following protocol was employed: 80V for 4h, 100V for 2h, 500V for 1.5h, 1000V for 1h, 2000V for 1h, 4000V for 1h, 6000V for 2h and finally 8000V for 2.5h. Following isoelectric focusing, the IPG strips were equilibrated for 20min firstly in buffer containing 6M urea, 30% (v/v) glycerol, 2% (w/v) SDS, 100mM Tris-HCl, pH 8.8 with the addition of 100mM DTT and subsequently for 20min in buffer supplemented with 0.25M iodoacetamide [49]. Strips were briefly washed in sodium dodecyl sulfate-containing running buffer (125mM Tris, 0.96M glycine, 0.1% (w/v) SDS) and placed on

top of 12.5% (v/v) resolving gels. To seal the strip gels, they were overlaid with the above-described running buffer containing 1% (w/v) agarose. The separation of the cardiac proteins was carried out in the second dimension by standard SDS polyacrylamide gel electrophoresis using the DodecaCell system from Bio-Rad Laboratories (Hemel Hempstead, Herts., UK). Slab gels contained 50 μg protein per gel. Electrophoresis was carried out overnight for approximately 18 hours in the dark at 1.5V per 21cm-gel until the Bromophenol Blue tracking dye just ran off the gel.

2.2.4 Protein visualization and data analysis

Fluorescent CyDye-labelled cardiac and extraocular proteins were visualized using a Typhoon Trio variable mode imager form Amersham Biosciences/GE Healthcare (Little Chalfont, Bucks., UK). For image acquisition, Cy5- and Cy3-labelled proteins were scanned at a wavelength of λ=650nm and λ =550nm, respectively. Photomultiplier tube values were optimised so that the volume of the most abundant spot was between 80,000 and 99,000 when scanned at a resolution of 100μm. This guaranteed that no spot would be saturated on the gel, therefore interfering with accurate analysis. The Cy3 images were then analysed using Progenesis Samespots software version 3.2.3 from NonLinear Dynamics (Newcastle upon Tyne, UK) and normalised against their corresponding Cy5 image. Gels were aligned to the reference image. Following detection of spots, the gels were placed into groups (MDX versus normal) and analysed to determine significant differences in 2-D spot abundance. An ANOVA score of 0.5 was required for spots to be included in the subsequent analysis. Then principal component analysis was verified with changes displaying power of <0.8 being removed from the analysis. All remaining changed spots that met the significance criteria were visually checked on the aligned gels to ensure feasibility and were subsequently identified by LC-MS/MS analysis.

2.2.5 Mass spectrometric identification of cardiac and extraocular proteins

Preparative gels containing 400μg of protein (1:1 MDX to normal) were stained with the dye Ruthenium II Bathophenanthroline Disulfonate Chelate (RuBPs) [50]. RuBPs-stained gels were scanned at a wavelength of λ=550nm using the criteria outlined above. Prior to identification via LC-MS/MS technology, 2-D protein spots of interest were excised using the automated Ettan spot picker system from Amersham Biosciences (Little Chalfont, Bucks., UK). Spots were digested as outlined by Shevchenko and colleagues (2006). Briefly, gel pieces were destained before the addition of 400ng trypsin per spot, incubated for 30min at 4^0C before being digested overnight at 37^0C. 100μL of extraction buffer (1:2 v/v of 5% (v/v) formic acid/acetonitrile) was added to the peptides and incubated for 15min at 37^0C. All supernantant was then transferred into fresh tubes and extracts were dried down completely in a vacuum centrifuge. Peptides were reconstituted in 12μL of 0.1% (v/v) formic acid, vortexed, sonicated and the mixture was centrifuged for 20min in cellulose spin filter tubes to remove any gel particles. The remaining solution was placed into LC-MS vials. Samples were analysed on an Agilent 6340 Ion Trap LC mass spectrometer using electrospray ionization (Agilent Technologies, Santa Clara, CA, USA) on a 10min gradient of 5-100% (v/v) acetonitrile/0.1% (v/v) formic acid with a post run of 1min (Lewis et al., 2010b). Separation of peptides was performed with a nanoflow Agilent 1200 series system, equipped with a Zorbax 300SB C18 μm, 4mm 40nl pre-column. Mobile phases used were A: 0.1% (v/v) formic acid, B: 50% (v/v) acetonitrile and 0.1% (v/v) formic acid. Samples (8μl) were loaded onto the enrichment column with capillary flow rate set at 4μL/min with a mix of A:B at a ratio of 19:1. Elution was carried out with the nano pump flow rate set at 0.6μL/min. Database searches were carried out using Mascot MS/MS Ion search. Criterion for each search was set at (i) species *Mus musculus*, (ii) two missed cleavages by trypsin, (iii) variable modification: oxidation of methioine, (iv) fixed modification: carboxymethylation of cysteines and (v) mass tolerance of precursor ions ±2Da and product ions ±1Da.

2.2.6 Immunoblot analysis

In order to determine the fate of select proteins, 1-D gel electrophoresis, Coomassie staining and immunoblotting was performed. Gel electrophoretic separation and transfer was carried out with a Mini-Protean II electrophoresis and transfer system from Bio-Rad Laboratories (Hemel-Hempstead, Herts, UK). Muscle proteins were transferred to nitrocellulose for 70min at 100V and at 4^0C Blocking of nitrocellulose sheets was achieved with a milk protein solution (5% (w/v) fat-free milk powder in 0.9% (w/v) NaCl, 50 mM sodium phosphate, pH 7.4) for 1h. Incubation with sufficiently diluted primary antibody was carried out overnight with gentle agitation. Nitrocellulose sheets were washed and then incubated for 1h with secondary horseradish peroxidase-conjugated antibodies, diluted in blocking solution. Immuno-decorated bands were visualized by the enhanced chemiluminescence method using chemiluminescence substrate (Roche Diagnostics, Mannheim, Germany). Densitometric scanning of immunoblots was performed using ImageJ (NIH, Bethesda, Maryland, USA).

2.2.7 Immunofluorescence microscopy

For the localization of nuclei, mitochondria and select marker proteins, confocal microscopy was used (Doran et al., 2006b). Normal and dystrophic MDX hearts were mounted on cyrocassettes at -20ºC and transverse cryosections of 10μm thickness were cut on a Shandon Cryotome (Life Sciences International, Cheshire, UK). Unfixed tissue sections were transferred to Superfrost Plus positively-charged microscopy slides. For labeling of mitochondria, freshly cut tissue sections were incubated with a 1:100 diluted solution of MitoTracker Red Chloromethyl-X-Rosamine (CMXRos) dye for 30 min, briefly washed in phosphate-buffered saline and then immediately examined by microscopy (Poot et al., 1996). CMXRos is a well-established lipophilic cationic fluorescent dye that is highly specific for mitochondria (Pendergrass et al., 2004) and is routinely used to measure mitochondrial function and morphology cell culture and in

whole tissues (Chazotte, 2009). For immunofluorescence microscopy, cryosections were submersed in blocking solution (0.2% (w/v) bovine serum albumin, 0.2% (v/v) Triton X-100, and 2.5% (v/v) goat serum in phosphate-buffered saline) for 30 min, followed by incubation with primary antibodies diluted in washing solution (0.2% (w/v) bovine serum albumin and 0.2% (v/v) Triton X-100 in phosphate-buffered saline) for 4 hours. Tissue sections were washed twice for 30 min in above washing solution omitting antibodies and then labelled with secondary antibodies for 1 hour, followed by repeated washing procedure. In order to determine the number of nuclei in normal versus MDX hearts, cardiac tissue sections were labelled with 1 μg/ml diamidinophenyindole (DAPI) for 30 min. One drop of p-phenylenediamine (PPD)-glycerol was applied to the immuno-decorated tissue sections and then coverslips carefully placed over the sections, avoiding the introduction of air bubbles. Fluorescent labelling patterns were visualised with an Olympus IX81 microscope (Olympus Life and Material Science Europe, Hamburg, Germany).

2.2.8 1D gel electrophoresis for subsequent digestion

Protein samples were separated on 3-12% (v/v) gradient sodium dodecyl sulfate polyacrylamide gels and stained with Coomassie Brilliant Blue or transferred to nitrocellulose (Ohlendieck et al., 1991). Importantly, gel electrophoresis was carried out in the absence of combs so that several centimeter-long horizontal strips of individual muscle protein bands could be separated. The successful electrophoretic transfer of muscle proteins was evaluated by staining of nitrocellulose membranes with the reversible stain MemCode. Individual MemCode-stained bands were cut out for subsequent treatment with trypsin.

2.2.9 On-membrane digestion

Protein bands were excised from membranes, placed in a small plastic tube, destained and washed 5 times with distilled water. Nitrocellulose strips were then

blocked with 0.5% (w/v) polyvinylpyrrolidone (PVP-40) at 37^{0}C for 37 min with gentle shaking (Luque-Garcia et al., 2008). Membranes were subsequently washed 5 times with distilled water. For digestion, a fresh stock solution of 20μg trypsin in 1.5 ml of buffer (1:1 (v/v) 100mM ammonium bicarbonate/10% (v/v) acetonitrile) was prepared. Membrane strips were digested overnight at 37^{0}C in 100μl trypsin solution (Shevchenko et al., 2006). Subsequently, 100μl extraction buffer (1:2 (v/v) 5% (v/v) formic acid/acetonitrile) was added to the trypsin-treated membranes and gently agitated for 15 min at 37^{0}C. All supernatant fractions were placed into fresh plastic tubes and peptides dried down by vacuum centrifugation (Doran et al., 2006b). Peptides were reconstituted in LC running buffer (0.1% (v/v) formic acid), centrifuged for 20min in 22μm cellulose spin filter tubes to remove any membrane particles and then aliquoted into LC-MS vials.

2.2.10 Mass spectrometric identification of on-membrane digestion

Recovered peptides were analysed on an Agilent 6340 LC/MS with a 3D Ion Trap configuration (Agilent Technologies, Santa Clara, CA, USA) on a gradient of 5-100% (v/v) acetonitrile/ 0.1% (v/v) formic acid for 10 min. Separation of peptides was performed with a nanoflow Agilent 1200 series system, equipped with a Zorbax 300SB C18 5 μm, 4mm 40nl pre-column and an Zorbax 300SB C18 5 μm, 43 mm x 75 μm analytical reversed phase column using the HPLC-Chip technology. Mobile phases utilized were A: 0.1% (v/v) formic acid, B: 90% (v/v) acetonitrile and 0.1 % (v/v) formic acid. Samples (5μl) were loaded into the enrichment at a capillary flow rate set to 4 μL/min with a mix of A and B at a ratio 19:1. Tryptic peptides were eluted with a linear gradient of 5-70% (v/v) solvent B over 6 min, 70-100% (v/v) for 1 min and 100% (v/v) for 1 min with a constant nano pump flow of 0.60mL/min. A 1 min post time of Solvent A was used and a blank run injected after each sample injection to remove sample carryover. The capillary voltage was set to 2000V. The flow and the temperature of the drying gas was 4 L/min and 300ºC, respectively. Identified peptides were utilized to determine the protein species present in distinct protein bands. Database searches

were carried out with Mascot MS/MS Ion search (Matrix Science, London, UK; NCBI database, release 20100212).

3 Proteomic profiling of the dystrophin-deficient MDX heart reveals drastically altered levels of key metabolic and contractile proteins

3.1 Introduction

X-linked Duchenne muscular dystrophy represents the most commonly inherited neuromuscular disease. Although primarily known as a skeletal muscle wasting disease, its progressive degenerative effect on the cardiac muscle is not fully understood. Hence, we decided to carry out a comprehensive proteomic study involving difference in-gel electrophoresis, on the heart, to attempt to identify some biomarkers of this muscle wasting disease.

The identification of the Duchenne muscular dystrophy gene by Koenig and colleagues (1987) lead to the discovery of dystrophin, a membrane cytoskeletal protein. The Dystrophin gene located at Xp21 is the largest gene in the human genome. It covers 2.4 megabases of the X-chromosome and codes for 3585 amino acids. Therefore, it is not surprising that there is a very high mutation rate; with many Duchenne patients suffering from deletions in the gene (Moser, 1984) and point mutations (Den Dunnen et al., 1989).

The 427kDa protein is located at the surface membrane of the muscle cell. Dystrophin forms part of a large supramolecular complex, which provides stability across the membrane and within the cell. In the dystrophic cell the protein is almost completely absent from the cell surface (Bonilla et al., 1988). This absence leads to the phenotype of muscle weakness and fibre wasting. Most symptoms are due to the secondary effects caused by the rupturing of the membrane, alterations in the excitation-contraction coupling and ion leakage (Menke and Jockusch, 1991; Emery, 2002).

3.1.1 Duchenne muscular dystrophy and the heart

Dystrophin is linked to many membrane glycoproteins, making up the dystrophin-glycoprotein complex (DGC). Although the function of all the membrane spanning proteins within the complex are not fully understood, mutations lead to muscular dystrophies, lending weight to how important they are in stabilizing and strengthening the membrane (Campbell, 1995; Lim and Campbell, 1998). The DGC binds other complexes such as calveolin-3 and the integrin complex. These dystrophin-associated complexes can recruit proteins and enzymes, facilitate phosphorylation and up-regulate alternative proteins/kinases activating cell signalling and growth and survival pathways (Ahn et al., 1996; Newey et al., 2000; Sotgia et al., 2000).

There are a number of tissue-specific isoforms of dystrophin, leading to varying degrees of severity of tissue damage. Variations of full-length isoforms are found in brain, heart and skeletal muscles (Culligan and Ohlendieck, 2002; Lohan et al., 2005). Unlike skeletal tissue, cardiac tissue does not undergo degenerative-regeneration cycles and the cardiac fibres become replaced by connective and fatty tissue (Leferovich et al., 2001). This is brought about by the loss of dystrophin anchoring extracellular laminin via the DGC to the cytoskeleton. The membrane becomes ruptured by the loss of membrane proteins and calcium channels are used to reinforce the gaps. This leads to an influx of calcium ions into the cytoplasm, which becomes toxic to the cell, triggering stress responses. Along with structural integrity being lost there are the secondary effects of destruction and abnormal calcium handling. Excitation-contraction coupling in the heart also takes place at the transverse tubules. Therefore physical stresses along this region of the membrane in dystrophic myofibrils may exacerbate the cardiac muscular dystrophic phenotype (Knudson et al., 1988).

Duchenne muscular dystrophy is primarily a skeletal muscle disorder and better treatment of the limb and respiratory systems has extended the life expectancy of sufferers. Cardiac involvement in muscular dystrophies is now becoming significant whereby nearly 20% of DMD and 50% of the milder form Becker muscular dystrophy patients are dying from cardiomyopathy by their third decade (Finsterer and

Stollberger, 2003). In this study, we are using the established animal model of the X-linked muscular dystrophy (MDX) mouse. Although missing the Dp427 protein dystrophin, it is argued that the MDX mouse does not match the DMD phenotype entirely in relation to cardiomyopathies (Bridges, 1986). DMD patients display left ventricular (LV) wall abnormalities and lose LV contractile force, whereas many studies show mice displaying this hypokinesia throughout the heart muscle. In addition, DMD hearts show patchy fibrosis and fatty replacement affecting the LV most, whereas the MDX mouse appears not to be affected quite so severely. In saying that, aged studies of MDX mice at 9-10 months have shown comparable dystrophic cardiomyopathies to DMD patients (Quinlan et al., 2004; Spurney et al., 2008). Mice missing cardiac dystrophin begin with normal heart functions but then develop tachycardia, impaired contractile properties increase in fibrosis, infiltration of fatty tissue and necrosis (Bridges, 1986; Bia et al., 1999; Quinlan et al., 2004). Based on these findings we have used a 9-month-old animal to test the proteomic alterations of the diseased heart.

3.1.2 Proteomics and the heart

A useful tool within proteomics is the availability of mass spectrometry (MS) to identify proteins of interest. Mass spectrometry can be used to identify biomarkers of a comparative biomedical study. Identification of markers characterized from diseased versus normal animal study is useful in enhancing our knowledge of the disease pathways and progression. Coupled with fluorescent dyes, the number of identifiable spots from two-dimensional gels has increased so much that fluorescent difference in-gel electrophoresis (DIGE) and mass spectrometry is considered a sensitive and powerful tool. With DIGE being capable of detection down to originally nanogram (Unlu et al., 1997) and now femtomole (fmol) quantities (Viswanathan et al., 2006) mass spectrometry detection has striven to gain its lowest detection level also. The liquid-chromatography electrospray ionization mass spectrometer (LC-MS ESI) used during this study certainly detects down to fmols of protein. The limitation of this is that complex samples are more difficult to detect than purified bovine serum albumin and MS running buffers, protocols and sample digestion all play a role in MS sensitivity.

DMD patient samples show large variation in expressed proteins and large experimental repeats would be needed; therefore inbred genetically homogeneous animal models can be more useful in gaining initial insight into disease pathology. The fact that animal models usually do not represent perfectly the human pathology of diseases adds a limitation to the research. High-throughput proteomic studies means that information can be gained quickly and when combined with genomic and metabolomic data different models can quickly be assessed for matching tissue-specific pathology. Proteomic profiling can examine thousands of samples and give back information on protein and isoforms abundance and post-translational modifications. Recent proteomic data has catalogued the 2D spot pattern of many small animal models and shown how similar the distribution of protein markers are to human fibre proteome (Sanchez et al., 2001; Yan et al., 2001). Similar workflows have then been used to analyze animal tissue to show fibre type shifting (Donoghue et al., 2005) and glycosylation and phosphorylation due to tissue ageing (O'Connell et al., 2007; Gannon et al., 2008). Proteomic changes in the heart have been previously studied using DIGE and MS. Forner and colleagues (2006) showed the differences in mitochondria between heart and skeletal muscle and the proteomic profile of contractile dysfunction in a failing heart was studied with respect to the molecular mechanisms (Phillips et al., 2010). With respect to X linked muscular dystrophy, studies on the MDX skeletal and diaphragm tissues have revealed a number of biomarkers involved in abnormal calcium handling, sarcolemmal integrity, necrosis and stress responses (Culligan et al., 2002; Doran et al., 2006a; Doran et al., 2006b). Dystrophin deficient cardiomyopathy has been investigated by other laboratories using genomic and metabolomic studies, their recent findings showed that there were large perturbations in the energy producing pathways and mitochondria in cardiac tissue and that hormones related to necrosis were up-regulated. In addition, the expression of taurine directly related to the increase seen in utrophin in MDX tissue. Taurine has previously been correlated with muscle regeneration after necrosis. Transcription levels of Nox4, a gene involved in cardiac fibrosis and cell survival were increased five fold in aged MDX mice hearts (Gulston et al., 2008; Spurney et al., 2008). Combining these

studies with a proteomic investigation into the dystrophic heart may give a more detailed knowledge of a primarily genetic disorder that develops a perturbed downstream phenotype.

3.1.3 Experimental design

To gain insight into the changes occurring in the dystrophic myofibres we decided to study crude cardiac muscle. It is hoped that this study may be useful in enhancing knowledge about the molecular mechanisms involved in dystrophic heart and that in the future it could be used to evaluate drugs or novel therapies affect on the heart. This report describes the detailed analysis of DIGE labeled normal and dystrophic cardiac *MDX* tissue. Firstly, their isoelectric point separated the proteins across the ranges of pH 4-7 and pH 6-11. In the second dimension, the proteins were separated based on their molecular mass. The fluorescently tagged proteins were visualized and densitometric measurements determined the expression levels of all spots across all gels. Finally, proteins of interest were digested and identified *via* ESI LC-MS. Changes in the protein regulation were then confirmed by immunoblotting and confocal microscopy.

3.2 Results

DIGE allows the separation of multiple samples within one two-dimensional gel. This reduces the artefacts that can be introduced due to gel-to-gel variation. We have carried out a comparative proteomic study of 9-month old normal versus age-matched MDX mouse heart. The number of mice was kept to a minimum due to the considerable cost of maintaining aged mice and the high cost of the fluorescent dyes. A two-dye set was chosen because the analysis was being carried out on only two sample types and they were inbred mice, so show less genetic variability as opposed to complex human samples where a three dye system would be suggested. The recommendations of Karp and Lilley (2005) were taken into consideration and three biological replicates for each sample type was run. During first separation, isoelectric

focusing was carried out over the 4-7 and 6-11 pH ranges to maximize the separation of cardiac proteins. Figure 3-1 shows the acidic to neutral proteins separated out over a 12% (v/v) SDS-PAGE gel and Figure 3-2 shows the separation of the more basic end of the soluble heart proteins. Shown are the representative two-dimensional gels of the Cy3 labeled normal muscle (Figure 3-1A; Figure 3-2C), Cy3 labeled MDX muscle (Figure 3-1C, Figure 3-2G) and the corresponding Cy5 labeled pooled standards (Figure 3-1B;D; Figure 3-2F,G), which were scanned on a Typhoon Trio variable imager and analysed using Progenesis SameSpots software. Across the entire pH range 2,509 distinct spots were recognized, with 2,048 spots on the pH 4-7 gels and 487 spots detected on the pH 6-11 range. 79 spots showed a drastic differential expression pattern, with 3 proteins being increased and 26 distinct proteins being decreased. Electrospray ionization mass spectrometry analysis was carried out to identify the cardiac proteins with changes abundance in dystrophic heart tissue.

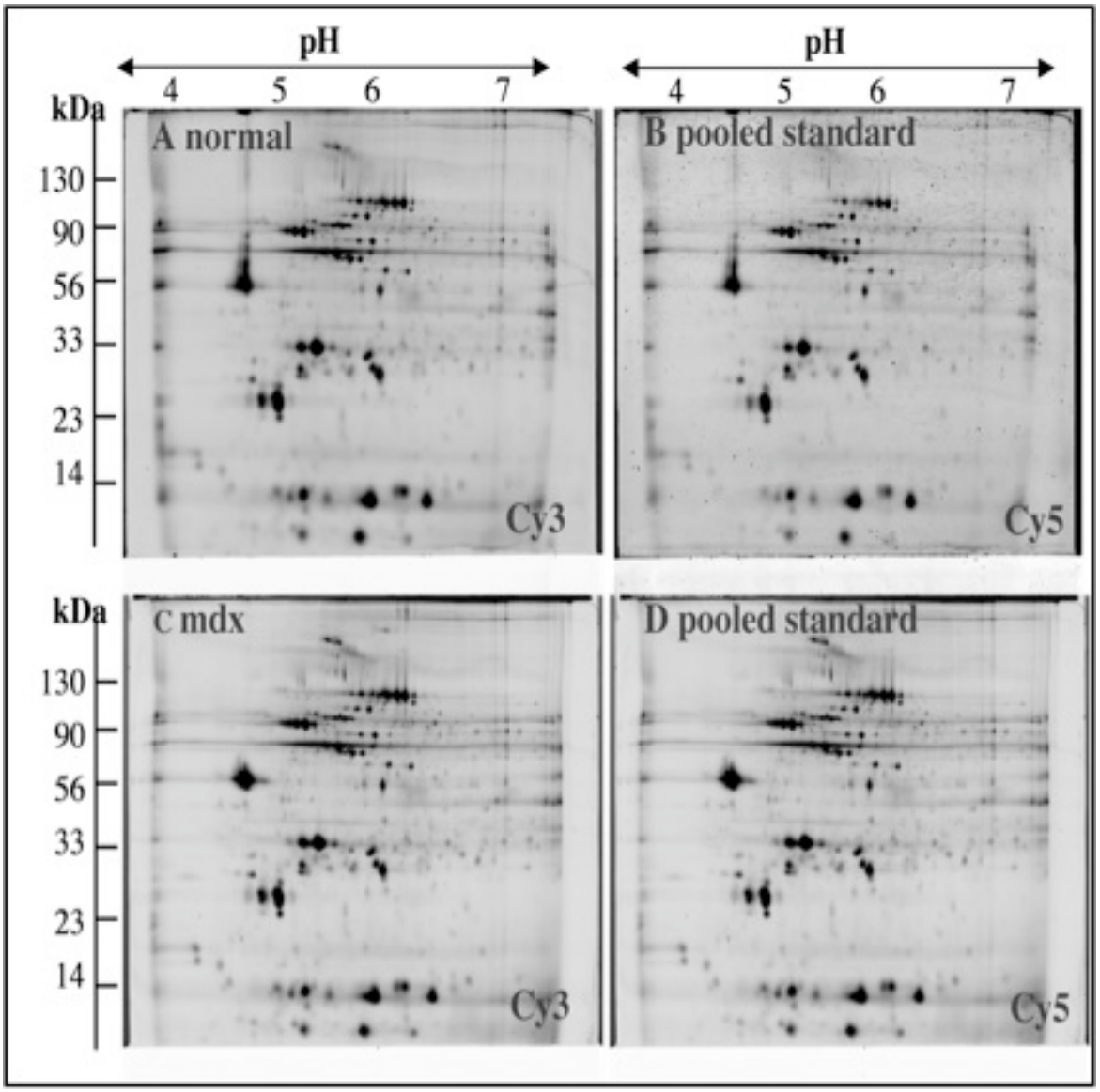

Figure 3-1 2-D DIGE analytical gel of normal versus MDX cardiac muscle in the pH 4-7 range.

Shown are Cy3-labeled gels of the soluble fraction of crude normal (A) and dystrophic MDX (C) cardiac muscle as well as Cy5-labeled gels containing all samples combined to form a pooled standard (B, D). Representative fluorescent DIGE gels with electrophoretically separated proteins are shown for the pH 4-7 range. The pH-values of the first dimension gel system and molecular mass standards (in kDa) of the second dimension are indicated on the top and the left of the panels, respectively.

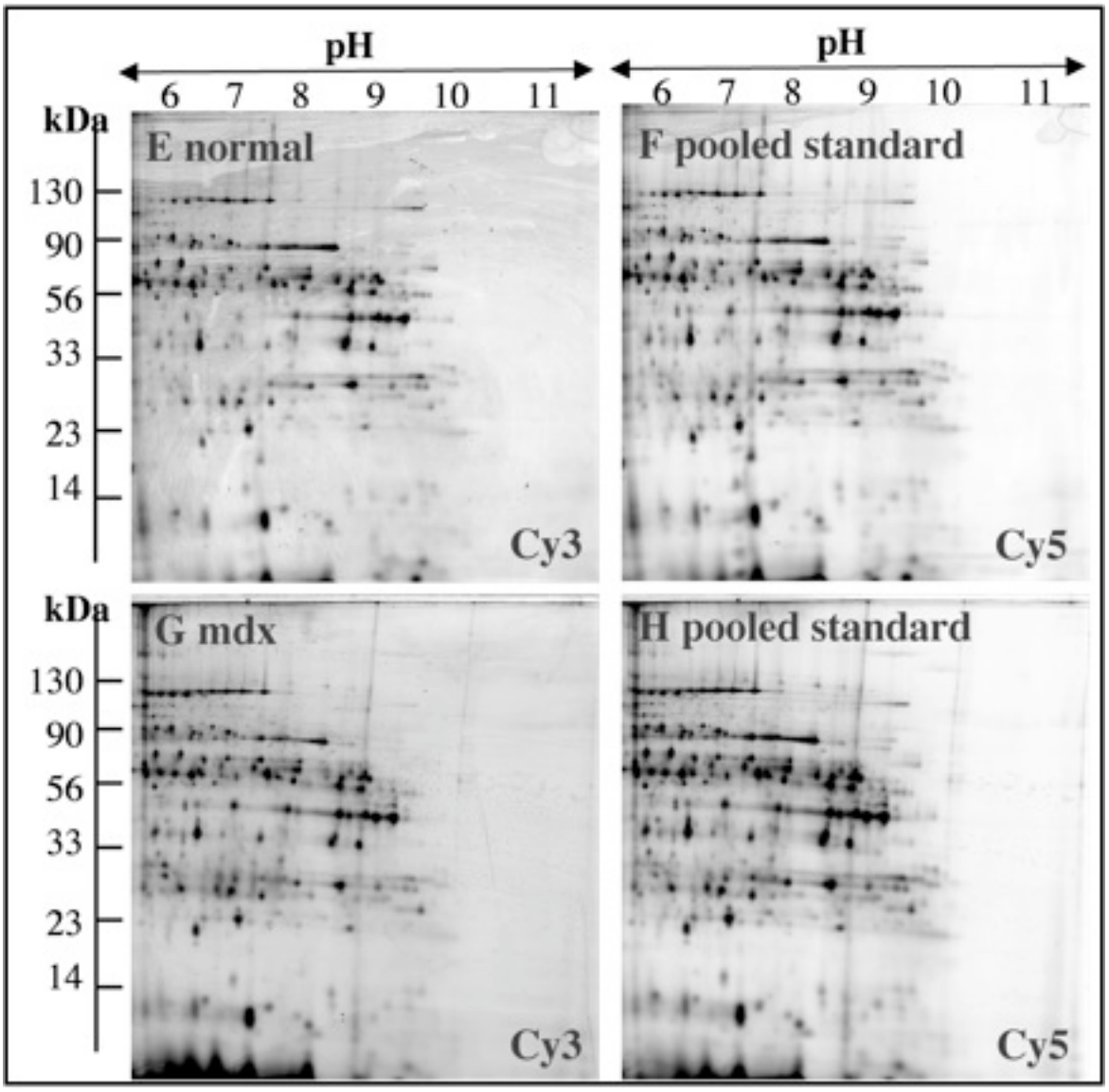

Figure 3-2 2-D DIGE analytical gel of normal versus MDX cardiac muscle in the pH 6-11 range.

Shown are Cy3 labeled gels of the soluble fraction of crude normal (A) and dystrophic MDX (C) cardiac muscle as well as Cy5 labeled gels containing the pooled standards (B,D). Representative fluorescent DIGE gels with electrophoretically separated proteins are shown for the pH 6-11 range. The pH-values of the first dimension gel system and molecular mass standards (in kDa) of the second dimension are indicated on the top and the left of the panels, respectively.

3.2.1 DIGE analysis of the dystrophin-deficient heart

A list of the cardiac proteins with significantly altered expression level in the dystrophic MDX tissue is shown in Table 3-1. The information on the 79 DIGE identified protein spots combines data from both the pH 4-7 and pH 6-11 separations and contains protein name, protein ID, number of matched peptides, percentage sequence coverage, the relative molecular mass, p*I* values and Mascot score and fold change of individual proteins affected by deficiency in dystrophin. The majority of identified cardiac proteins belonged to the main classes of metabolic or contractile proteins. Components of the actomyosin apparatus, enzymatic and regulatory elements of mitochondria, glycolytic enzymes, metabolic transporters, cellular stress proteins and cytoskeletal components were clearly identified by MS analysis. Cardiac proteins with a dystrophy-related change in abundance ranged in molecular mass from apparent 14 kDa to 90 kDa and covered a p*I* range from approximately 5 to 9. DIGE Cy5 master gels of both the pH 4-7 and pH 6-11 range are shown in Figure 3-3 so that it is possible to correlate MS identified protein species, listed in Table 3-1, with distinct two-dimensional spots of altered density in the dystrophic heart. An increased expression level was shown for 3 cardiac proteins. These are listed as nucleoside diphosphate kinase B (spot 1), the nuclear lamina matrix protein lamin A/C (spot 2) and a component of the electron-transferring flavoprotein dehydrogenase (spot 3). All other identified protein species exhibit decreased abundance in dystrophic-deficient myocardial tissue. These cardiac proteins are marked and numbered 4 to 79 in the Cy5 labeled master gels of Figure 3-3. The protein species with the highest decrease in concentration was identified as the anti-oxidant enzyme peroxiredoxin-6 (spot 79). In addition, mitochondrial ATP synthase (spots 50,55, 69, 72, 74, 77), isocitrate dehydrogenase (spots 38, 42), NADH dehydrogenase (spot 40), pyruvate dehydrogenase (spots 11, 14, 15, 20, 25, 34), isoveryl-CoA dehydrogenase (spots 8 and 19), oxoglutarate dehydrogenase (spot 7), prohibitin (spot 6), electron-transferring flavoprotein (spot 5, 17, 36), myozenin-2 (spot 4), voltage-dependent anion-selective

channel VDAC1 (spot 41), the slow/cardiac isoforms of myosin light chain MLC2 (spots 26, 48, 62, 65, 70, 78), myosin light chain MLC3 (spots 53, 61, 76), cardiac alpha-actin (spots 21, 39, 45, 46, 56, 60, 64, 66, 67, 71, 75), alpha-1 tropomyosin (spots 35, 59), adenylate kinase AK1 (spot 68), creatine kinase (spot 16), cytochrome c oxidase (spots 22, 51), cytochrome b-c complex (spots 10, 30, 57, 63), desmin (spots 43, 47, 52, 54, 58), vimentin (spots 12, 23), cardiac fatty acid binding-protein FABP3 (spots 27, 33, 49), heat shock protein Hsp27 (spot 18), heat shock protein Hsp60 (spots 31, 37, 44), enolase (spots 13, 28, 32), DJ-1 protein (spot 27), valosin-containing protein VCP (spot 24) and albumin (spot 9) were identified. The results for 2 additional decreased protein spots have not been included in Table 3-1, since they only contained 1 matched peptide per cardiac protein as determined by MS analysis. The peptide sequences LGANSLLDLVVFGR (2% sequence coverage) and LTFDSSFSPNTGK (4% sequence coverage) identified the non-listed cardiac proteins as succinate dehydrogenase (73.6 kDa; p*I* 7.1) and porin isoforms VDAC1 (32.5 kDa; p*I* 8.6), respectively.

Table 3-1 List of the DIGE-identified proteins with a changed abundance in 9-month old dystrophic MDX heart muscle

Spot No.	Protein	Protein ID	Fold change	Peptides matched	Coverage (%)	Molecular mass (kDa)	Isoelectric point (p*I*)	*Mascot score
1	Nucleoside diphosphate kinase B	NDKB_MOUSE	4.4	4	34	17.5	7.0	69
2	Lamin-A/C	LMNA_MOUSE	1.9	4	6	74.5	6.5	111
3	Electron transfer flavoprotein-ubiquinone oxidoreductase, mitochondrial	ETFD_MOUSE	1.8	8	15	68.9	7.3	45
4	Myozenin-2	MYOZ2_MOUSE	-1.5	4	20	29.8	8.5	145
5	Electron transfer flavoprotein subunit alpha, mitochondrial	ETFA_MOUSE	-1.5	2	12	35.3	8.6	89
6	Prohibitin	PHB_MOUSE	-1.5	8	41	29.9	5.6	290
7	Dihydrolipoyllysine-residue succinyltransferase component of 2-oxoglutarate dehydrogenase complex, mitochondrial	ODO2_MOUSE	-1.6	3	6	49.3	9.1	86

8	Isovaleryl-CoA dehydrogenase, mitochondrial	IVD_MOUSE	-1.7	7	23	46.7	8.5	89
9	Serum albumin	ALBU_MOUSE	-1.7	3	5	70.7	5.8	82
10	Cytochrome b-c1 complex subunit Rieske, mitochondrial	UCRI_MOUSE	-1.8	4	13	29.6	8.9	84
11	Dihydrolipoyllysine-residue acetyltransferase component of pyruvate dehydrogenase complex, mitochondrial	ODP2_MOUSE	-1.9	10	20	68.5	8.8	117
12	Vimentin	VIME_MOUSE	-1.9	11	20	53.7	5.1	118
13	Beta-enolase	ENOB_MOUSE	-2.0	8	19	47.3	6.7	111
14	Pyruvate dehydrogenase E1 component subunit beta, mitochondrial	ODPB_MOUSE	-2.0	8	31	39.3	6.4	279
15	Pyruvate dehydrogenase E1 component subunit beta, mitochondrial	ODPB_MOUSE	-2.0	3	19	39.3	6.4	134
16	Creatine kinase M-type	KCRM_MOUSE	-2.0	2	4	43.3	6.6	47
17	Delta(3,5)-Delta(2,4)-dienoyl-CoA isomerase, mitochondrial	ECH1_MOUSE	-2.0	4	24	36.4	7.6	201

18	Heat shock protein beta-1 Hsp27	HSPB1_MOUSE	-2.0	2	8	23.1	6.1	50
19	Isovaleryl-CoA dehydrogenase, mitochondrial	IVD_MOUSE	-2.0	7	17	46.7	8.5	98
20	Pyruvate dehydrogenase protein X component, mitochondrial	ODPX_MOUSE	-2.1	5	11	54.3	7.6	63
21	Actin, alpha cardiac muscle 1	ACTC_MOUSE	-2.1	6	19	42.3	5.2	104
22	Cytochrome c oxidase subunit 5B, mitochondrial	COX5A_MOUSE	-2.1	2	14	14.1	8.7	52
23	Vimentin	VIME_MOUSE	-2.1	13	27	53.7	5.1	122
24	Transitional endoplasmic reticulum ATPase (valsolin-containing protein)	TERA_MOUSE	-2.2	5	10	90.0	5.1	171
25	Pyruvate dehydrogenase E1 component subunit beta, mitochondrial	ODPB_MOUSE	-2.3	4	14	39.3	6.4	100
26	Myosin regulatory light chain 2, ventricular/cardiac muscle isoform	MLRV_MOUSE	-2.3	9	52	18.9	4.9	209
27	Fatty acid-binding protein, heart	FABPH_MOUSE	-2.3	5	37	14.8	6.1	149
28	Alpha-enolase	ENOA_MOUSE	-2.3	2	3	47.5	6.4	43

29	Protein DJ-1	PARK7_MOUSE	-2.3	4	26	20.2	6.3	90
30	Cytochrome b-c1 complex subunit 1, mitochondrial	QCR1_MOUSE	-2.3	6	17	53.4	5.8	83
31	60 kDa heat shock protein, mitochondrial	CH60_MOUSE	-2.4	2	6	61.1	5.9	63
32	Beta-enolase	ENOB_MOUSE	-2.4	3	7	47.3	6.7	92
33	Fatty acid-binding protein, heart	FABPH_MOUSE	-2.4	7	52	14.8	6.1	162
34	Pyruvate dehydrogenase protein X component, mitochondrial	ODPX_MOUSE	-2.4	2	4	54.3	7.6	66
35	Tropomyosin alpha-1 chain	TPM1_MOUSE	-2.5	15	43	32.7	4.7	302
36	Electron transfer flavoprotein subunit alpha, mitochondrial	ETFA_MOUSE	-2.5	8	33	35.3	8.6	235
37	60 kDa heat shock protein, mitochondrial	CH60_MOUSE	-2.5	12	32	61.1	5.9	346
38	Isocitrate dehydrogenase [NAD] subunit alpha, mitochondrial	IDH3A_MOUSE	-2.5	9	29	40.1	6.3	164
39	Actin, alpha cardiac muscle 1	ACTC_MOUSE	-2.6	12	31	42.3	5.2	317

40	NADH dehydrogenase [ubiquinone] flavoprotein 2, mitochondrial	NDUV2_MOUSE	-2.6	6	29	27.6	7.0	370
41	Voltage-dependent anion-selective channel protein 1	VDAC1_MOUSE	-2.6	10	29	32.5	8.6	292
42	Isocitrate dehydrogenase [NAD] subunit alpha, mitochondrial	IDH3A_MOUSE	-2.6	13	39	40.1	6.3	376
43	Desmin	DESM_MOUSE	-2.6	30	50	53.5	5.2	1184
44	60 kDa heat shock protein, mitochondrial	CH60_MOUSE	-2.7	25	38	61.1	5.9	842
45	Actin, alpha cardiac muscle 1	ACTC_MOUSE	-2.8	10	26	42.3	5.2	276
46	Actin, alpha cardiac muscle 1	ACTC_MOUSE	-2.8	4	14	42.3	5.2	88
47	Desmin	DESM_MOUSE	-2.8	15	37	53.5	5.2	349
48	Myosin regulatory light chain 2, atrial isoform	MLRA_MOUSE	-2.8	9	57	19.6	4.8	299
49	Fatty acid-binding protein, heart	FABPH_MOUSE	-2.9	12	61	14.8	6.1	425

50	ATP synthase subunit beta, mitochondrial	ATPB_MOUSE	-2.9	18	40	56.3	5.2	1093
51	Cytochrome c oxidase subunit 5A, mitochondrial	COX5A_MOUSE	-2.9	7	28	16.3	6.1	286
52	Desmin	DESM_MOUSE	-2.9	26	62	53.5	5.2	1657
53	Myosin light chain 3	MYL3_MOUSE	-2.9	6	41	22.5	5.0	90
54	Desmin	DESM_MOUSE	-3.0	12	30	53.5	5.2	431
55	ATP synthase subunit d, mitochondrial	ATP5H_MOUSE	-3.0	3	21	18.8	5.5	48
56	Actin, alpha cardiac muscle 1	ACTC_MOUSE	-3.1	16	40	42.3	5.2	598
57	Cytochrome b-c1 complex subunit 1, mitochondrial	QCR1_MOUSE	-3.1	12	27	53.4	5.8	330
58	Desmin	DESM_MOUSE	-3.1	36	68	53.5	5.2	1289
59	Tropomyosin alpha-1 chain	TPM1_MOUSE	-3.1	21	46	32.7	4.7	605
60	Actin, alpha cardiac muscle 1	ACTC_MOUSE	-3.2	18	59	42.3	5.2	450

61	Myosin light chain 3	MYL3_MOUSE	-3.3	11	63	22.5	5.0	231
62	Myosin regulatory light chain 2, ventricular/cardiac muscle isoform	MLRV_MOUSE	-3.4	13	73	18.9	4.9	118
63	Cytochrome b-c1 complex subunit 1	QCR1_MOUSE	-3.4	12	31	53.4	5.8	342
64	Actin, alpha cardiac muscle 1	ACTC_MOUSE	-3.5	7	36	42.3	5.2	160
65	Myosin regulatory light chain 2, ventricular/cardiac muscle isoform	MLRV_MOUSE	-3.5	7	46	18.9	4.9	354
66	Actin, alpha cardiac muscle 1	ACTC_MOUSE	-3.6	4	24	42.3	5.2	91
67	Actin, alpha cardiac muscle 1	ACTC_MOUSE	-3.7	17	62	42.3	5.2	294
68	Adenylate kinase isoenzyme 1	KAD1_MOUSE	-3.8	5	31	21.6	5.7	174
69	ATP synthase subunit beta, mitochondrial	ATPB_MOUSE	-3.8	4	21	56.3	5.2	92
70	Myosin regulatory light chain 2	MLRA_MOUSE	-3.9	6	47	19.6	4.8	168
71	Actin, alpha cardiac muscle 1	ACTC_MOUSE	-3.9	18	61	42.3	5.2	302

72	ATP synthase subunit d, mitochondrial	ATP5H_MOUSE	-3.9	5	36	18.8	5.5	69
73	ATP synthase subunit beta, mitochondrial	ATPB_MOUSE	-3.9	18	51	56.3	5.2	640
74	ATP synthase subunit beta, mitochondrial	ATPB_MOUSE	-3.9	25	71	56.3	5.2	1102
75	Actin, alpha cardiac muscle 1	ACTC_MOUSE	-3.9	6	16	42.3	5.2	119
76	Myosin light chain 3	MYL3_MOUSE	-4.0	6	30	22.5	5.0	99
77	ATP synthase subunit beta, mitochondrial	ATPB_MOUSE	-4.1	24	70	56.3	5.2	871
78	myosin light chain 2, ventricular/cardiac	MLRV_MOUSE	-4.1	11	77	18.9	4.9	206
79	Peroxiredoxin-6	PRDX6_MOUSE	-5.3	3	19	25.0	5.7	102

* The Mascot score has a 95% confidence level if >20

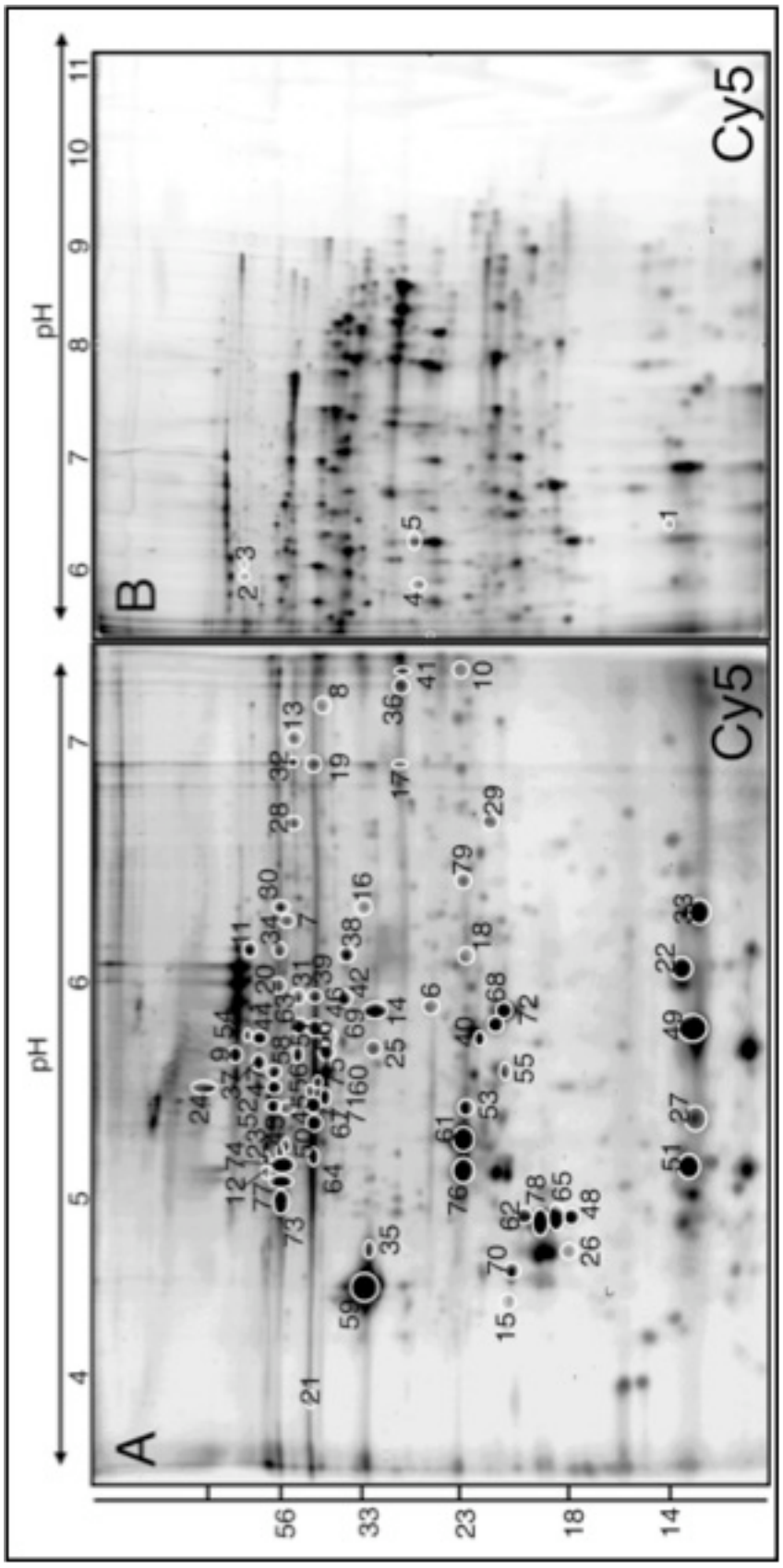

Figure 3-3 DIGE analysis of normal versus dystrophic MDX cardiac muscle

Shown are the pooled sample Cy5-labeled master gels of the soluble fraction from murine heart. The map covers the pH 4-7 (A) and pH 6-11 (B) ranges. Protein spots with significantly changed expression levels are marked by circles and numbered 1 - 79. See Table 3-1 for a detailed listing of the identified cardiac proteins with a change in abundance in the dystrophic phenotypic tissue. The pH-values of the first dimension gel system and molecular mass standards (in kDa) of the second dimension are indicated on the top and the left of the panels, respectively.

3.2.2 Decreased proteins in dystrophic heart muscle

Examples of key cardiac proteins with a significantly decreased expression in dystrophic fibres are shown as enlarged images of DIGE-identified protein spots in Figure 3-4. Minimal labelling allows for direct comparison of fluorescence-labeled 2D protein spots which have been unequivocally identified by mass spectrometric analysis (Table 3-1). Shown are the mitochondrial proteins ATPase synthase, porin isoform VDAC1, isocitrate dehydrogenase, succinate dehydrogenase and prohibitin as well as DJ-1 protein, the stress protein Hsp60 and myosin light chain isoforms MLC2. Figure 3-5 shows additional enlarged images of DIGE-identified proteins of the cytosolic AK1 isoform of adenylate kinase and metabolitic cardiac isoform FABP with corresponding examples of 3D images. A large proportion of the cardiac proteins identified in this study by DIGE analysis belong to the contractile apparatus, the cellular stress response and the cytoskeletal network, as well as mitochondrial metabolism including oxidative phosphorylation, the citric acid cycle and fatty acid transportation.

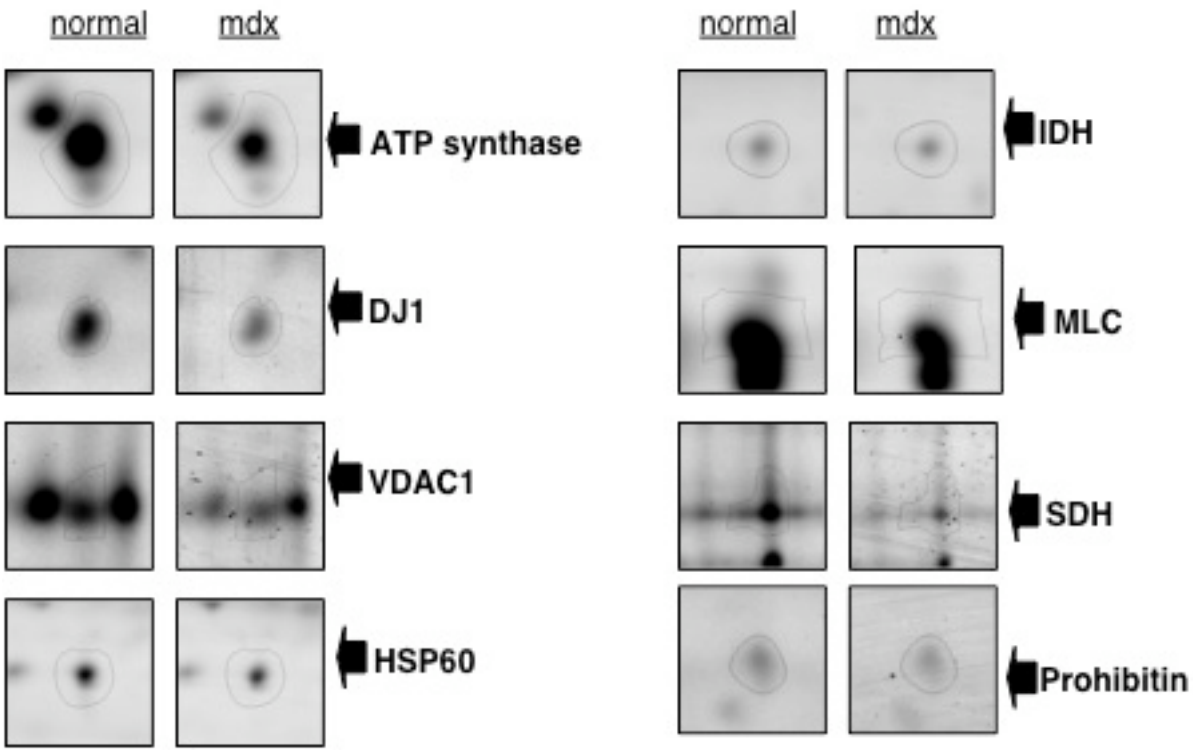

Figure 3-4 Decreased expression of key proteins in the dystrophic-deficient MDX heart

Shown are expanded views of 2D gels of normal versus dystrophic MDX heart tissue. Shown are ATP synthase, DJ-1 protein, porin isoform VDAC1, stress protein Hsp60, isocitrate dehydrogenase (IDH), myosin light chain MLC2, succinate dehydrogenase (SDH) and prohibitin.

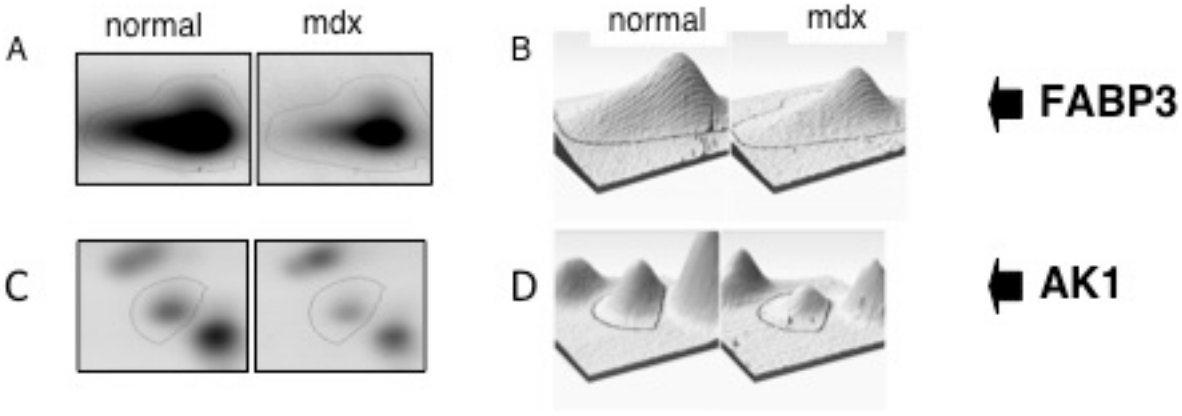

Figure 3-5 Decreased expression of key proteins with 3D comparative images

Shown are the expanded views of 2D gels of normal versus dystrophic MDX heart tissue with matching 3D views of AK1 isoform of adenylate kinase and fatty acid binding protein FABP3.

3.2.3 Immunoblot analysis of dystrophic heart muscle

We employed Western blotting here to verify the results from our DIGE analysis by immunoblotting a selected group of cardiac proteins. At this point, it is important to state that mass spectrometry-based proteomic analysis is of individual 2D spots excised from an SDS-PAGE gel and therefore one can isolate isoforms of a particular protein. 1D immunoblotting or immunohistochemistry may not be capable of separating isoforms due to lack of antibody specifity. Our analysis shows that many isoforms of a particular protein appear in the gel but that not all isoforms may hold the same fate and, as we have found, proteomic findings from biochemical or cell biological analysis of total protein often does not correlate fully with individual 2D spots. Figure 3-6 shows Coomassie stain 1D gel and an equally loaded immunoblot of laminin of crude preparations from normal and dystrophic heart tissue and it illustrates that no major differences exist in the overall protein expression levels between the two different phenotypes. Figure 3-7 shows immunoblot analysis and relates to the combination of all isoforms of cardiac desmin in total crude tissue and is found not to be significantly different. The analysis of mitochondrial marker proteins (Figure 3-8) shows that the majority of the energy production mitochondrial components are drastically down-regulated. This holds for ATP synthase, porin isoform VDAC1, the fatty acid transporter protein cardiac fatty acid binding protein FABP3, isocitrate dehydrogenase IDH and succinate dehydrogenase SDH. Shown in the stress regulatory protein analysis figure (Figure 3-9) are the immuno-decorated bands of antibodies to Hsp60 and DJ1. The statistical analysis shows neither of these proteins to be significantly decreased in expression between normal and dystrophic preparations. Thus the overall isoform population of Hsp60 and DJ1 does not appear to be reduced in dystrophinopathy, although the above-described DIGE analysis showed a lower level of distinct sub-species of these cardiac elements. In general, the immunoblotting results support the main findings from our DIGE analysis of normal versus dystrophic heart tissue and demonstrate independently that the deficiency in dystrophin has a profound effect in the expression pattern of the cardiac protein complement.

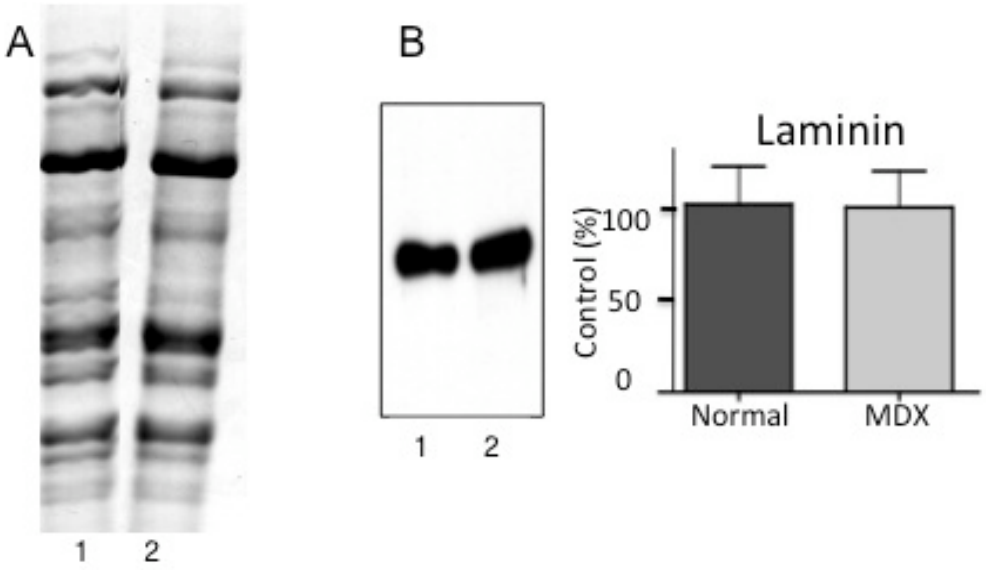

Figure 3-6 Immunoblotting survey of equally loaded cardiac tissue

Shown is a Coomassie-stained gel (A) of normal and MDX tissue showing equal loading and an immunoblot of Laminin (B) an unchanged protein in dystrophic myofibres shown not to be significantly between normal and dystrophic preparations. The comparative blotting was statistically evaluated using as unpaired Student's *t*-test (n=3 replicates). Error bars represent standard deviation. Lanes 1 and 2 represent normal and dystrophic muscle extracts from control and MDX mice, respectively.

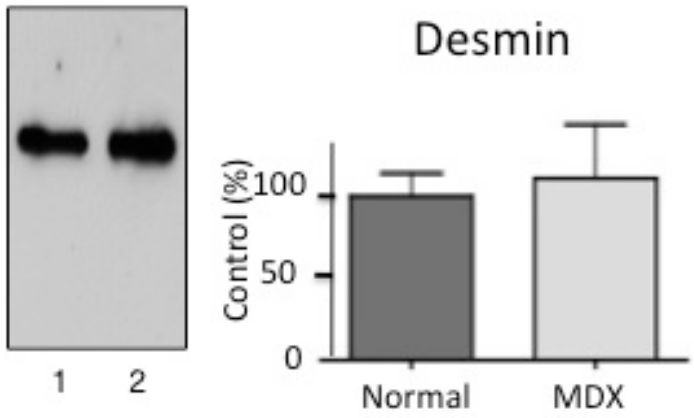

Figure 3-7 Immunoblot analysis of filament protein

Shown is the cytoskeletal marked protein desmin from crude total extract of normal and MDX tissue with graphical presentation of the statistical evaluation. The expression of desmin was found not to be significantly different between normal and dystrophic preparations. The comparative blotting was statistically evaluated using as unpaired Student's *t*-test (n=3 replicates). Error bars represent standard deviation. Lanes 1 and 2 represent normal and dystrophic muscle extracts from control and MDX mice, respectively.

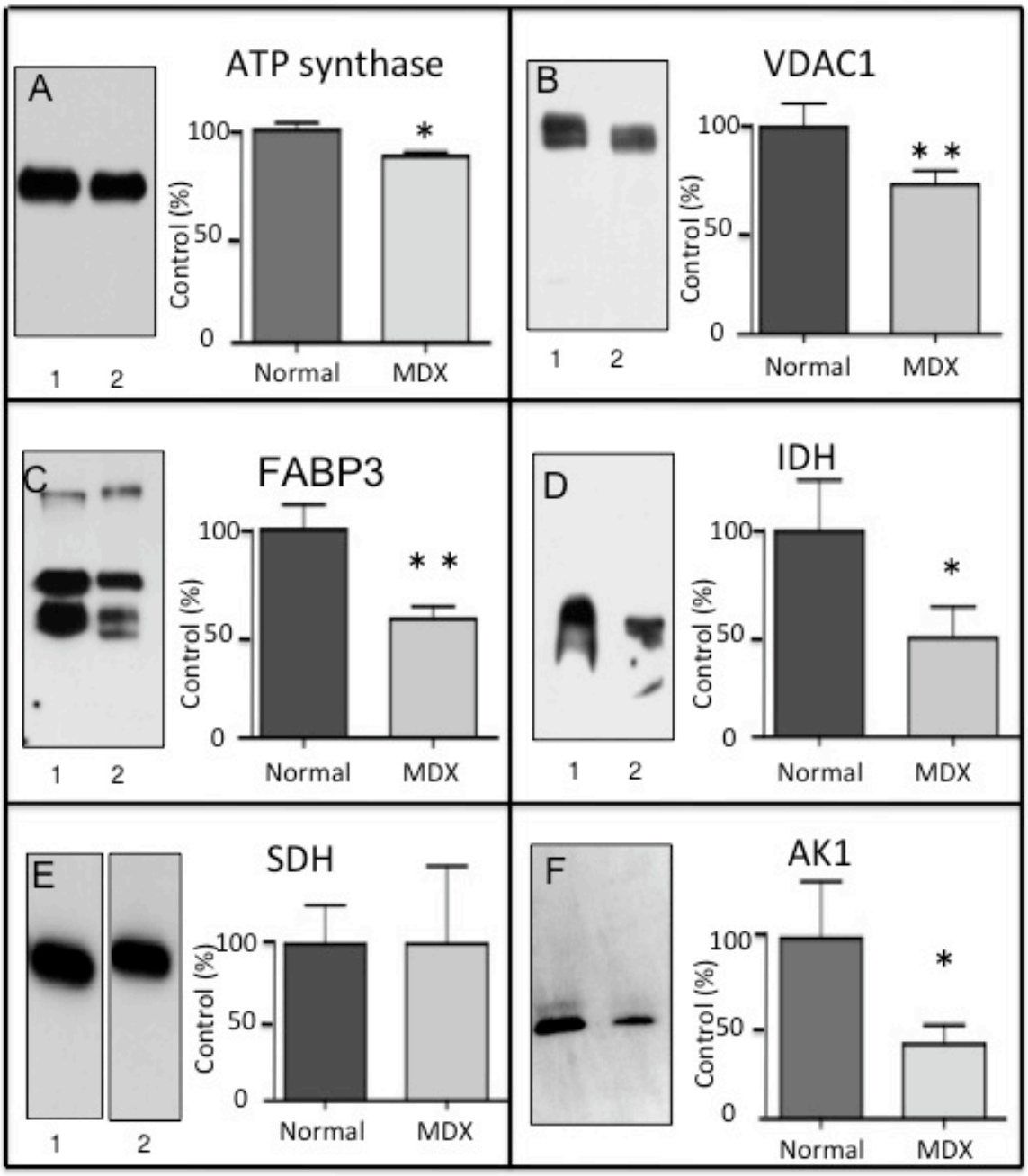

Figure 3-8 Immunoblotting survey of cardiac mitochondrial proteins in dystrophic tissue

Shown are the immunoblots with graphical presentation of the statistical evaluation of immuno-decoration using antibodies to ATP synthase (A), porin isoform VDAC1 (B), fatty acid binding protein FABP3 cardiac isoform (C), isocitrate dehydrogenase IDH (D), succinate dehydrogenase SDH (E) and adenylate kinase AK1 (F). The comparative blotting was statistically evaluated using as unpaired Student's *t*-test ($n=3$; $^{*}p<0.05$, $^{**}p<0.01$). Error bars represent standard deviation. The concentration of succinate dehydrogenase was found not to significantly different between normal and dystrophic preparations. Lanes 1 and 2 represent normal and dystrophic muscle extracts from control and MDX mice, respectively.

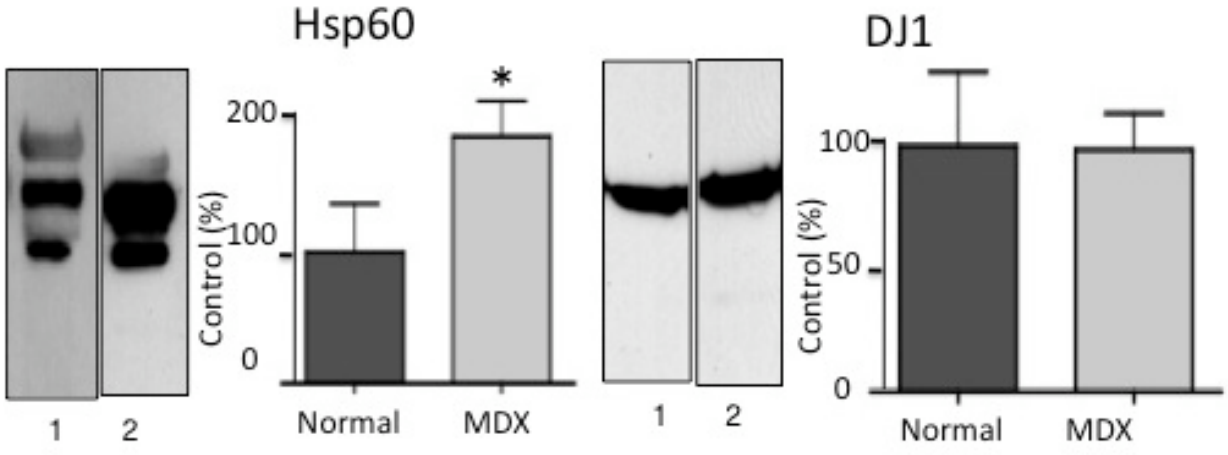

Figure 3-9 Immunoblot analysis of cardiac stress regulatory proteins

Shown are the immuno-decorated bands of altered expression stress regulation proteins in dystrophin-deficient myofibres. The comparative blotting was statistically evaluated using an unpaired Student's *t*-test (n=3; *$p<0.05$). Error bars represent standard deviation. Lanes 1 and 2 represent normal and dystrophic muscle extracts from control and MDX mice, respectively. The concentration of crude total cardiac Hsp60 and DJ1 was found to have opposite fate to the DIGE analysis, where a number of isoforms of both proteins shown were down-regulated.

3.2.4 Immunofluorescence microscopy analysis of dystrophic heart muscle

Since the DIGE analysis of the normal versus the dystrophic MDX heart has revealed changes in a variety of mitochondrial components, it was important to determine whether this alteration was due to a reduction in the number of mitochondria. Figure 3-10 shows representative results from a mitochondrial stain marker, a zoom view with nuclei and survey of nuclei number. DAPI staining revealed 229±6 and 270±18 nuclei per examined tissue section in normal versus dystrophic sections, respectively (Figure 3-10E,F). The slight increase in MDX preparations was not statistically significant (n=4). Thus, the proteomic finding of a dystrophic-dependent increase in lamin-A/C is therefore not directly related to a drastic change in the number of nuclei per cardiac tissue unit. Fluorescent labelling of mitochondria with the MitoTracker dye CMXRos showed a characteristic internal staining pattern in cardiac fibres (Figure 3-10A-D). The intensity values of fluorescing mitochondrial bundles measured at 1470±36 and 1384±40 for normal versus MDX preparations and were found not to be significantly different (n=4). Hence, lower levels of mitochondrial enzymes do not seem to be a consequence of a drastic decrease in mitochondrial density in the dystrophic MDX heart. Cryosections of MDX tissue showed a complete absence of the dystrophin isoform Dp427 (Figure 3-11A-D), a down-regulation of the sarcolemmal marker ß-dystroglycan (Figure 3-11E-H) and an unchanged concentration in the slow/cardiac myosin heavy chain (Figure 3-11I-L) protein. In addition, confocal microscopy was employed for the localization of cardiac mitochondrial marker proteins. The immunofluorescence labelling of desmin (Figure 3-12A-D), succinate dehydrogenase (Figure 3-12E-H) and prohibitin (Figure 3-12I-L) appear to be comparable between normal and dystrophic tissue cryosections. The microscopical localization study revealed similar bundling patterns as the mitochondria staining dye but no decrease of these proteins in the dystrophic tissue sections, as found by DIGE analysis. This, like immunoblotting, indicates although distinct sub-species of certain cardiac proteins are affected in linked muscular dystrophy as determined by mass-spectrometry-based

proteomics, the overall isoform complement of these elements is not drastically altered. This indicates that no major differences exist in the expression levels of desmin-containing intermediate filament structures and the population of cardiac mitochondria in normal versus dystrophin-deficient cells.

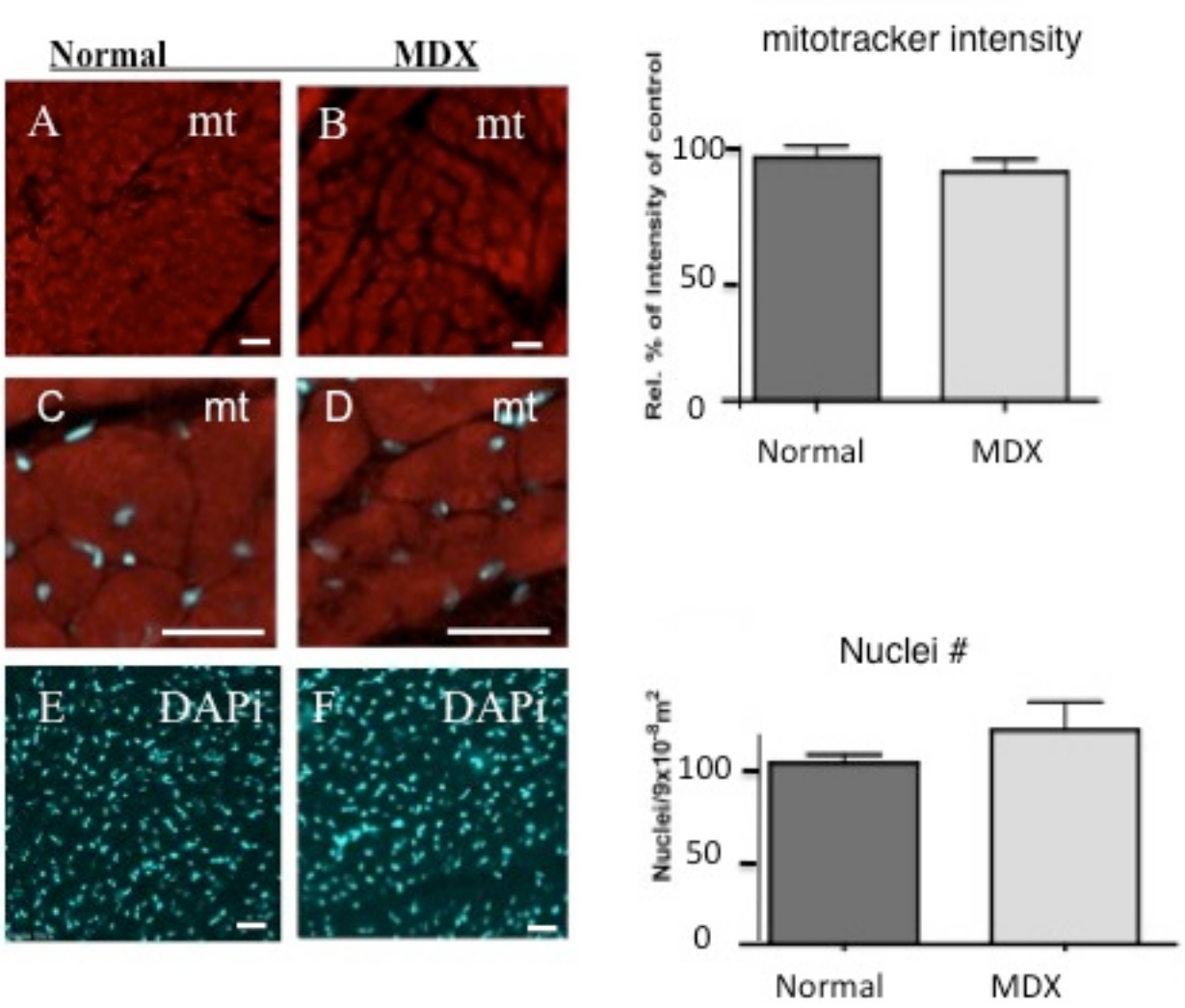

Figure 3-10 Immunofluorescence survey of mitochondrial content and nuclei number in dystrophic cardiac tissue

Confocal microscopy was used for the localization of mitochondria and nuclei in normal (A, C, E) and dystrophic MDX (B, D, F) heart cryosections. Shown is the labelling of nuclei with the DNA binding dye DAPI (E, F) and the visualization of mitochondria with the red-fluorescent MitoTracker dye CMXRos (A, B), with an overlay image of both dyes showing a zoom view of mitochondria and nuclei in selected cells (C, D). Graphical presentation of the statistical evaluation of fluorescence intensity of the mitotracker dye and nuclei number is shown using an unpaired Student's *t*-test (n=4). Bar in panels A to F equals 30μm.

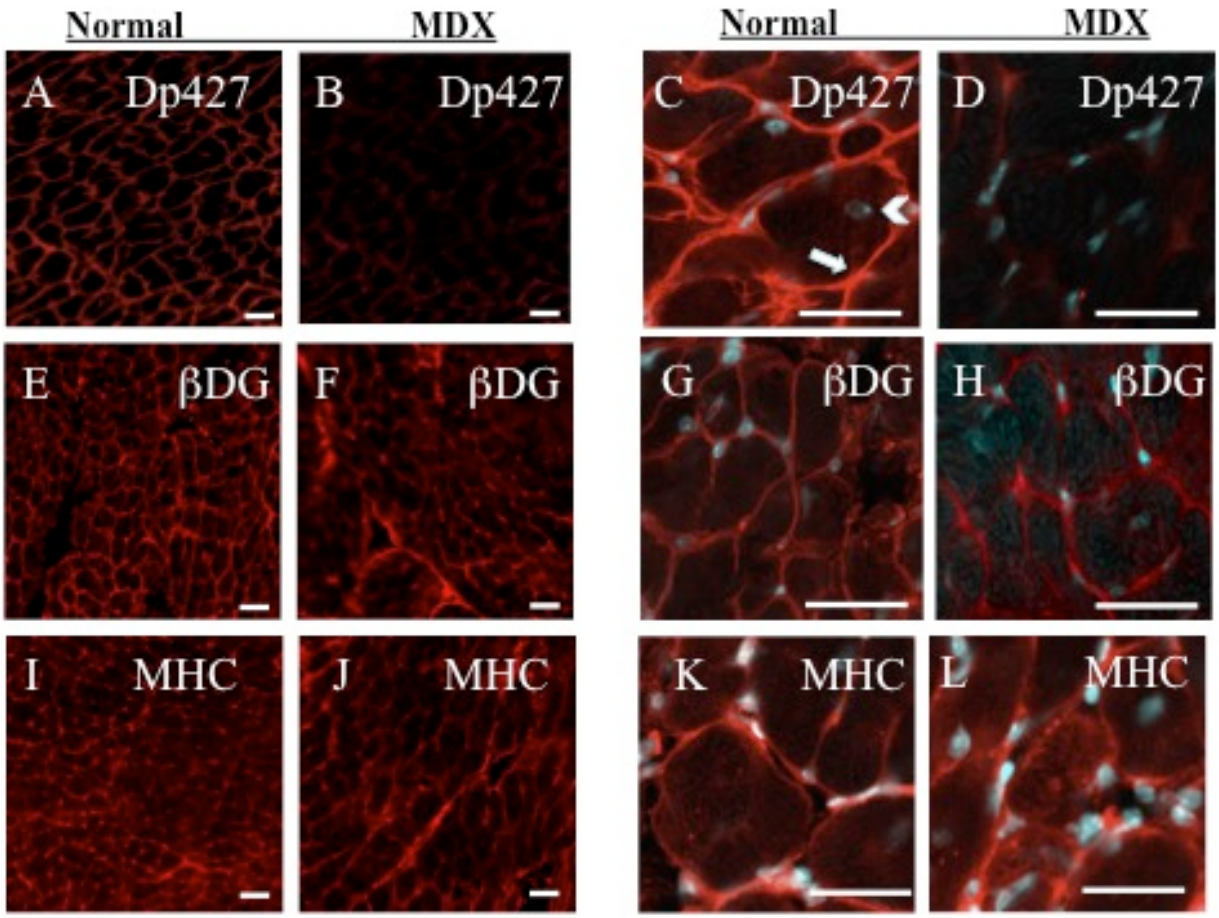

Figure 3-11 Immunofluorescence survey of cardiac marker proteins in dystrophic cardiac tissue

Confocal microscopy was used for the localization of cellular dystrophic markers in normal (A, E, I, C, G, K) and dystrophic (B, F, J, D, H, L) heart cryosections. Shown is labelling with fluorescent antibodies to full-length dystrophin isoform Dp427 (A-D), ß-dystroglycan ßDG (E-H) and myosin heavy chain (MHC) (I-L). White arrowhead marks a nuclei and white arrow marks the cell membrane. Bar in panels A to L equals 30μm

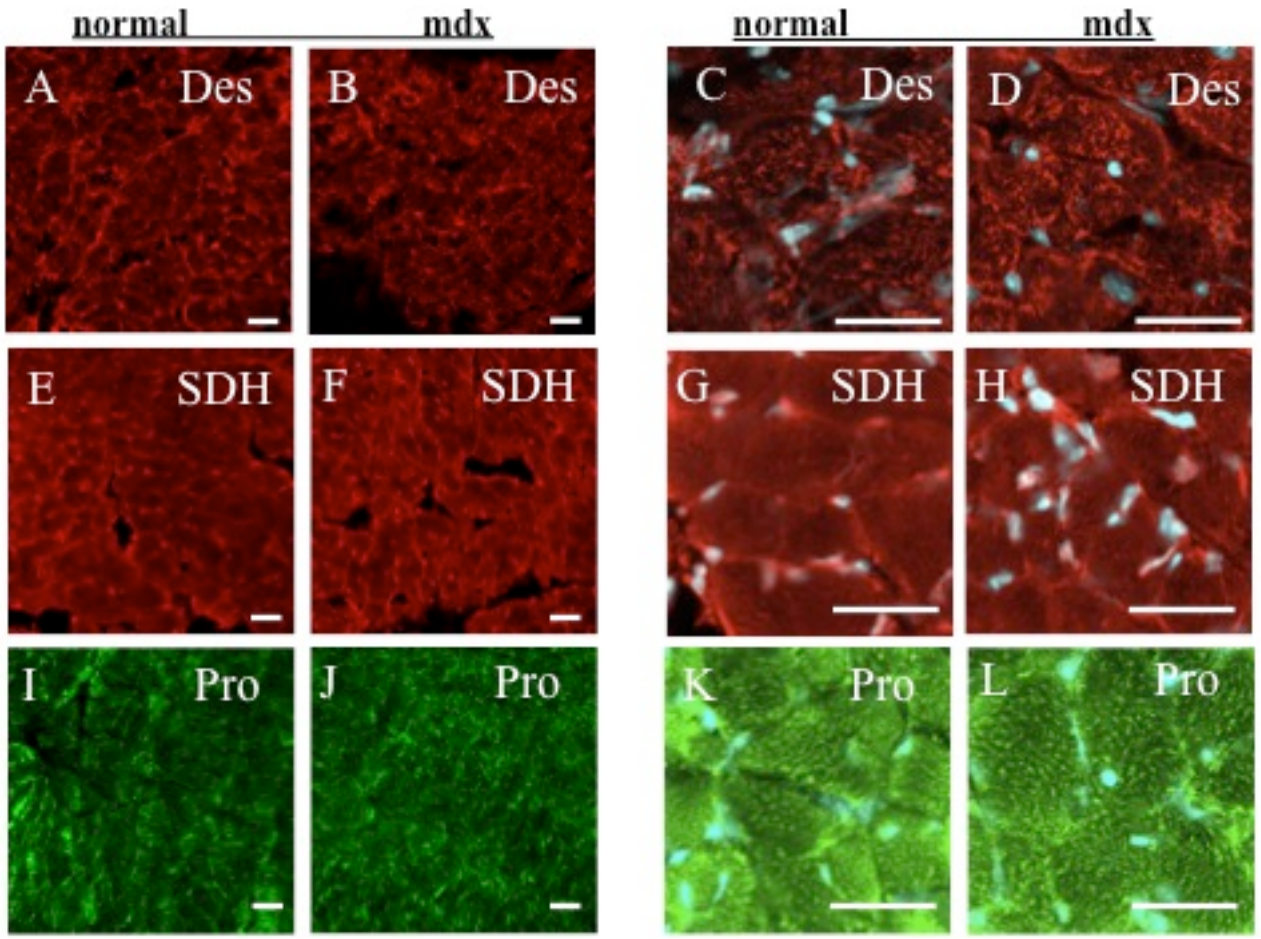

Figure 3-12 Immunofluorescence survey of cardiac mitochondrial marker proteins in dystrophic cardiac tissue

Confocal microscopy was used for the localization of mitochondrial dystrophic markers in normal (A, E, I, C, G, K) and dystrophic (B, F, J, D, H, L) heart cryosections. Shown are labelling of antibodies to full-length dystrophin isoform desmin Des (A-D), succinate dehydrogenase SDH (E-H) and prohibitin Pro (I-L). Bar in panels A to L equals 30μm

3.3 Discussion

Protein expression profiling was used to analyze protein expression of normal and diseased cardiac tissue to elucidate markers of linked muscular dystrophy. We wish to enhance our knowledge of the molecular pathogenesis of cardiomyopathy of the dystrophic heart. Separation, identification and characterization of biomarkers are important for (i) the progress of improved diagnostic methods, (ii) the development of better therapies to address the secondary affects of the loss of dystrophin, and (iii) the evaluation of novel therapeutic methods for the correction of the primary abnormality of cardiac dystrophinopathy (Seow et al., 2000). Proteomic profiling is routinely used to test the effects and side effects of possible drugs, as published recently by Colussi and colleagues (2010) looking for biomarkers of muscle regeneration in an MDX mouse. Other MDX protein expression studies look at the protein profiles of double knockout mice to give additional insight into the compensatory mechanisms involved in dystrophic mice, which furthers our knowledge on possible therapeutic methods (Li et al., 2009). Again, the proteomic profiling of MDX skeletal muscle has recently established altered expression levels of soluble proteins involved in nucleotide metabolism, Ca^{2+}-handling and the cellular stress response (Ge et al., 2003; Doran et al., 2004). Mass spectrometry analysis was subsequently carried out on similar biochemical samples that were subjected to experimental exon skipping therapy. The treatment revealed a partial reversal of dystrophic changes by the change in expression of previously identified biomarkers (Doran et al., 2009), demonstrating the potential of proteomic technologies to decisively enhance the capabilities of biochemical research into the molecular mechanisms that underlie the pathogenesis of diseases. In contrast to skeletal dystrophinopathies, little is known about the molecular pathogenesis that leads to the cardiac complications of the dystrophin-deficient animal. Here, we have successfully applied the fluorescent DIGE method to the large-scale analysis of the dystrophic heart. We divided the experiment into two pH ranges, to obtain enhanced separation, in an attempt to gain further insights into the down-stream

effects of the loss of dystrophin on cardiac tissue. MS-based proteomics clearly revealed a drastic decrease in proteins belonging to the contractile apparatus, the energy production pathways, cellular stress response and cytoskeletal proteins. Figure 3-13 displays the divisions in the functions of the identified proteins of the dystrophic heart as compared to normal muscle.

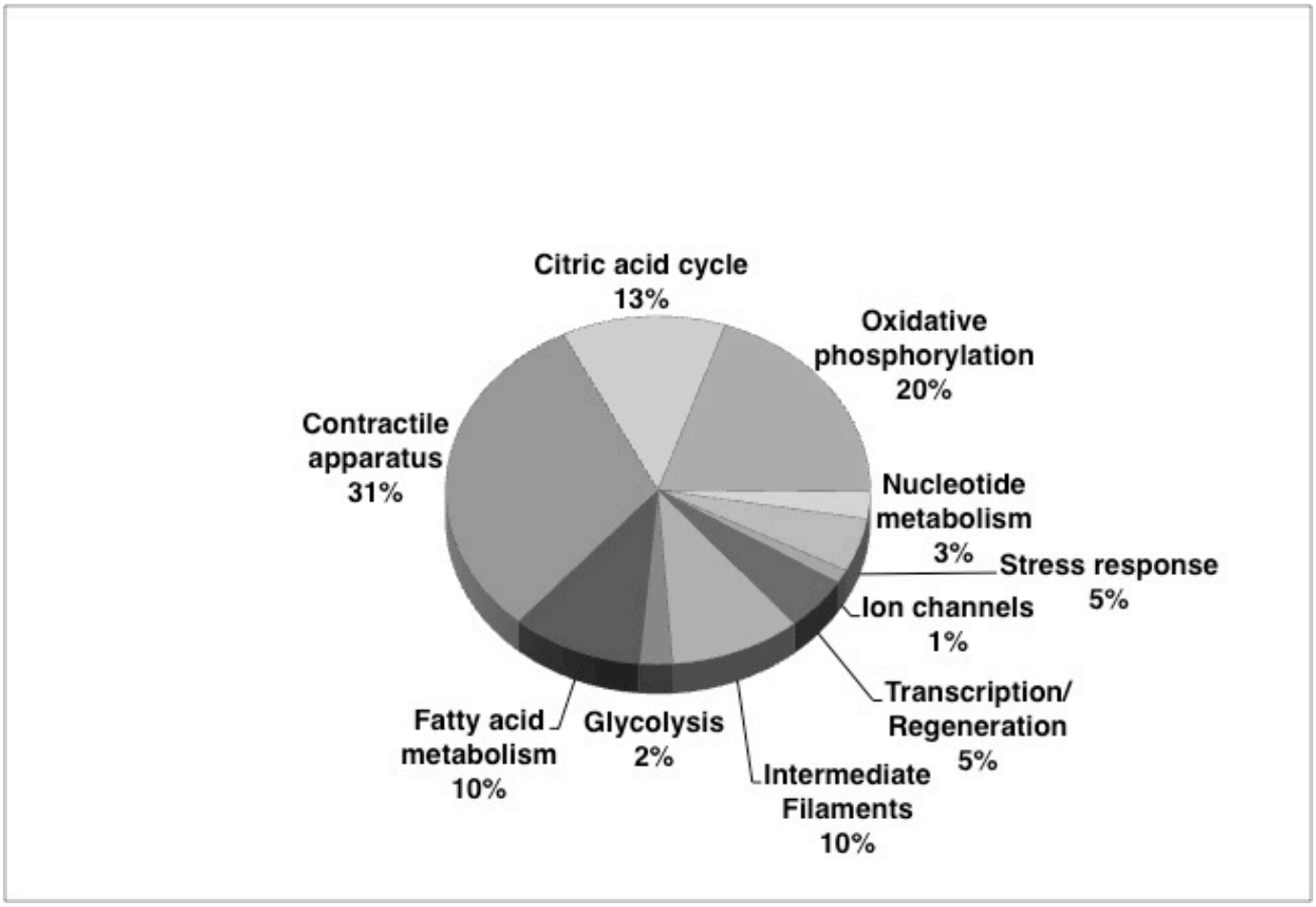

Figure 3-13 Overview of biological functions of DIGE-identified proteins with an altered expression in dystrophic heart muscle

Shown are the apparent functions of DIGE-identified proteins with a significantly different expression in normal versus dystrophic-deficient MDX cardiac tissue. A large portion of these proteins are involved in contraction of the muscle and mitochondrial metabolic proteins including elements of oxidative phosphorylation, the citric acid cycle and fatty acid metabolism.

3.3.1 Drastically increased concentration of proteins by DIGE analysis

The DIGE analysis presented has shown a significant increase in lamin-A/C, a nuclear lamin. This intermediate filamentous protein is a component of the cytoskeleton of the inner nuclear membrane and may provide chromatin stability leading to gene expression in the heart. Comparative DAPI staining of nuclei numbers in normal versus dystrophic heart cryosections indicated no significant increase in nuclei numbers in dystrophin-deficient tissue, therefore, the increase in this lamin protein is due to the disease pathogenesis rather than an increase in nuclei.

The largest increase in concentration of a protein was identified as a 4-fold change in expression of nucleoside diphosphate kinase (NDK) B. Nucleoside diphosphate kinases are regulatory enzymes involved in the transport of phosphate groups and are involved in homeostasis of intracellular di- and tri-phosphonucleosides. Additionally, NDKB has been identified to carry out transcriptional activation and to bind DNA (Kimura et al., 2000). These kinases' functions are implicated in cell growth and proliferation, differentiation and signal transduction, which suggests that this up-regulation may be involved in compensating the severely stressed dystrophin-deficient heart myofibres. Another up-regulated protein was an isoform of the electron transfer flavoprotein dehydrogenase. Other DIGE-identified proteins involved in electron transferring in oxidative phosphorylation and fatty acid metabolism show a decrease in protein expression, showing how complex the molecular mechanisms are in a human disease and shows the importance of using animal models to reveal changes in protein expression. The majority of our protein profiling analysis showed a massive decrease in a diversity of cardiac proteins. Many different cellular pathways and range of functions are affected in dystrophin-deficient heart cells and our analysis is consistent with the severity of cardiomyopathic complications seen in MDX mice and DMD patients (Durbeej and Campbell, 2002; Finsterer and Stollberger, 2003).

3.3.2 Drastically decreased concentration of protein by DIGE analysis

Proteins involved with the cardiac contractile apparatus, oxidative phosphorylation, nucleotide metabolism, transcription, fatty acid transportation and structurally important skeletal proteins were affected by the deficiency of dystrophin in the heart cells. Braun and colleagues (2001) could show that MDX slow-twitch tissues are affected in their ability to transfer energy via the ATPases in the mitochondria. The altered transfer of ATP energy to the mitochondria may contribute to the phenotypic muscle weakness in MDX mice and therefore DMD patients. The disturbance in the energy transfer in dystrophic tissue can lead to oxidative stress in the cells. Our DIGE study identified the largest decrease in expression to be the 6-fold decrease in peroxiredoxin-6, an antioxidative enzyme that protects the cell against oxidative stresses. This drastic decrease may have severe effects on how the cardiac cell counteracts the detrimental stressors. Many other cellular stress response proteins have also found to be decreased in the dystrophic heart tissue, including the small heat shock protein Hsp27 and Hsp60 as well as DJ-1. Small heat shock proteins act as chaperones, helping the cell maintain homeostasis by assisting in protein folding and transporting dysfunctional proteins around the cell and they are up-regulated in the heart following exercise (Boluyt et al., 2006). Mutations in the DJ-1 protein cause neurodegenerative diseases and has been implicated in oxidative stress response and in transcriptional regulation (Chen et al., 2010). An impaired stress response could then lead to a detrimental aggregation of misfolded proteins and oxidative damage occurring within the dystrophic heart cell leading to dysfunction and muscle weakness. The dystrophinopathy-related decrease in endoplasmic reticulum ATPase might impair cardiac function as the valsolin containing protein is involved in several cellular pathways such as membrane fusion and cell-cycle control.

3.3.3 Decreased concentration of cytoskeletal proteins

The DIGE analysis presented here of the MDX heart clearly displays an altered protein expression of many important members of the cytoskeletal network. Dystrophin

is involved in anchoring numerous proteins in and around the membrane. This allows the connection of contractile proteins to the membrane, which provides the force against which the myosin pulls and permits the muscle to contract. In contrast to comparable myosin heavy chain concentrations between normal and dystrophic muscle, other critical contractile proteins are negatively affected by the loss of dystrophin. The thick and thin filaments of the contractile unit are formed from a complex arrangement of myosin. Myosin arrangement is such that two heavy chains form a dimer and two pairs of myosin light chains strengthen the 'lever arm' that pulls against the actin. Mutations in myosin light chains have been implicated in familial hypertrophic cardiomyopathy (Szczesna, 2003). Therefore, the reduction in the ventricular and atrial isoforms of myosin light chain, and cardiac alpha-actin might have a severe impact on the contractile apparatus in the dystrophic heart. Arrhythmias, contractile dysfunction and lower heart rates which are observed in dystrophic cardiac muscle, could be directly related to the altered concentration of myosin light chains and actin (Quinlan et al., 2004). Cardiac cells are activated by calcium binding to tropomyosin, in the thin filament, which alters the conformation of actin, allowing a cross bridge to form. The observed 3-fold decrease in the tropomyosin alpha-1 chain isoform in MDX heart may also be of significant pathophysiological consequence. This alteration in myosin and actin concentrations represents a significant structural change, which may impair function during sliding of the thick and thin filaments, leading to impaired sarcomeric shortening.

3.3.4 Decreased expression level of intermediate filament proteins

A reduction was seen in the DIGE analysis of a number of intermediate filament (IF) proteins. IF proteins are important for the structural integrity of the muscle cell; they help provide elasticity within the contracting fibres. Our proteomic study provided information that a number of isoforms of desmin were reduced in expression, but this was not confirmed by either immunoblotting or confocal microscopy, which showed the overall population of desmin to be unchanged in crude soluble cardiac tissue. However, other IF proteins were shown to be down-regulated between normal and MDX heart

tissue. Myozenin-2 and vimentin appeared to be reduced in MDX cardiac tissue. A mutation of the sarcomeric protein myozenin-2, has shown to cause cardiac hypertrophy and arrhythmias (Osio et al., 2007). Vimentin protein coils around itself to form a sheet-like structure and provides structural stability to nuclei, endoplasmic reticulum and mitochondrial membrane (Herrmann and Aebi, 2004). The abnormal expression levels of these proteins might therefore cause a disrupted interfilament interaction and an impaired cytoskeletal matrix, thereby causing cellular instability in the dystrophic heart.

3.3.5 Decreased concentration of mitochondrial proteins as identified by DIGE analysis

A significant finding as a part of this study was the drastically reduced concentration of numerous mitochondrial proteins and metabolic transporter proteins. Mass spectrometry analysis noted a reduction in many proteins belonging to the oxidative phosphorylation pathway, the citric acid cycle, glycolysis and fatty acid metabolism. As energy production is centred on the massive numbers of mitochondria in the heart, a reduction in these elements will have a profound effect on the bioenergetic status of the dystrophic heart. Many complex processes are involved in production of ATP in the heart. Hydrogen ions are built up outside the mitochondrial membrane, usually donated from pyruvate dehydrogenase and NADH, via glycolysis and the citric acid cycle. The protons then pass through the electron chain transport system and into the mitochondrial membrane spanning enzyme complex ATP synthase. Here oxidative phosphorylation occurs using oxygen to convert ADP into the high-energy protein ATP that accumulates inside the mitochondria (Lemieux and Hoppel, 2009). This energy is then transported throughout the cell including to the contractile filaments and used to power the cross-bridge action that ultimately causes the overlap of the thick and thin filaments and generates sarcomeric shortening. Previous studies of the dystrophic heart have shown that the reduction in intermediate filaments results in a disorganized sarcomere and a lower affinity of the mitochondria to ADP and that the dystrophic heart

displays disturbances of oxidative phosphorylation (Dunn et al., 1993; Dupont-Versteegden et al., 1994). Cardiac mitochondria also regulate signalling pathways by providing surface receptors to the cytosolic proteins and also allow exchange of solutes into the matrix of the mitochondria. Concentrations of cytochrome c found in the mitochondrial intermembrane along with adenylate kinase and creatine kinase enzymes play a role in cell apoptosis (Benz and Brdiczka, 1992). In the dystrophin-deficient heart evidence was provided that creatine kinase coupling to oxidative phosphorylation was impaired (Braun et al., 2001). Altered expression levels of mitochondrial proteins have previously been shown to affect many aspects of normal development, diseases and exacerbate the aging process (O'Connell et al., 2007). The dysfunction has lead to many forms of heart failure including ischemic reperfusion injury (Rouslin, 1983) and dilated cardiomyopathy (Liao et al., 1996). Therefore, a reduced concentration of many mitochondrial proteins associated with the outer and inner membrane, intermembrane and matrix suggests an impaired metabolism in the dystrophic heart. Reduced expression within the mitochondrial proteome appears to affect functioning of ATP synthase, creatine kinase, adenylate kinase, cytochrome b-c complex, ER ATPase, NADH dehydrogenase, oxoglutarate dehydrogenase, pyruvate dehydrogenase, isovaleryl-CoA dehydrogenase, isocitrate dehydrogenase, electron transfer flavoprotein and alpha- and beta-enolase which all show reduced expression levels in our DIGE analysis of the dystrophic heart. This agrees with a previous study by Zhang and colleagues (2008) who reported a perturbed mitochondrial proteome, with reductions in citrate synthase and creatine kinase enzymes and lowered ATP affinity of the mitochondria, leading to cardiac dysfunction and abnormal energy handling. Another recent study showed that a drastic cytosolic calcium concentration increase, as seen in dystrophic affected fibres, led to mitochondrial calcium overload, a collapse of the potential gradient and dysfunction leading to cell death (Jung et al., 2008). Our confocal microscopy analysis of the dystrophic heart shows no significant changes in the mitochondrial mass between normal and dystrophin-deficient heart, as judged by labelling with the chloromethyl-X-rosamine MitoTracker dye, which is drawn inside the mitochondria by their negative potential (Pendergrass et al., 2004).

3.3.6 Other proteins

A contrasting result revealed in our DIGE analysis was that individual protein spots representing electron-transferring flavoprotein showed both an increased and decrease expression level. Electron transfer flavoprotein ubiquinone oxidoreductase transports electrons derived from the fatty acid oxidation pathway into the matrix of the mitochondria to aid in the respiratory chain system (Swanson et al., 2008). The effect of different isoforms of this protein is hard to interpret, but dystrophin deficiency must affect distinct isoform species in differing ways, applying post –translational modifications to adapt to a stressed environment. Pyruvate dehydrogenase is a large enzyme complex involved in cellular respiration, and highly aerobic tissues are dependant on the conversion of pyruvate to acetyl-CoA (Koukourakis et al., 2005). In this study, we observed that a number of isoforms of pyruvate dehydrogenase had a decrease in protein expression between normal and MDX heart tissue. A reduction in this enzyme could have a detrimental impact on the overall bioenergetics of the MDX heart. Isoforms of cardiac prohibitin are present in inner mitochondrial membrane and are responsible for efficient assembly of mitochondrial respiratory chain enzymes, and provide scaffolding duties for the mitochondrial membranes (Koukourakis et al., 2005). Although a decrease was not confirmed by immunochemistry in overall prohibitin expression, distinct subspecies may be affected in muscular dystrophy. Enolase is the only enzyme in the glycolytic pathway appears to be down-regulated, indicating that mitochondrial metabolism and stability is more affected in dystrophic related cardiomyopathy than glycolysis. Another of the energy supply pathways affected is oxidative metabolism. Fatty acids are bound to albumin to overcome their low solubility in the cytoplasm as they are transported across the mitochondrial membrane (Bassingthwaighte et al., 1989). A reduction, seen with the DIGE analysis, in both albumin and the cardiac isoform fatty acid binding protein would starve the cell of essential energy supplies, which may trigger loss of contractile strength in dystrophic myofibres. An outer mitochondrial ion channel identified as a porin isoform forms a voltage-dependent anion channel, VDAC1. The large complex of proteins form

membrane spanning channels that function to maintain ion homeostasis. A reduction in porin channels would indicate an abnormal ion handling leading to further disruption in the mitochondria.

In contrast to a combined metabolomic and proteomic study of the MDX heart (Gulston et al., 2008) but in agreement with two comprehensive proteomic studies on MDX skeletal muscle (Doran et al., 2004; Doran et al., 2006b) we showed here a decrease in adenine nucleotide transport enzyme, the AK1 isoform of adenylate kinase. This finding was clearly confirmed using immunoblot analysis. Another nucleotide metabolism enzyme, creatine kinase also followed this disturbed concentration in the dystrophic heart tissue. These ATP transport pathways may be useful for the future development of a comprehensive biomarker signature of cardiomyopathy associated with muscular dystrophy.

3.4 Conclusion

Overall, our DIGE-based screening of the soluble proteome from dystrophic MDX hearts revealed a severely disturbed perturbed protein expression pattern due to the deficiency in dystrophin. A significant portion of this change was found in energy transport and metabolism proteins. As the stability of the mitochondria may be affected, indirectly by the loss of dystrophin, their affinity to bind phosphonucleosides is being influenced. The drastic increase in regulatory enzymes involved in homeostasis of intracellular ADP and ATP molecules may signal this loss in affinity of the mitochondria, as the dystrophin-deficient muscle responds to this stress of an increase in serum ATP. Furthermore, the drastic reduction in an antioxidative stress protein means that the myofibre is less able to counteract the increased disturbance due to the altered energy transfer and this may augment the stress and damage occurring in the dystrophic heart fibre. The phenotypic muscle weakness seen in dystrophic cardiac tissue may be due to loss of available energy to perform actions and of structural disorganization due in part to the decrease in concentration of the large myosin-related proteins. The observed changes in essential proteins involved in cardiac contraction, mitochondrial metabolism, the cellular stress response and nucleotide metabolism

might be useful for the future improvement of early cardiac diagnostic procedures, the identification of novel therapeutic targets to treat cardiomyopathic complications in Duchenne muscular dystrophy and the evaluation of novel treatment strategies to counteract the loss in cardiac dystrophin.

4 Proteomic profiling of naturally protected extraocular muscles from the dystrophin-deficient MDX mouse

4.1 Introduction

X-linked Duchenne muscular dystrophy is an extremely progressive neuromuscular disorder of childhood, however, not all types of muscle are affected similarly. While diaphragm is drastically weakened, the gastrocnemius is progressively affected and the laryngeal and extraocular muscles are usually spared. We carried out a comparative proteomic study of naturally protected extraocular muscle of the established MDX mouse model of X-linked muscular dystrophy.

4.1.1 Duchenne muscular dystrophy and the extraocular muscle

Dystrophinopathies are characterized by a primary deficiency in the Dp427 isoform of the membrane cytoskeletal protein dystrophin (Ahn and Kunkel, 1993). The loss in this large protein causes secondary effects leading to muscle damage and weakness due to sarcolemmal instability, alterations in ion homeostasis, metabolic pathways and cellular signalling and disturbance of the excitation-contraction coupling (Emery, 2002). As dystrophin anchors large membrane spanning glycoprotein complexes within the cell, membrane rupturing due to its deficiency leads to loss of membrane integrity. The reduced presence of the dystroglycan (DG) complex is believed to play a fundamental role in the degeneration of dystrophic muscles. However, not all subtypes of skeletal muscle are affected to the same extent in X-linked muscular dystrophy. The laryngeal and certain distal muscle fibres, as well as extraocular muscle (EOM), are protected from a severely degenerative phenotype in dystrophic organisms (Dowling et al., 2002; Dowling et al., 2003; Marques et al., 2007).

4.1.2 Properties of extraocular muscle

Characterization of these naturally protected muscles may lead to the identification of constitutive properties or adaptive mechanisms that may cause the sparing of EOM in dystrophinopathies (Andrade et al., 2000). Although described as a skeletal muscle the histology, biochemical and physiological character of EOM is markedly different from other skeletal muscles. In limb muscle fibres, the speed of contraction is controlled principally by the type of myosin heavy chain (MHC) isoform expressed. An extraocular specific (MHC) isoform along with cardiac MHC and a developmental MHC are expressed in the fast twitch, fatigue resistant EOM. MHC_{EOM} although abundantly expressed in EOM is not found in skeletal muscle. Usually fast-twitching muscles are not fatigue resistant. However, large bunches of mitochondria found in EOM may contribute to this muscle subtype physiology (Fischer et al., 2002; Stirn Kranjc et al., 2009). Another physical difference between EOM and other skeletal muscles is the finding by Porter and colleagues (2003a) of the lack of an M-line in the contractile apparatus of EOM. The co-ordination action of six EOMs (see Figure 4-1) allows the eye to perform a variety of movements, with the rectus fibres located around the globe of the eye providing a rotation function and the oblique muscle providing a pulley system, to allow the eye to move about its vertical, horizontal and anteroposterior axis.

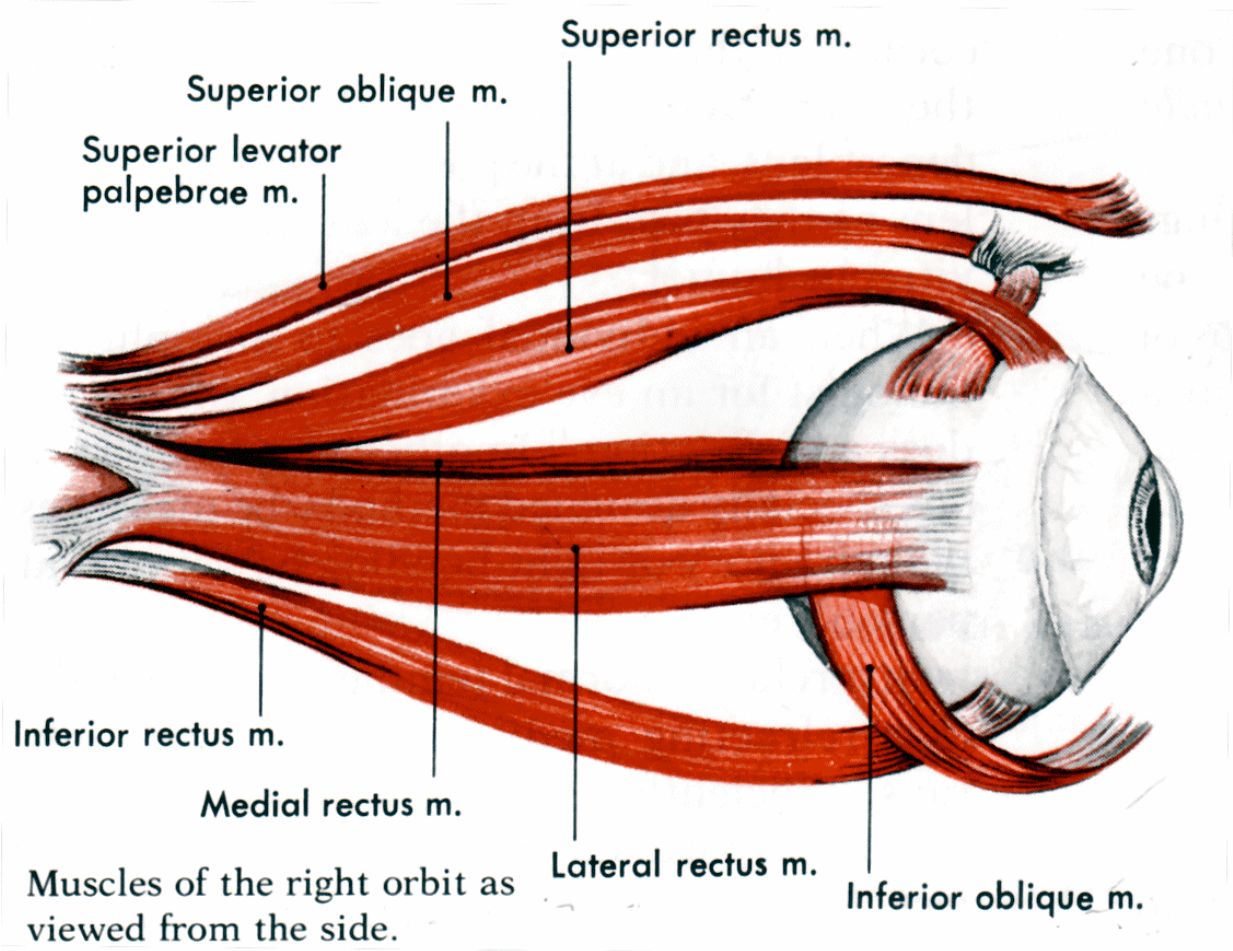

Figure 4-1 Diagrammatic representation of the extraocular muscles

Shown is the location of the six fatigue-resistant extraocular muscles; Superior rectus, Inferior rectus, Lateral rectus and Medial rectus muscles allowing for rotational upward, downward, outward and inward movement respectively and Superior oblique and Inferior oblique muscles co-ordinating rolling movements. The accessory extraocular muscle Superior levator palpebrae lifts the eyelid
http://www.arthurs-clipart.org/medical/senseorgans/page_01.htm

4.1.3 Proteomics and extraocular muscle

Proteomic profiling of Dp427-deficient leg, diaphragm and cardiac muscles has revealed drastic changes in the expression levels of adenylate kinase, heat shock proteins, calcium binding proteins and many proteins involved in the energy generating metabolic pathways and contractile muscle proteins (Dowling et al., 2004b; Doran et al., 2006b; Lewis et al., 2010b). Porter and colleagues (2003b) have shown that within the six different dystrophin-deficient EOM muscle types, all are absent in dystrophin but

that three fibre types have up-regulated dystrophin homologue, utrophin. Contrary to skeletal muscle they demonstrate that there are no degeneration-regeneration cycles in the spared dystrophic EOM. In contrast to skeletal muscle fibre types, immunoblotting for ß-dystroglycan (ßDG) demonstrates the membrane complex to be preserved in naturally protected phenotypes of MDX myofibres (Dowling et al., 2004a).

4.1.4 Experimental design

Since Dp427-deficient fibres appear not to be affected in a major way, we have carried out a mass spectrometry (MS)-based proteomic comparison of normal versus MDX EOM fibres. The MDX mouse represents an established animal model of DMD, which exhibits severe muscle degeneration in the diaphragm, segmental necrosis in limb muscles and a mild phenotype in EOM (Bulfield et al., 1984). Here we have used fluorescence difference in-gel electrophoresis (DIGE), one of the most powerful tools available in biochemistry (Viswanathan et al., 2006), to study potential changes in protein expression levels in Dp427-deficient versus normal EOM preparations. This report describes analysis of DIGE labeled normal and dystrophic EOM *MDX* tissue of 9-week old dystrophin-deficient versus age-matched normal extraocular muscle. Using a pH 4-7 range, out of 1,088 recognized protein spots we identified a moderate expression change in only 7 protein species. These proteins of interest were digested and identified *via* ESI LC-MS. An immunoblotting study revealed drastic up-regulation of dystrophin homologue protein and also an increased concentration of stress response proteins.

4.2 Results

4.2.1 Comparative proteomic analysis of MDX versus normal extraocular muscle

Since EOM tissues exhibit a uniquely mild phenotype in a dystrophic tissue, we performed a comparative proteomic analysis of normal versus MDX preparations of extraocular muscle. Optimized for the small size of murine extraocular tissue and following the recommendations of Karp and Lilley (2007) three biological replicates for each sample type was run using a two dye system. Each replicate contained a pool of two pairs of extraocular muscle. Figure 4-2 illustrates representative two-dimensional gels of Cy3-labelled normal and dystrophic EOM tissue and corresponding Cy5-labelled pooled standards. Gel electrophoretically separated protein spots were analyzed with the help of a Typhoon Trio variable imager and Progenesis 2-D analysis software. Overall, 1,088 distinct muscle protein species were recognized in slab gels with an isoelectric focusing range of pH 4-7. We employed this pH-range in the first dimension step taking into account the high cost of DIGE materials, the limited sample size and from a previous study, showing that the majority of separated soluble crude muscle proteins are identified within this range (Lewis et al., 2010b). Seven spots showed a moderate differential expression pattern, with three proteins being increased and four proteins showing decreased expression. Electrospray ionization mass spectrometry analysis was carried out to identify the extraocular proteins with changes abundance in dystrophic tissue.

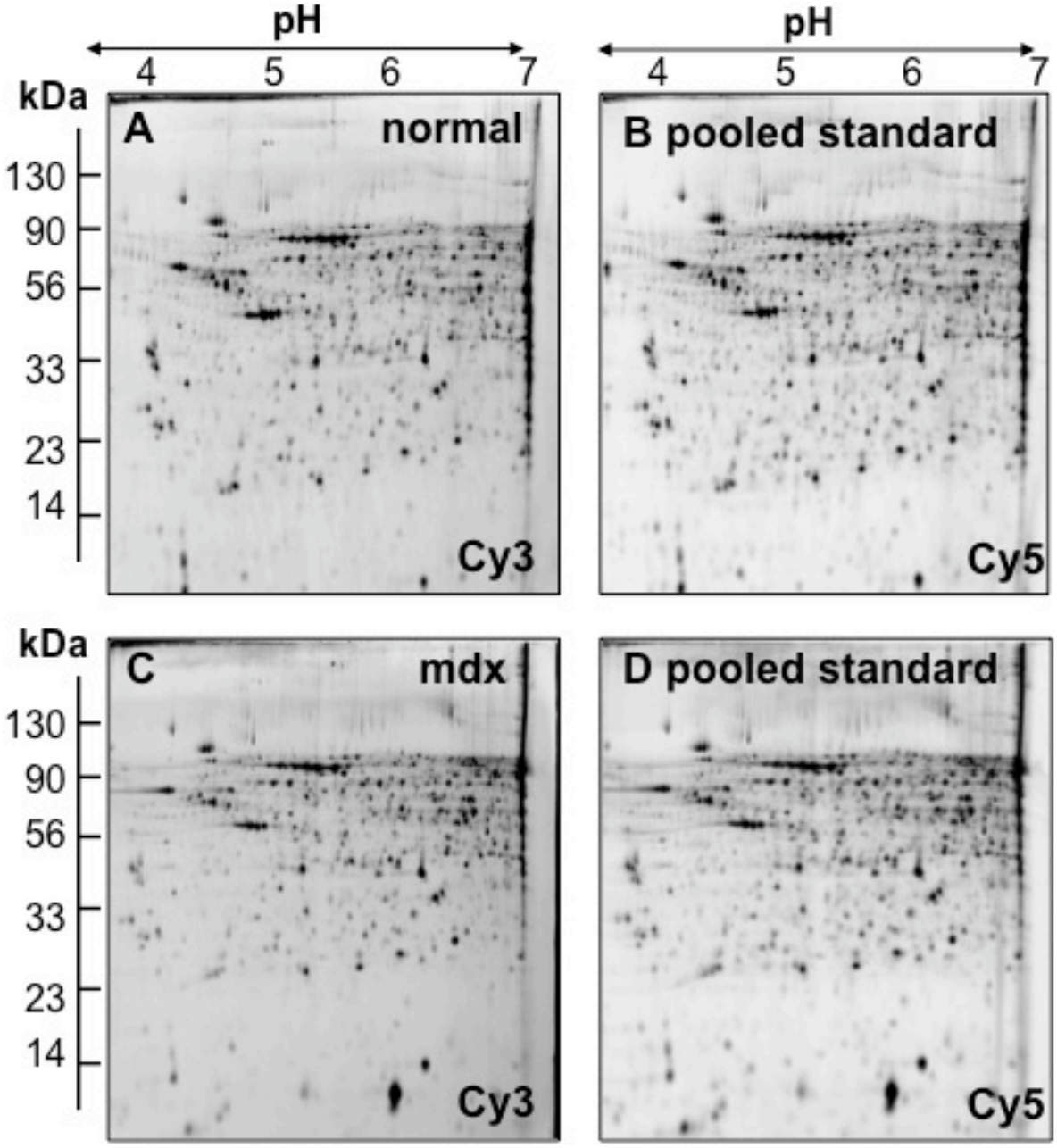

Figure 4-2 2-D DIGE analytical gel of normal versus MDX extraocular muscle in the pH 4-7 range

Shown are the Cy3-labelled gels of total extract from normal (A) and dystrophic MDX (C) EOM tissue, as well as Cy5-labelled gels containing pooled standards (B,D). DIGE images are shown for the pH4-7 range. The pH-values of the second dimension are indicated on the top and the left of the panels, respectively.

4.2.2 DIGE analysis of dystrophin-deficient extraocular muscle

A list of the extraocular proteins with significantly altered expression level in the dystrophic MDX tissue is shown in Table 4-1. The information on the seven DIGE identified protein spots from the 4-7 pH range contains protein name, fold change, matched peptides, number of matched peptides, percentage sequence coverage, the relative molecular mass, p*I* values, Mascot score and protein ID of individual proteins affected by deficiency in Dp427. An analytical master gel (Figure 4-3) shows the moderate changes that were found in muscle proteins marked and numbered 1 to 7 in the Cy5-labelled gel, so that it is possible to correlate MS-identified protein species, listed in Table 4-1, with distinct two-dimensional spots of altered density in MDX EOM preparations. MS analysis identified the increased proteins as the muscle-specific intermediate filament protein desmin (spot 1), apolipoprotein A-I binding protein (spot 2) and perilipin-3 (spot 3) and the decreased proteins as cytosolic gelosin (spot 4), gephyrin (spot 5), transaldolase (spot 6) and acyl-CoA dehydrogenase (spot 7).

Table 4-1 List of the DIGE-identified proteins with a changed abundance in dystrophic MDX extraocular muscle

Ranked	Protein	Fold Change	Number of matched peptides	% coverage	Molecular mass (kDa)	p/	*Mascot score	Accession No.
1	Desmin	2.1	2	4	53.5	5.21	51	gil33563250l
2	Apolipoprotein A-I binding protein precursor	1.8	5	30	31.3	7.59	65	gil21553309l
3	Perilipin-3	1.5	6	21	47.3	5.45	204	gil13385312l
4	Gelsolin, cytosolic	-1.4	1	2	81.1	5.53	92	gil90508l
5	Gephyrin	-1.7	6	11	82.0	5.45	139	gil148670669l
6	Transaldolase	-1.8	12	33	37.5	6.57	147	gil33859640l
7	Acyl-CoA dehydrogenase precursor	-1.9	16	45	48.3	8.34	321	gil31982520l

* The Mascot score has a 95% confidence level if >20

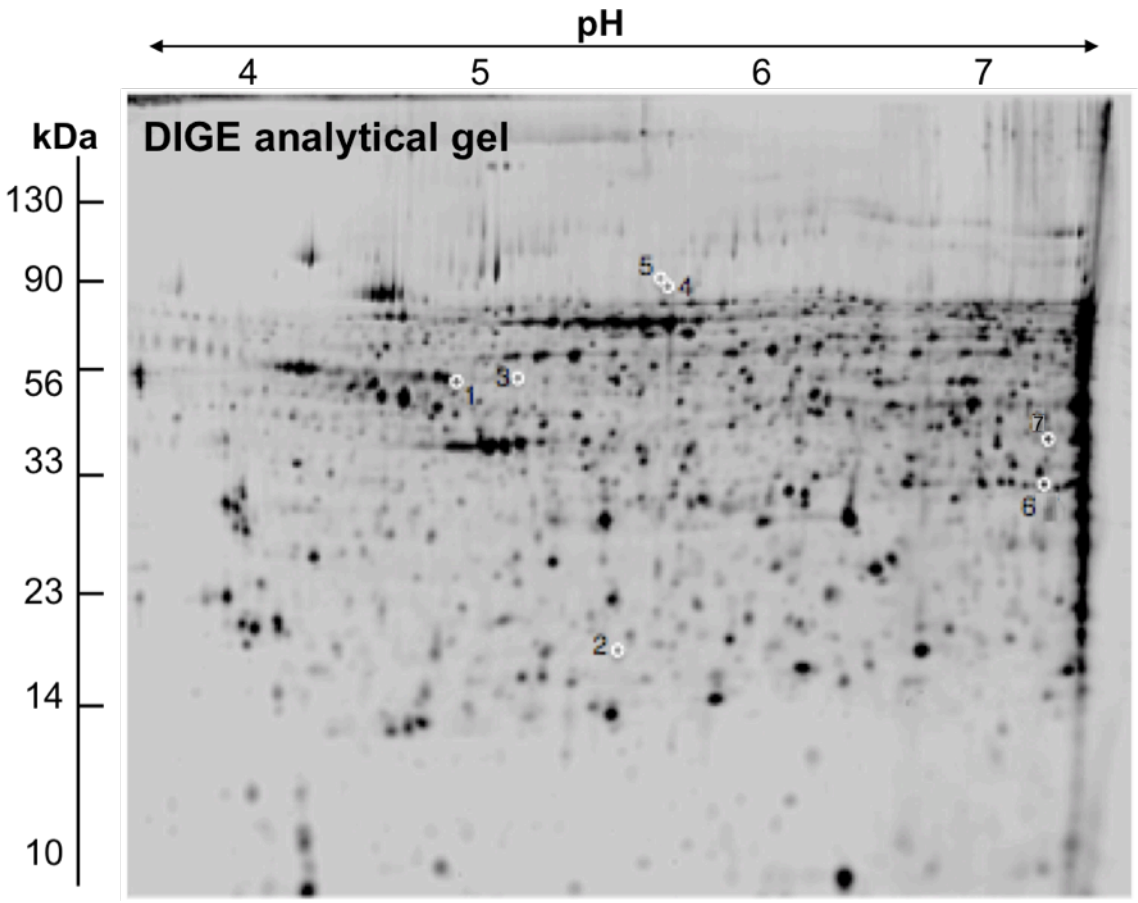

Figure 4-3 DIGE analysis of MDX extraocular tissue

Shown is a Cy5-labelled master gel of crude tissue extracts from EOM tissue covering the pH 4-7 range. Protein spots with a moderately changed expression in MDX preparations are marked by circles and are numbered 1-7. See Table 4-1 for a detailed listing of these EOM-associated proteins with a changed abundance in the MDX mouse. The pH-values of the first dimension gel system and molecular mass standards (in kDa) of the second dimension are indicated on the top and on the left of the panels, respectively.

4.2.3 Immunoblot analysis of dystrophin-deficient extraocular muscle

In order to further characterize the EOM phenotype, comparative immunoblotting was carried out. The immunoblot analysis shown in Figure 4-4 reveals a drastic down-regulation of dystrophin and a drastic up-regulation of Up395, in Dp427-deficient EOM preparations. Immuno-decoration experiments clearly illustrate that the expression of the dystrophin-associated glycoprotein ß-DG is drastically reduced in severely degenerative MDX diaphragm, but is of comparable levels in MDX EOM tissue as shown in Figure 4-5. The same is true for CSQ where a previous study shows a reduction in MDX diaphragm preparation (Doran et al., 2006a), our study confirms this decrease in MDX diaphragm but shows a rescue in the expression of this calcium storage protein in MDX EOM tissue (Figure 4-6). This figure also shows the calcium pump SERCA1 not to be changed in any major way in MDX mice. An immunoblot of laminin and ATPß synthase mitochondrial isoform, unchanged in MDX tissue shows equal loading of the PAGE gels (Figure 4-7). An immunoblotting survey of key stress proteins demonstrated a drastic increase of essential Hsp elements in mildly dystrophic EOM preparations. The expression of the small stress proteins αßCrystallin, cvHsp and Hsp25 was elevated in Dp427-deficient EOM tissue (Figure 4-8). In contrast to decreased levels of Hsp90 in the dystrophic diaphragm, this large stress protein was shown to be increased in MDX EOM (Figure 4-9).

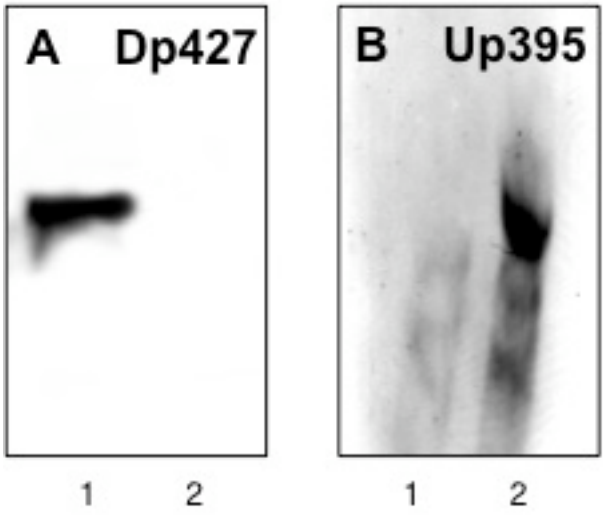

Figure 4-4 Immunoblotting analysis of MDX EOM tissue.

Shown are the immunoblots using antibodies to dystrophin full-length isoform Dp427 (A) and utrophin Up395 (B). The concentration of dystrophin was shown to be drastically down-regulated between normal lane 1 (A) and and dystrophic lane 2 (A) EOM preparation. Whereas the concentration of utrophin was shown to be drastically up-regulated between normal lane 1 (B) and dystrophic lane 2 (B) EOM preparation.

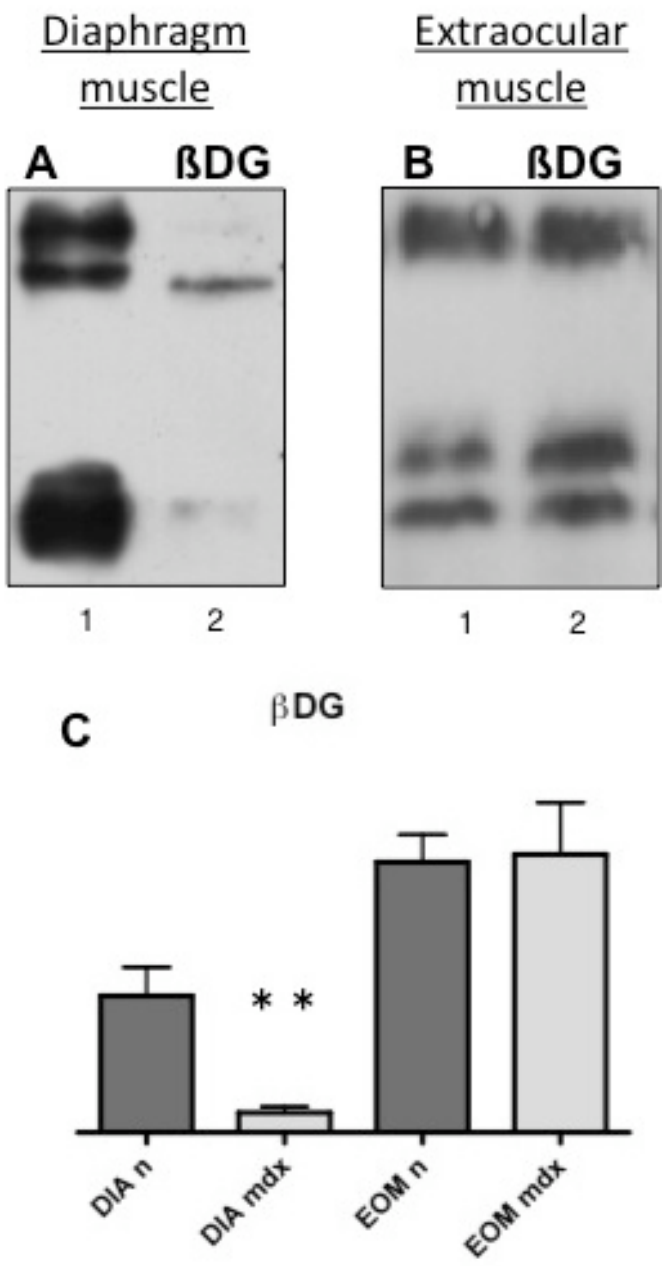

Figure 4-5 immunoblotting analysis of ßDG in MDX tissues

Shown is the immunoblot using antibody specific ßDG in severely affected diaphragm muscle, showing a significant difference in the concentration of ßDG between normal diaphragm lane 1 (A) and dystrophic diaphragm lane 2 (A). Shown also is the immunoblot using ßDG antibody in mildly affected EOM muscle (B). The concentration of ßDG was found not to significantly different between normal lane 1 (B) and dystrophic lane 2 (B) EOM preparation. Graphical presentation of the statistical evaluation (C) carried out of the comparative blotting was statistically evaluated using an unpaired Student's *t*-test (n=3;**p<0.01).

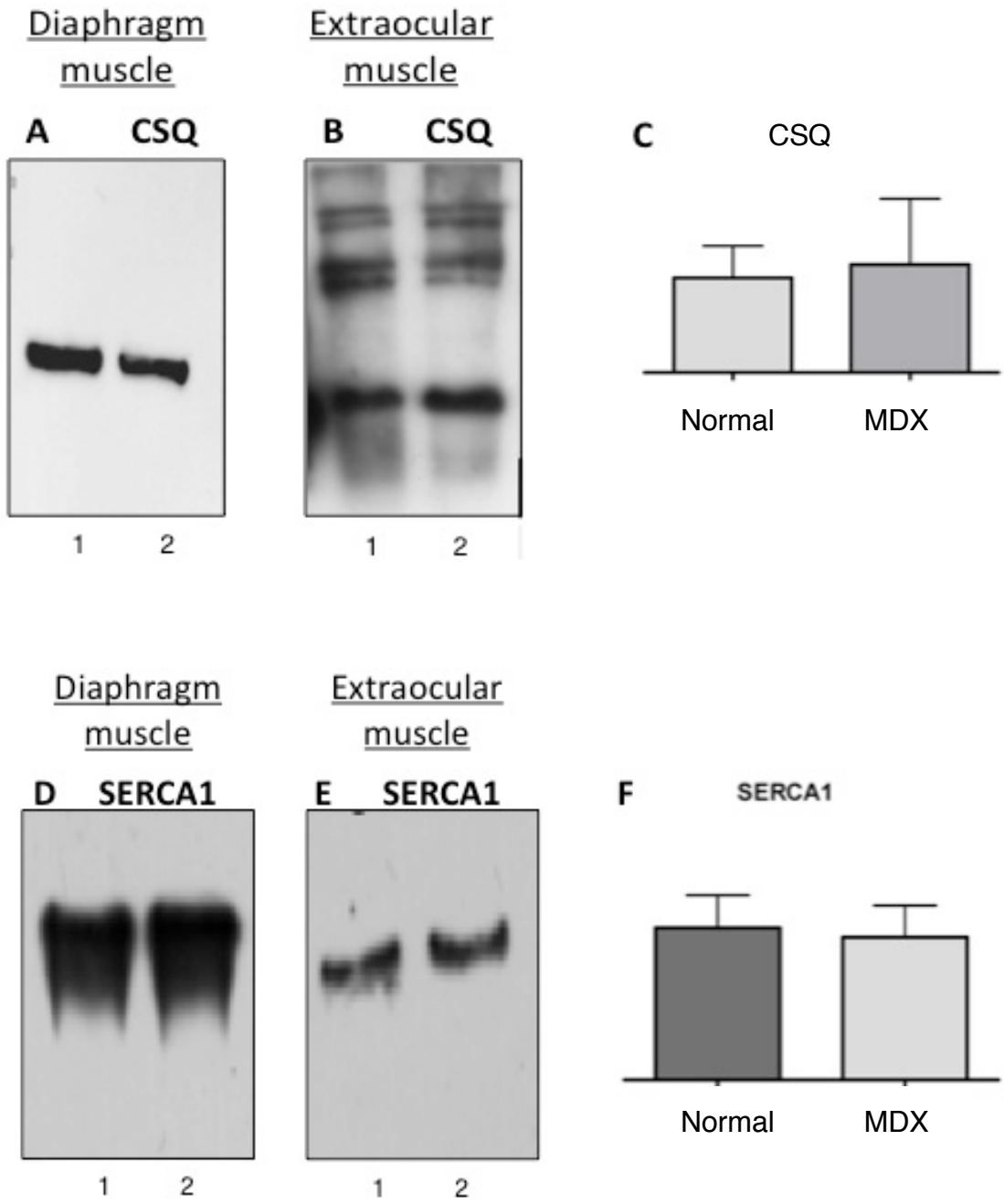

Figure 4-6 Immunoblot analysis of calcium-handling proteins in MDX tissue

Shown are the immunoblots with graphical presentation of the statistical evaluation of immuno-decoration using antibodies to calcium handling calsequestrin CSQ (A,B) and SERCA1 skeletal isoform (D,E). The comparative blotting was statistically evaluated using an unpaired Student's *t*-test (n=3). The concentration of calsequestrin (C) and SERCA1 (F) was found not to significantly different between normal and dystrophic EOM preparation. Lanes 1 and 2 represent normal and dystrophic muscle extracts from control and MDX mice, respectively.

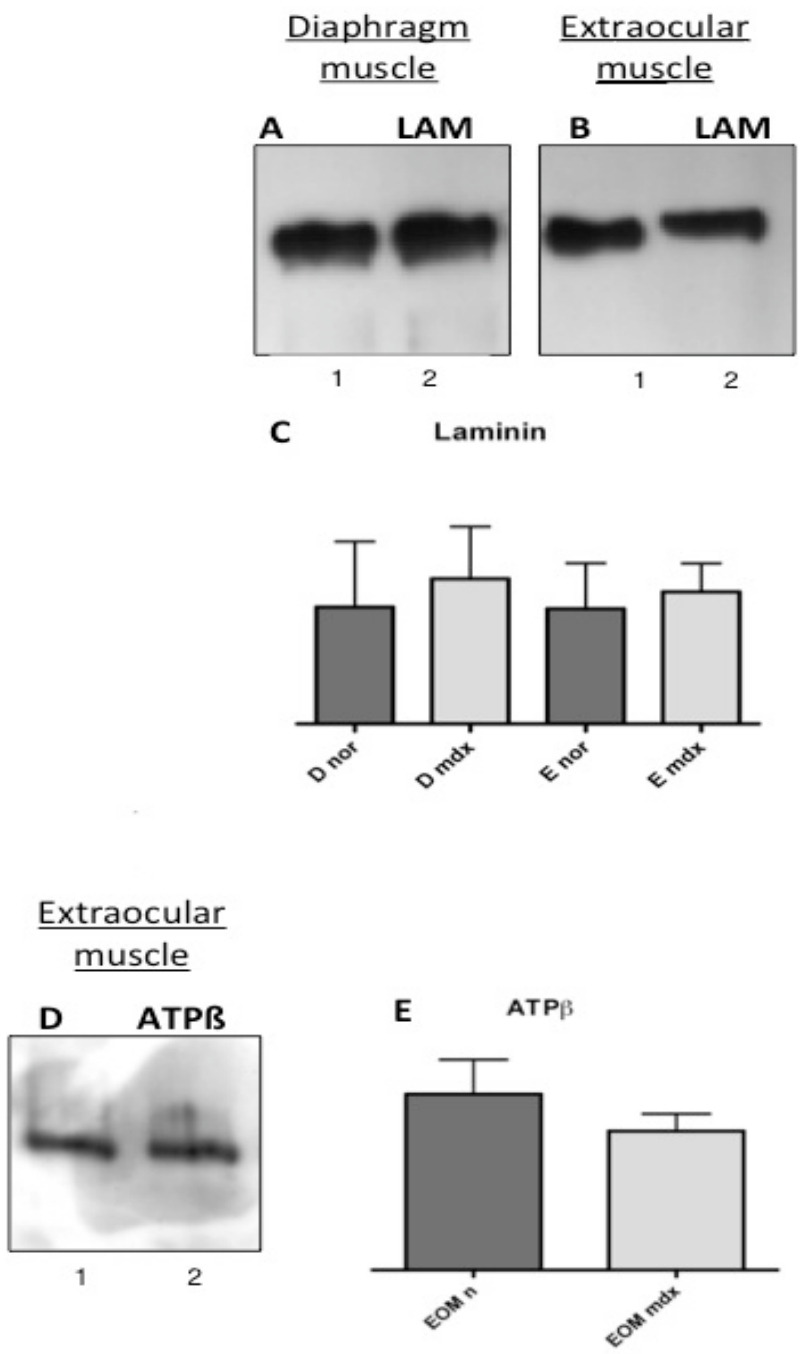

Figure 4-7 Immunoblot analysis of unchanged proteins

Shown are representative blots of the equal loading protein laminin and the unchanged protein ATP synthase. Laminin was shown to be equally loaded in MDX diaphragm (A) and also in MDX EOM (B). ATPß synthase (D) was shown to be unchanged in MDX EOM. The comparative blotting was statistically evaluated using an unpaired Student's *t*-test (n=3). The concentration of Laminin (C) and ATP synthase (E) was found not significantly changed in dystrophic tissue preparations. Lanes 1 and 2 represent normal and dystrophic muscle extracts from control and MDX mice, respectively

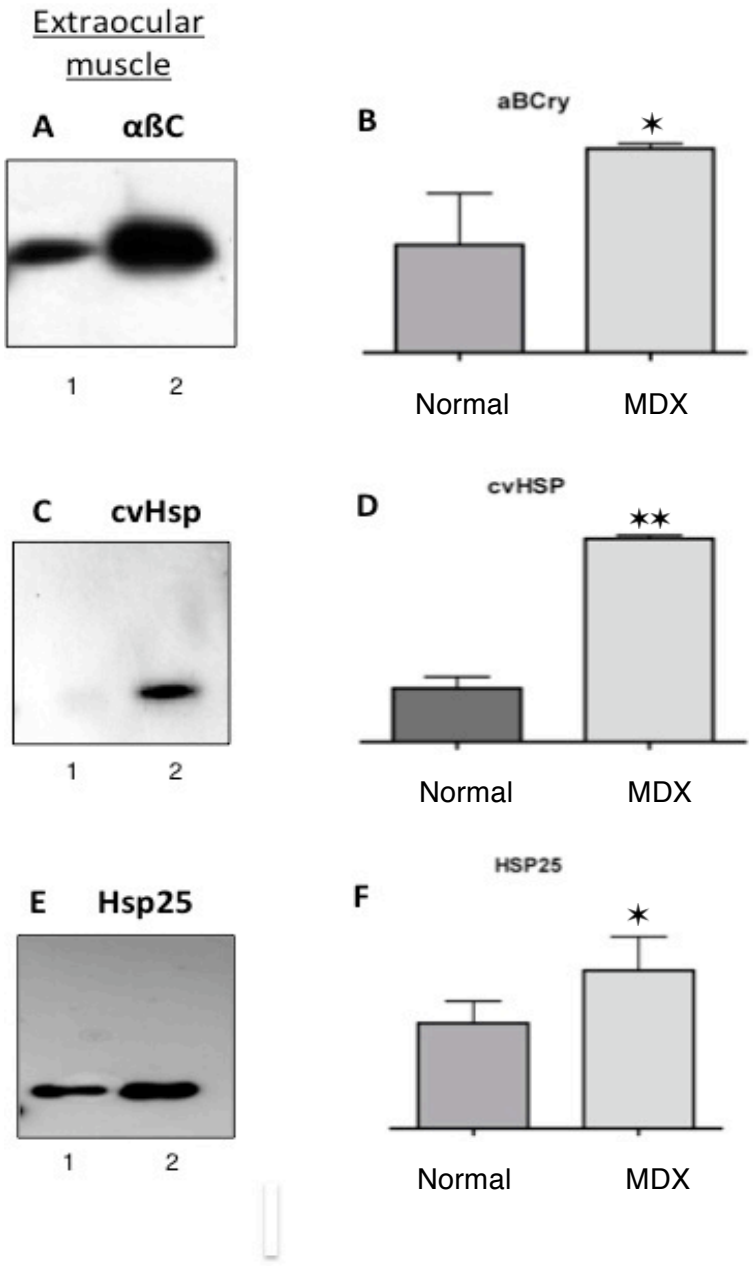

Figure 4-8 Immunoblot analysis of small heat shock proteins

Shown are the representative immunoblots expanded views of immuno-decorated bands labeled with antibodies to αßCrystallin (A), cvHsp (C) and Hsp25 (E). The comparative blotting was statistically evaluated using an unpaired Student's *t*-test (n=3;*p<0.05, **p<0.01). The concentration of all small heat shock proteins were found to be significantly increased between normal and dystrophic EOM preparation. Lanes 1 and 2 represent normal and dystrophic muscle extracts from control and MDX mice, respectively

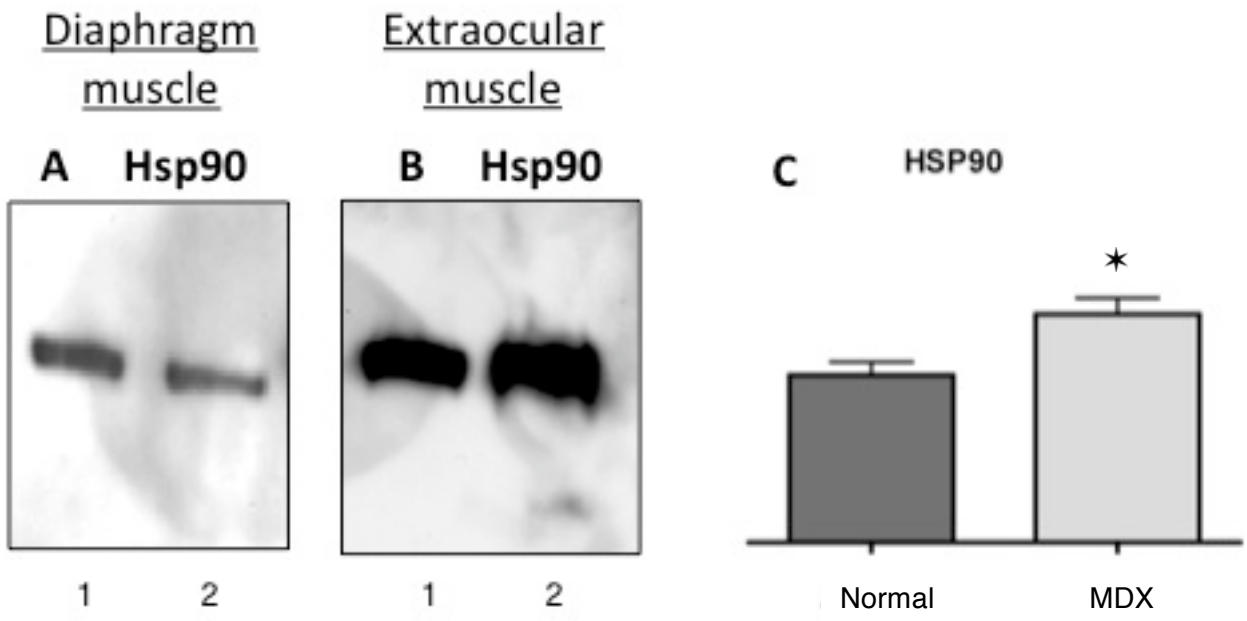

Figure 4-9 Immunoblot analysis of large heat shock protein 90

Shown are the representative immunoblots with expanded views of immuno-decorated bands labeled with antibody to a large heat shock protein Hsp90. Dystrophic diaphragm preparation (A) and dystrophic EOM (B) show opposite fates. The comparative blotting was statistically evaluated using an unpaired Student's *t*-test (n=3; $^{*}p<0.01$). The concentration of Hsp90 was found to be significantly different in MDX EOM preparation (C). Lanes 1 and 2 represent normal and dystrophic muscle extracts from control and MDX mice, respectively

4.3 Discussion

As compared to non-fluorescent protein dye approaches, the application of fluorescent CyDyes has decisively improved the dynamic range of protein coverage in comparative proteomic studies (Karp and Lilley, 2005; Viswanathan et al., 2006). We have therefore used the highly accurate quantitative DIGE technique for the analysis of the mildly affected EOM from the MDX model of DMD. In other subtypes of skeletal muscles, the deficiency in Dp427 causes downsteam alterations (Emery, 2002). Proteomic studies have clearly established a generally perturbed protein expression pattern in MDX diaphragm muscle (Doran et al., 2006b). It is crucial to employ an extremely sensitive biochemical method in order to be able to detect minor changes in a naturally protected phenotype of dystrophinopathy. Since the fluorescent DIGE technique enables multiple protein samples to be separated on the same two-dimensional gel, potential artefacts due to gel-to-gel variations are greatly reduced (Viswanathan et al., 2006). Hence, DIGE analysis suggests itself as an ideal analytical tool to conduct a comparative investigation into the proteomic changes in MDX EOM versus normal EOM preparations. The proteomic findings presented here agree with the idea that EOM tissue is only marginally affected by the loss in Dp427.

4.3.1 Moderate expression changes of DIGE EOM analysis

A moderate change in abundance in seven EOM-associated proteins, as shown here by DIGE analysis, is in stark contrast to major alterations in 35 diaphragm proteins, as previously shown by MS-based studies (Doran et al., 2006b). The approximately 2-fold increase in muscle-specific desmin is an interesting finding, since it supports the hypothesis that the loss in Dp427 is partially compensated in EOM tissue by strengthening the intermediate filament network. High levels of desmin might stabilise the small diameter EOM fibres and thereby protect them from extensive contraction-induced injury in the absence of Dp427. The higher concentration of apolipoprotein A-I

binding and perilipin-3 suggests an increased utilisation of lipid metabolism. Apolipoprotein A-I binding protein interacts with apolipoprotein A-I, a crucial constituent of high-density lipoprotein, and is involved in cholesterol efflux mechanisms. Perilipin-3 is a lipid droplet-associated protein that functions as a protective coating against lipases. An increased level of both proteins might support the altered metabolic needs of Dp427-deficient EOM fibres. The decreased levels of gelosin, gephyrin, transaldolase and acyl-CoA dehydrogenase have probably an effect on structural and metabolic mechanisms. Gelosin is an actin-binding element that regulates actin filament assembly and disassembly and gephyrin is a tubulin-binding protein involved in clustering of glycinergic and GABAergic receptors. Hence, a reduced density in these two binding proteins might affect actin-based cytoskeletal stability and trigger a certain degree of post-synaptic disturbances in Dp427-deficient EOM fibres. Lower levels of transaldolase and acyl-CoA dehydrogenase indicate moderate changes in metabolite utliisation. Transaldolase represents a non-oxidative enzyme of the pentose phosphate pathway and links this metabolic system to glycolysis. Acyl-CoA dehydrogenase is a crucial mitochondrial enzyme involved in fatty acid metabolism. Decreased densities of these two enzymes might therefore impair key metabolic processes, including the glycolytic pathway and fatty acid ß-oxidation.

4.3.2 Immunoblotting survey of MDX EOM tissue

In contrast to the above discussed moderate changes in structural and metabolic elements as determined by DIGE analysis, immunoblotting demonstrated on one hand the rescue of key muscle proteins in MDX EOM and on the other hand a drastic up-regulation of proteins belonging to the Hsp family of molecular chaperones. These alterations were probably not detected by proteomics due to the low abundance of these proteins in conventional two-dimensional gels. Interestingly, the drastic increase in Up395 in Dp427-deficient EOM tissue is associated with comparable levels of the crucial dystrophin-associated glycoprotein ß-DG and the luminal Ca^{2+}-binding protein CSQ. Both proteins are greatly reduced in the dystrophic diaphragm and are believed to be major pathophysiological factors in DMD (Pertille et al., 2010). The secondary

loss in ß-DG causes the disintegration of sarcolemmal stability and subsequent Ca^{2+}-dependent necrotic changes in muscular dystrophy. Low levels of CSQ seem to exacerbate abnormal cytosolic Ca^{2+}-handling by impaired luminal Ca^{2+}-buffering in the dystrophic sarcoplasmic reticulum. These pathological alterations appear not to be present in MDX EOM tissue, which agrees with the previously reported resistance of dystrophic EOM fibres to Ca^{2+}-induced muscle degeneration (Khurana et al., 1995).

4.3.3 Perturbed stress response in MDX EOM tissue

The drastic increase in molecular chaperone protein suggests that MDX EOM is capable of sustained cellular stress responses, involving both low- and high-molecular-mass Hsp elements. Since small Hsps are especially associated with the repair of the cytoskeletal network in skeletal muscle (Nicholl and Quinlan, 1994), the up-regulation of Hsp25, αßC and cvHsp might be linked to the DIGE-determined increase in desmin. In general, stress proteins facilitate the stabilisation or elimination of misfolded proteins or peptide clusters in order to prevent the deleterious accumulation of non-functional protein aggregates (Boluyt et al., 2006). Chaperone activity probably plays an important role in the rescue mechanisms that are intrinsic to EOM fibres.

4.4 Conclusion

In conclusion, this proteomic and biochemical study clearly showed that the mild phenotype of MDX EOM is associated with (i) only a limited number of metabolic and structural systems being perturbed, (ii) a drastic increase in Up395 and a concomitant rescue of sarcolemmal ß-DG, (iii) comparable levels of key Ca^{2+}-handling proteins, and (iv) a drastic increase in molecular chaperones. Thus, the up-regulation of Hsps and the rescue of the luminal Ca^{2+}-uptake apparatus in MDX EOM tissue, as well as the extra-junctional expression of Up395, are probably crucial for preventing severe muscular dystrophy. This makes these proteins potential pharmacological targets for the development of future therapies to treat DMD. In addition, the small diameter and

limited load bearing of EOM fibres might also be critical factors that render this subtype of skeletal muscle extremely resistant to cellular degeneration.

5 Mass spectrometric identification of dystrophin isoform Dp427 by 'on-membrane' digestion of sarcolemma from skeletal muscle

5.1 Introduction

Although the membrane cytoskeletal protein dystrophin of 427kDa and its tightly associated glycoprotein complex are drastically affected in muscular dystrophy, recent large-scale proteomic investigations did not identify full-length dystrophin in muscle preparations and were unable to be determine its molecular fate in dystrophinopathy (Ge et al., 2003; Doran et al., 2006a; Doran et al., 2006b). Since conventional two-dimensional gel electrophoresis under-represents many low-abundance and membrane-associated protein species and in-gel trypsination is often hampered by an inefficient digestion of certain target proteins (Luque-Garcia et al., 2006), we have here applied direct on-membrane digestion of one-dimensional blots of the sarcolemma-enriched fraction and the isolated dystrophin-glycoprotein complex. This method described by Aebersold (1987) succeeded in the mass spectrometric identification of dystrophin isoform Dp427 and associated glycoproteins, as well as sarcolemmal dysferlin. In addition, protein bands representing established signature molecules of cross-contaminating membrane systems, such as the voltage-gated dihydropyridine receptor of transverse tubules, the ryanodine receptor Ca^{2+}-release channel of triad junctions and the Ca^{2+}-ATPase of the sarcoplasmic reticulum, were identified by mass spectrometry. Thus, proteomic approaches using on-membrane digestion might be suitable for future studies of low-abundance proteins, integral proteins, peripheral membrane proteins and high-molecular-mass proteins. On-membrane digestion has the potential to develop into the method of choice for studying these classes of

proteins, which presence is otherwise missed by conventional gel electrophoresis-based proteomics .

5.1.1 The sarcolemmal and associated proteins

The sarcolemma provides a crucial structural attachment site for the basement membrane at the outside of the muscle cell and for the membrane cytoskeleton on the inside of contractile fibres, which strengthens the muscle periphery during contraction-relaxation cycles. The membrane cytoskeletal protein dystrophin and its tightly associated glycoprotein complex play a key role in the stabilisation of the fibre surface by providing a linkage between the extracellular matrix component laminin and the cortical actin cytoskeleton (Ervasti and Campbell, 1993). Full-length dystrophin has an molecular mass of apparent 427kDa and exhibits a complex domain structure. The membrane cytoskeletal element consists of an N-terminal actin-binding domain, a central spectrin-like rod domain with proline-rich hinge regions, a cysteine-rich domain and a C-terminal region containing membrane-binding sites (Koenig and Kunkel, 1990). Although biochemical and cell biological studies have clearly shown that the primary genetic deficiency results in the drastic reduction of the dystrophin-associated glycoprotein complex in linked muscular dystrophy (Ohlendieck et al., 1993), recent large-scale proteomic studies have surprisingly not identified dystrophin isoform Dp427 in gel electrophoretically separated muscle preparations (Ge et al., 2003; Doran et al., 2004; Doran et al., 2006a; Doran et al., 2006b; Lewis et al., 2010b). These mass spectrometric gel-based proteomic studies have revealed many changes in many novel biomarkers of muscular dystrophy such as the adenylate kinase enzyme (Ge et al., 2003), the sarcoplasmic reticulum Ca^{2+}-binding protein calsequestrin (Lohan and Ohlendieck, 2004), the cytosolic Ca^{2+}-binding protein regucalcin (Doran et al., 2006a) and the small stress response protein cardiovascular heat shock protein (cvHsp) (Doran et al., 2006b), but appears not to be suitable for detecting alterations in elements of the dystrophin-glycoprotein complex, due to the large size of key proteins, integral transmembrane domains and tightly bound complexes.

5.1.2 Advantages of on-membrane digestion

Conventional two-dimensional gel electrophoresis under-represents many low-abundance and membrane-associated protein species when analysing complex protein mixtures (Wittmann-Liebold et al., 2006; Rabilloud et al., 2009). In addition, an inefficient digestion of certain target proteins often hampers in-gel trypsination procedures. To address these technical shortcomings in the proteomic identification and biochemical analysis of dystrophin, we have investigated here whether direct on-membrane digestion of one-dimensional blots containing the sarcolemma-enriched fraction or the isolated dystrophin-glycoprotein complex from skeletal muscle can overcome these methodological problems. In general, proteins adsorbed onto nitrocellulose sheets are more accessible to proteases increasing the digestion efficiency (Luque-Garcia et al., 2006). On-membrane trypsination methods have been applied in various biochemical studies (Towbin et al., 1979; Aebersold et al., 1987; Luque-Garcia et al., 2008). The advantages of on-membrane methodology are better protein sequence coverage and a shorter digestion time as compared to in-gel techniques. This reduces complications due to trypsin autolysis and makes this method especially useful for the mass spectrometric identification of low-abundance and large membrane associated proteins. This technique might also be useful for the routine analysis of the dystrophin-glycoprotein complex in normal and pathological muscle samples. Importantly, it may also be suitable for studying the fate of high-molecular-weight muscle proteins that would otherwise not be properly recognised using conventional two-dimensional gel electrophoretic approaches.

5.2 Results

5.2.1 Subcellular fractionation

In order to separate the high-molecular-mass band of the 427kDa dystrophin protein from other large muscle proteins and be able to visualise and identify a distinct Dp427-containing band, a combination of subcellular fractionation and gradient gel

electrophoresis was carried out on this complex protein mixture. This work was carried out prior to the beginning of this on-membrane study, by the supervisor of this project, Professor Kay Ohlendieck. I took no part in the subcellular fractionation portion of this study but I will provide a brief outline to clarify the workflow. The flowchart Figure 5-1 outlines the subcellular fractionation procedure to separate the sarcolemma-enriched fraction from the remaining cell contents. The nuclei, contractile apparatus, the cellular debris, mitochondria, cytosolic proteins were separated out to leave microsomes. Membrane fractions containing surface membranes, triad junctions, transverse tubules and the sarcoplasmic reticulum were isolated by density gradient centrifugation as described by Ohlendieck and colleagues (1991). The dystrophin-glycoprotein complex was then isolated from the microsome fraction by a chromatography and centrifugation method described by Ervasti and colleagues (1990). In skeletal muscle, the plasmalemma membrane, in contrast to the sarcoplasmic reticulum and associated triad structures, represents a much less abundant membrane system (Ohlendieck et al., 1991). Therefore, it is likely that that various abundant membrane species cross-contaminate sarcolemmal preparations during differential and density gradient centrifugation steps.

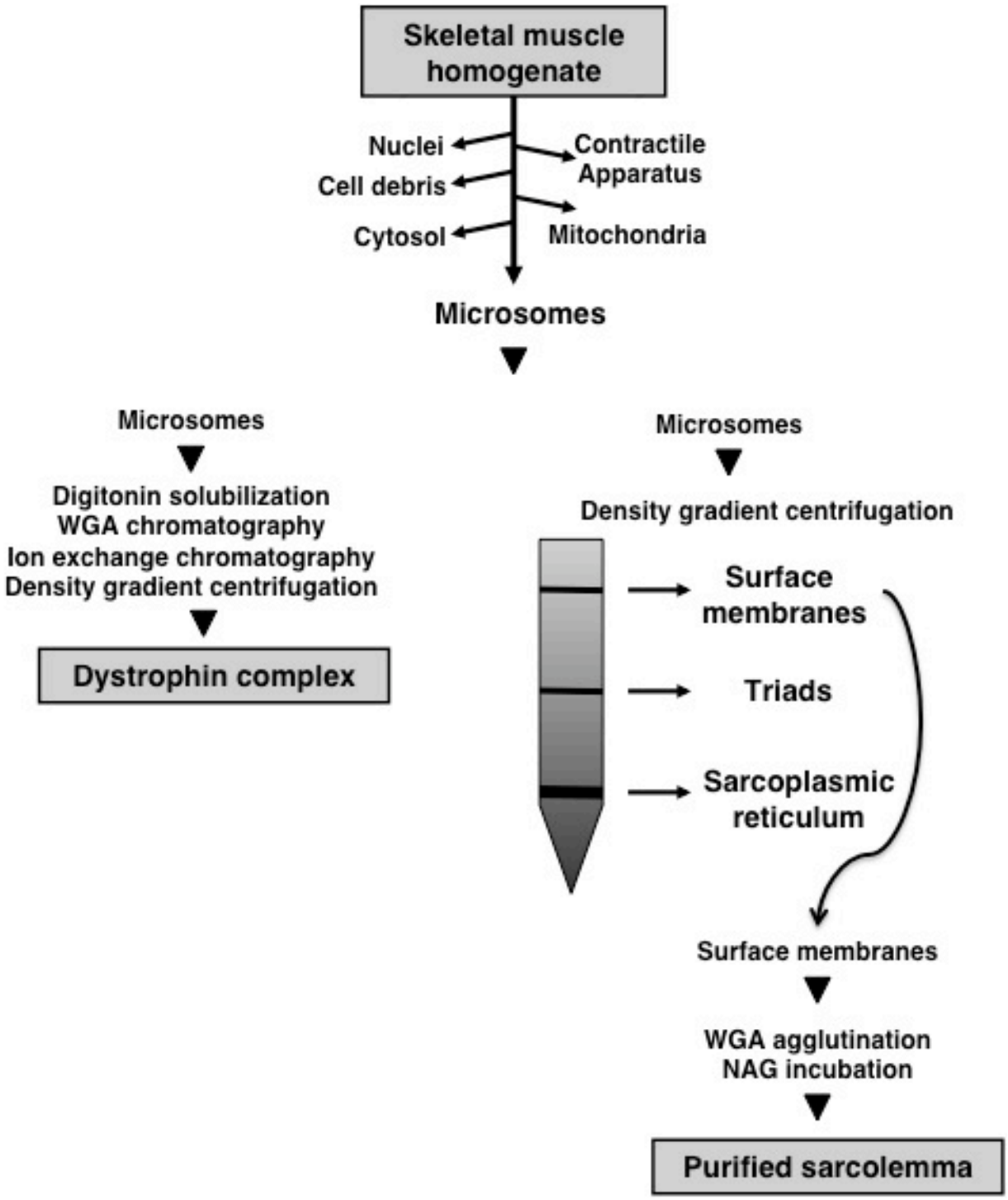

Figure 5-1 Enrichment of sarcolemmal proteins

Outline of the preparation of the sarcolemma-enriched fraction from skeletal muscle homogenates using differential centrifugation, sucrose density gradient centrifugation and lectin agglutination (WGA, wheat germ agglutinin; NAG, N-acetylglucosamine). A series of low speed centrifugation steps removed the nuclei, contractile apparatus, cell

debris, mitochondria and cytosolic elements with a final centrifugation step leaving supernatant containing only microsomes. The dystrophin-glycoprotein complex was isolated from microsomes by addition of the detergent, digitonin, to solubilise the membranes and separated by charge and size using liquid chromatography and density gradient centrifugation, respectively. The purified sarcolemma was isolated by performing a density gradient centrifugation step on a batch of microsomes. Different membrane cell elements separated out according to size and the surface membrane portion of the supernatant containing intact vesicles were separated out using wheat germ agglutination which bind to the glycoproteins displayed on the exterior of the sarcolemmal membranes.

5.2.2 SDS-PAGE fractionation

Following subcellular fractionation, a mass spectrometry-based study was carried out. The flowchart shown in Figure 5-2 outlines the proteomic analysis from polyacrylamide gel separation to protein identification via mass spectrometry. The major membranes of skeletal muscle tissues are diagrammatically shown in Figure 5-3. For comparative purposes, the subcellular localisation of marker proteins that were identified by mass spectrometry in this study is illustrated in the diagram. The Coomassie stained gel of Figure 5-4A illustrates the considerable difference in the protein band pattern of the sarcoplasmic reticulum, triad junctions, transverse tubules and sarcolemma. Following electroblotting, the successful transfer of proteins was visualised by staining of nitrocellulose replicas with the reversible stain MemCode (Figure 5-4B).

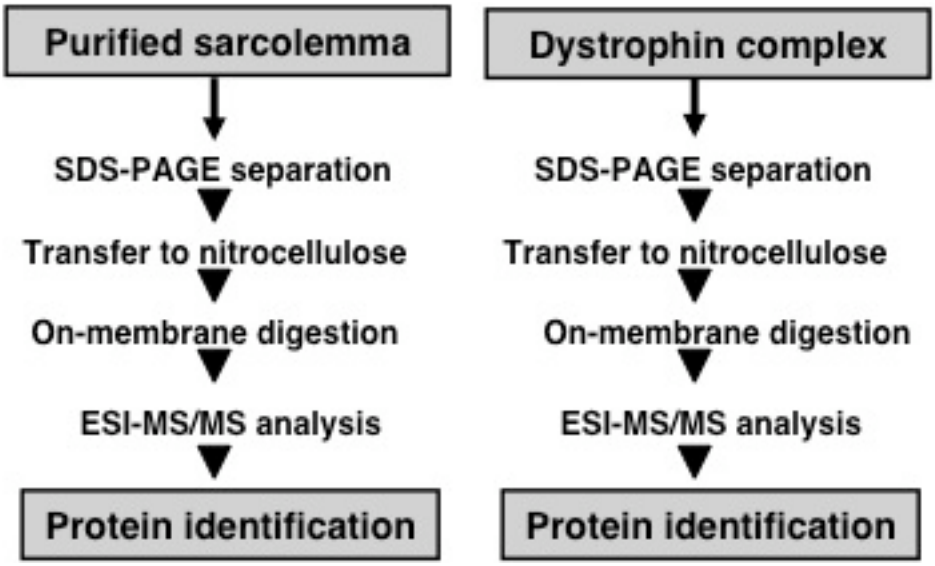

Figure 5-2 Analytical strategy to study the dystrophin-glycoprotein complex

Shown is the overview of the analytical strategy to study the isolated sarcolemma protein complexes by mass spectrometry-based proteomics. Sarcolemmal proteins were separated by sodium dodecyl sulfate polyacrylamide gel electrophoresis (SDS-PAGE). Transferred to nitrocellulose membrane and then individual bands digested by on-membrane trypsination. Muscle proteins were identified by electrospray mass spectrometry (ESI-MS).

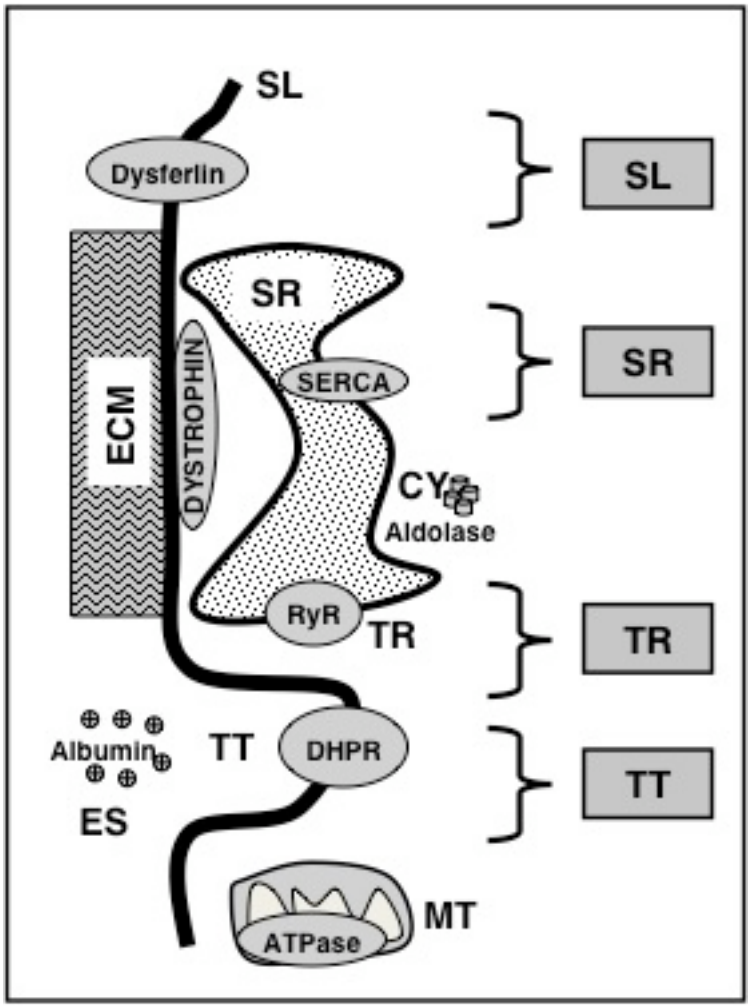

Figure 5-3 Major membranes of skeletal muscle

Shown is the diagrammatic presentation of major muscle membrane systems in skeletal muscle fibres and the subcellular localisation of established marker proteins. Membrane systems can be divided into the sarcolemma (SL), transverse tubules (TT), triad junctions (TR), the sarcoplasmic reticulum (SR) and mitochondria (MT), whereby established markers of these fractions are represented by dysferlin, the dihydropyridine receptor (DHPR) the ryanodine receptor (RyR), Ca^{2+}-ATPase isoform SERCA and the F1-ATPase, respectively. In addition, soluble elements of the extracellular space (ES), such as albumin, or abundant glycolytic enzymes of the cytosol (CYT), such as aldolase, may become entrapped in vesicular membrane preparations derived from muscle homogenates.

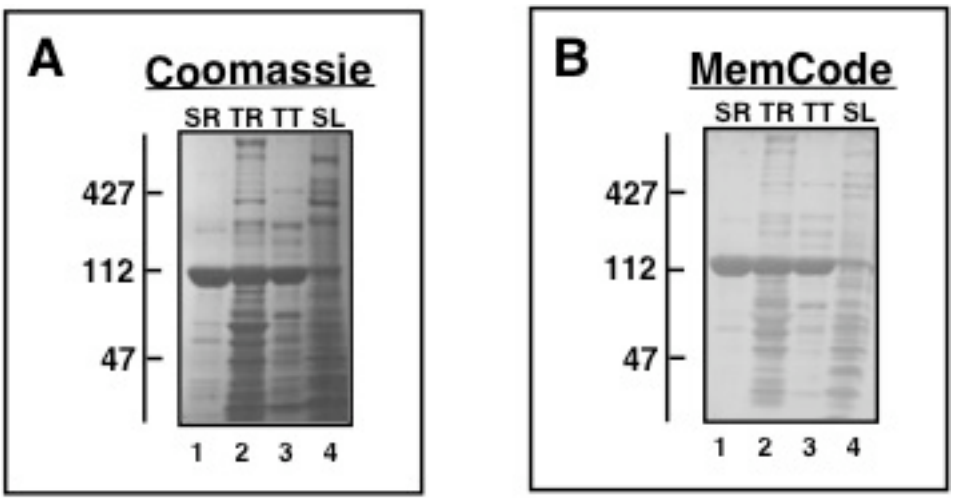

Figure 5-4 Protein band pattern of fractionated muscle membranes

Shown is the Coomassie-stained gel of the sarcoplasmic reticulum, triads, transverse tubules and sarcolemma (A). Also shown is the nitrocellulose replica of the sarcoplasmic reticulum, triads, transverse tubules and sarcolemma stained with the reversible dye MemCode (B). Molecular mass standards (in kDa) are shown on the left of the panels.

5.2.3 Sarcolemma-enriched fraction

As shown in the representative nitrocellulose sheet of Figure 5-5, for the mass spectrometric analysis of the sarcolemma-enriched fraction, gel electrophoresis of muscle proteins was performed without combs so that several centimetre-long horizontal strips of individual proteins bands could be separated. MemCode-stained nitrocellulose sheets were cut into 41 individual bands and then digested with trypsin. The mass spectrometric analysis identified 16 individual muscle proteins with a high Mascot score, as listed in Table 5-1. Protein bands 1 to 16 contained several established marker proteins of subcellular fractions from the skeletal muscle. Bands 1,3,4,5,6,11 and 16 represent the ryanodine receptor Ca^{2+}-release channel isoform RyR1 of the triad junction, dysferlin of the sarcolemma, myosin heavy chain MHC1 of the contractile apparatus, the voltage-sensing α_{1S}-subunit of the dihydropyridine receptor L-type Ca^{2+}-channel of the transverse tubules, the fast SERCA1 isoform of the sarcoplasmic reticulum Ca^{2+}-ATPase, the mitochondrial F1-ATPase and the abundant glycolytic enzyme aldolase of the cytosol, respectively. Thus, besides an enrichment of the sarcolemmal marker dysferlin, the plasma membrane preparation analysed in the report contained contaminating or associated structures from the actomyosin apparatus and most major membrane systems present in contractile fibres. Other proteins present in this subcellular fraction were phosphofructokinase, albumin, calsequestrin, TRIM72 protein and flotilin (Table 5-1). Several proteins ould only be identified by 1 matched peptide and are therefore not listed in the Table 5-1. This included succinate dehydrogenase (2% coverage; 73.670 kDa; pI 7.06; Mascot score; 75; gi|347134|), the α-subunit of sarcoglycan (3% coverage; 42.984 kDa; pI 5.76; Mascot score; 57; gi|126722611|), muscle creatine kinase (3% coverage; 43.247 kDa; pI 6.63; Mascot score: 56; gi|180576|) and the α-chain of G-protein (4% coverage; 43.41.100 kDa; pI 5.36; Mascot score: 68; gi|309255|).

Most importantly, as shown in Figure 5-5, the mass spectrometric analysis of the sarcolemma-enriched fraction by 'on-membrane' digestion identified the low-

abundance membrane cytoskeletal protein dystrophin (band 2), as well as the tightly dystrophin-associated protein α-syntrophin (band 10). Previous mass spectrometry-based proteomic profiling studies of total soluble skeletal muscle extracts have failed to detect dystrophin or its associated membrane proteins (Ge et al., 2003; Doran et al., 2006b; Lewis et al., 2010b).

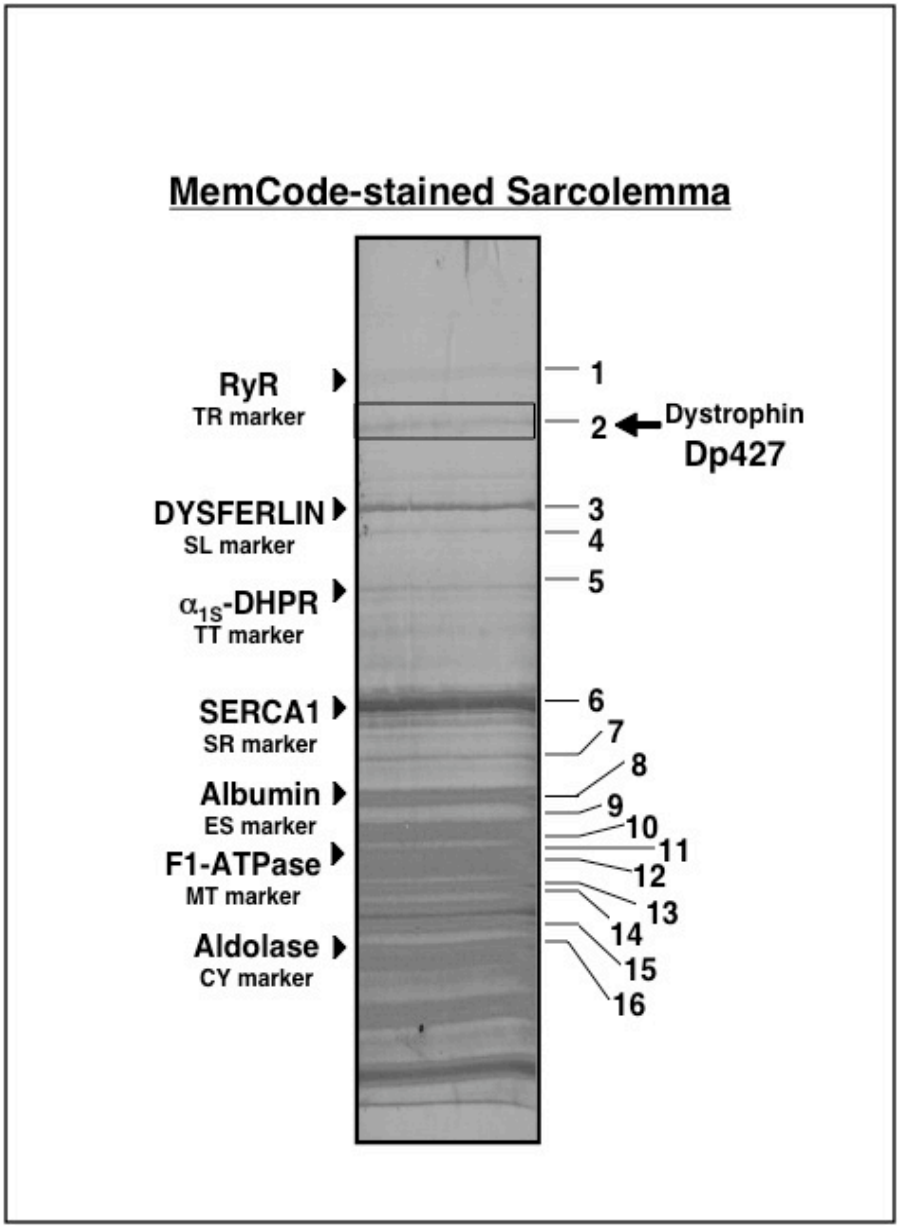

Figure 5-5 Identification of full-length dystrophin isoform Dp427 by on-membrane digestion ofhe sarcolemmal-enriched fraction from rabbit skeletal muscle.

Shown is a representative MemCode-stained nitrocellulose replica of the electrophoretically separated sarcolemmal-enriched fraction, using a gel system without a comb for the generation of several centimeter long horizontal bands for on-membrane digestion. Protein bands that were unequivocally identified by mass spectrometry are numbered 1 to 16 (Table 5-1), including elements of the dystrophin-glycoprotein complex, such as dystrophin isoform Dp427 (band 2) and α-syntrophin (band 10). On the left side of the panel are marked established marker proteins of the various subcellular fractions of muscle, as described in Figure 5-3

Table 5-1 Mass spectrometric identification of electrophoretically separated protein bands from the purified sarcolemma

Band No.	Name of identified protein	Peptides matched	Coverage (%)	Molecular mass (kDa)	Isoelectric point (p*I*)	*Mascot score	Accession No.
1	Ryanodine receptor, RyR1 isoform, skeletal muscle	3	1	570.381	5.61	176	gil156119408l
2	Full-length dystrophin, Dp427 isoform, skeletal muscle	4	1	427.067	5.63	224	gil5032283l
3	Dysferlin	4	2	241.329	5.42	245	gil156523092l
4	Myosin heavy chain MHC1, skeletal muscle	3	2	224.063	5.62	77	gil109113269l
5	Dihydropyridine receptor, subunit α-$_{1S}$, skeletal muscle	4	2	214.002	6.16	162	gil156119412l
6	Calcium-transporting ATPase, fast SERCA1 isoform, skeletal muscle	4	4	111.756	5.14	219	gil147903853l

7	Phosphofructo-kinase, skeletal muscle	2	3	86.005	8.49	154	gil125128l
8	Albumin	3	6	70.861	5.85	107	gil126723746l
9	Calsequestrin, isoform CSQ-1, skeletal muscle	2	7	45.762	3.99	152	gil149755961l
10	Syntrophin, alpha 1 subunit, skeletal muscle	2	4	54.187	6.06	104	gil1438772l
11	ATP synthase, mitochondrial F1 complex, beta subunit isoform 2	3	8	56.410	5.2	195	gil114644226l
12	Tripartite motif-containing TRIM72 protein	2	8	53.601	5.92	137	gil126723064l
13	Flotillin	2	6	47.769	6.71	79	gil6679809l
14	Enolase	2	2	47.381	7.63	58	gil126723437l
15	Muscle creatine kinase	4	11	43.433	6.63	186	gil6729828l
16	Aldolase	3	11	39.586	8.2	164	gil6730618l

* The Mascot score has a 95% confidence level if >20

5.2.4 Dystrophin-glycoprotein complex fraction

Shown in Figure 5-6 is the mass spectrometric analysis of the purified dystrophin-glycoprotein complex and Table 5-2 lists the details of the mass spectrometric identification of dystrophin (band 1), α-sarcoglycan (band 2) and γ-sarcoglycan (band 3). The dystrophin-associated protein dystrobrevin could only be identified by 1 matched peptide (2% coverage; 78.425 kDa; pI 6.34; Mascot score: 70; gi | 1246783 |) and is therefore not listed in Table 5-2. Representative results from LC-MS analysis and mass spectra of dystrophin from sarcolemmal preparations and the isolated dystrophin-glycoprotein complex are shown in Figure 5-7.

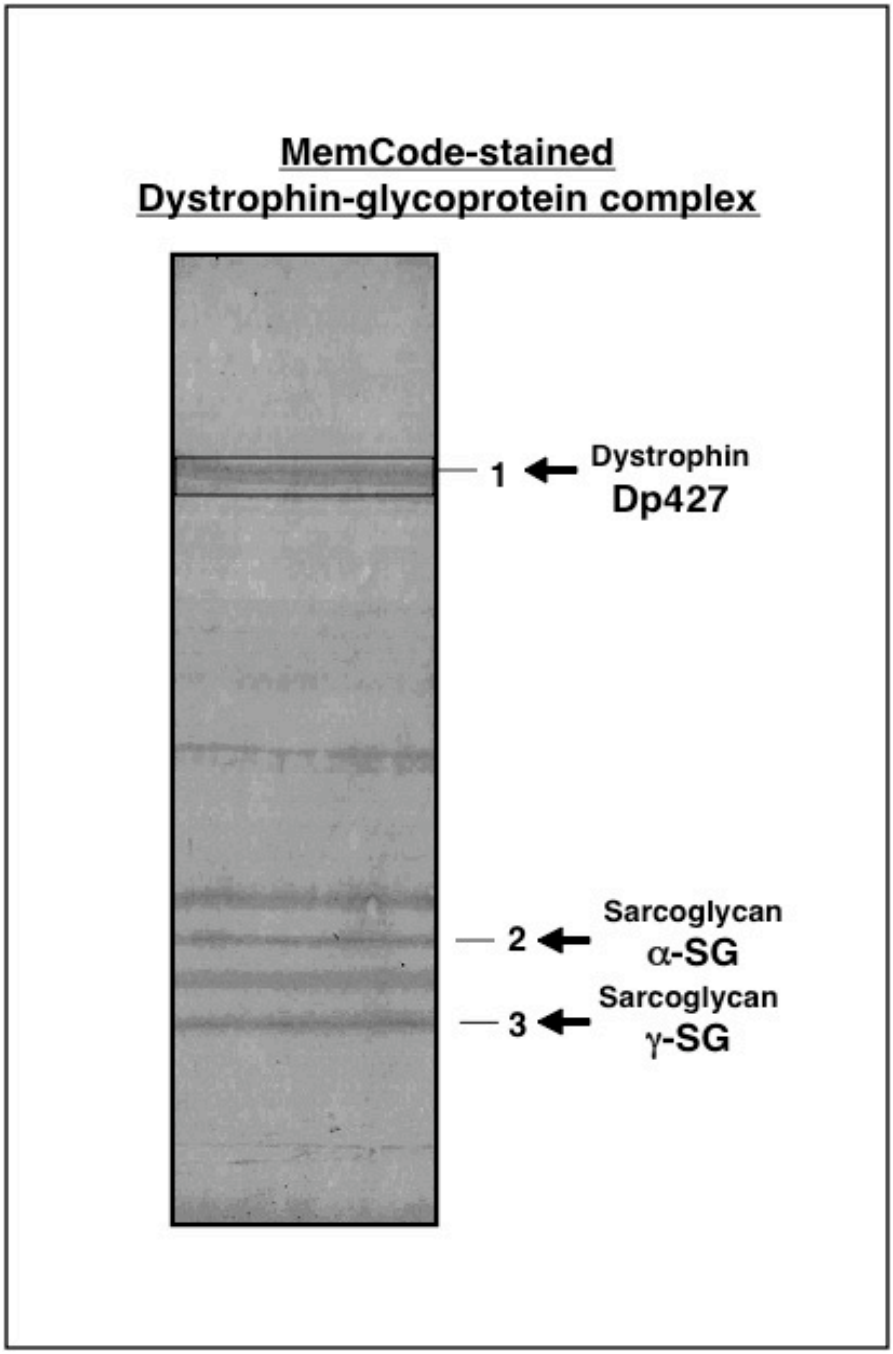

Figure 5-6 Identification of dystrophin by on-membrane digestion of the purified dystrophin-glycoprotein complex from rabbit skeletal muscle.

Shown is a representative MemCode-stained nitrocellulose replica of the electrophoretically separated dystrophin-glycoprotein complex, using a gel system without a comb for the generation of several centimetre long horizontal bands for on-membrane digestion. Protein bands that were unequivocally identified by mass spectrometry are numbered 1 to 3 (Table 5-2), including dystrophin isoform Dp427 (band 1), α-sarcoglycan (band 2) and γ-sarcoglycan (band 3).

Table 5-2 Mass spectrometric identification of electrophoretically separated protein bands from purified dystrophin-glycoprotein complex

Band No.	Name of identified protein	Peptides matched	Coverage (%)	Molecular mass (kDa)	Isoelectric point (p*I*)	*Mascot score	Accession No.
1	Full-length dystrophin, Dp427 isoform, skeletal muscle	4	2	430.340	5.67	249	gil119619468l
2	Sarcoglycan, α-subunit	3	10	42.993	5.76	158	gil126722611l
3	Sarcoglycan, γ-subunit	2	14	32.359	5.12	90	gil126723675l

* The Mascot score has a 95% confidence level if >20

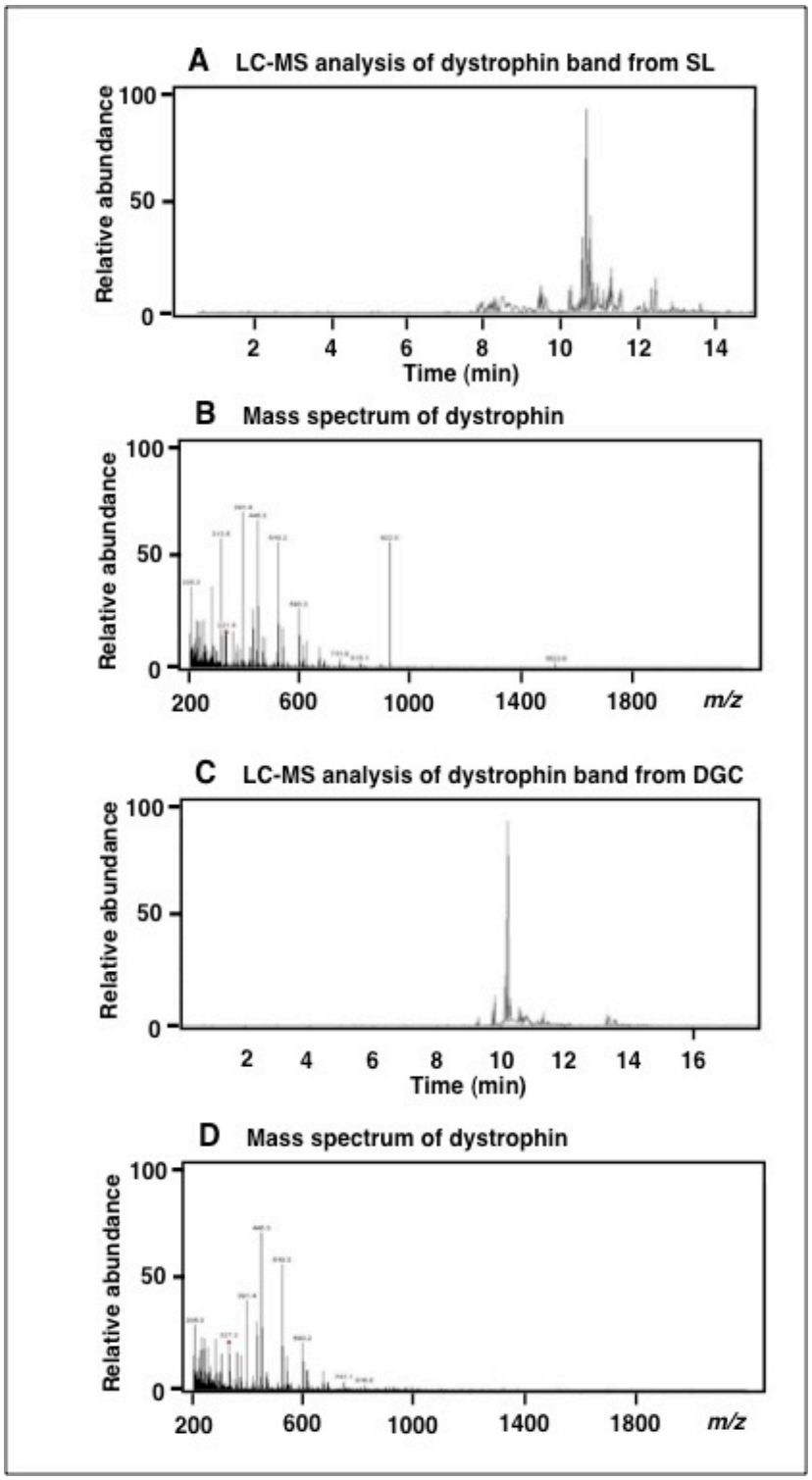

Figure 5-7 Identification of full-length dystrophin isoform Dp427.

Shown is the LC-MS analysis of the dystrophin band isolated from the sarcolemma-enriched membrane fraction (A) or the purified dystrophin-glycoprotein complex (C) from rabbit skeletal muscle. Mass spectra of dystrophin are presented in panels (B) and (D).

5.3 Discussion

Besides defining the physical integrity within contractile tissues by separating the fibre interior from the extracellular environment, the highly complex surface membrane system of skeletal muscle fibres plays a central physiological role in the neuromuscular transmission process, the propagation of action potentials, the maintenance on homeostasis, the regulation of excitation-contraction coupling, the control of metabolic fluxes and the provision of cellular signalling cascades for the swift physiological adaptation to changed functional demands. The biomedical fact that primary genetic abnormalities in proteins located on the surface membrane system are responsible for various neuromuscular pathologies emphasizes the importance for a detailed biochemical understanding of the composition and structure of the plasma membrane from skeletal muscle tissues. Individual sarcolemmal proteins have been studied for many years using conventional biomedical approaches, but its global protein composition is poorly understood. One possible way forward to catalogue the entire membrane protein complement of the fibre periphery is mass spectrometry-based proteomics.

5.3.1 Modified proteomics study

Proteomics had a major impact on the modern biosciences (de Hoog and Mann, 2004) and decisively enhanced the field of basic and applied myology (Isfort, 2002). Proteomic profiling of muscle development, fibre differentiation and muscle transformation has identified a large cohort of new potential markers of muscle biochemistry and their role in physiological adaptations to changed functional demands (Ohlendieck, 2010). Mass spectrometry was also instrumental in the global analysis of common neuromuscular disease mechanisms. The proteomic analysis of muscular disorders has identified novel signature molecules involved in the molecular pathogenesis of muscular dystrophy and age-related muscle weakness (Doran et al., 2006b; O'Connell et al., 2007; Lewis et al., 2010b). However, the majority of these studies have focused on the analysis of total extracts of the accessible skeletal muscle

proteome. Since the routine gel electrophoretic separation of crude protein extracts greatly under-estimates the presence of integral proteins, low-abundance elements, high-molecular-mass proteins and components with extremely acidic or basic pI-values, previous analysis have been restricted to relatively soluble protein species. This is probably the main reason why proteomic studies of skeletal muscle tissues identify mostly abundant and soluble proteins, such as heat shock proteins, glycolytic enzymes and contractile proteins (Doran et al., 2006a; Doran et al., 2006b; Doran et al., 2008; Lewis et al., 2010b). However, the results shown here suggest that a modified subproteomic approach can be employed to also study membrane-associated and high-molecular-mass muscle proteins.

5.3.2 'On-membrane' digestion

The successful identification of dystrophin isoform Dp427, as described in this report, demonstrates that one-dimensional gel electrophoresis, in combination with on-membrane digestion, can overcome some of the technical problems of conventional two-dimensional gel electrophoretic techniques. Thus, in order to include the analysis of membrane-associated proteins in mass spectrometric studies, it is recommended to combine two-dimensional gel electrophoretic analysis of crude muscle extracts with on-membrane digestion approaches and to enrich for low-abundance proteins by preceding on-membrane digestion with a subcellular fractionation step.

5.4 Conclusion

A more inclusive biochemical approach might be especially useful for the comparative proteomic screening of neuromuscular disorders where integral membrane proteins are often affected by complex down-stream abnormalities in muscle metabolism, signal transduction and ion homeostasis.

6 General Discussion

Progressive X-linked muscular dystrophy represents the most commonly inherited neuromuscular disorder in humans. Although the disintegration of the dystrophin-associated glycoprotein complex triggers the initial pathogenesis of Duchenne muscular dystrophy, secondary alterations in energy production, cellular signalling, cytoskeletal disorganisation and changes in ion homeostasis are probably critical factors that cause end-stage fibre degeneration (Carlson and Makiejus, 1990; Williams and Bloch, 1999). The application of mass spectrometry-based proteomics is routinely used to catalogue muscle biomarkers and has recently been applied to MDX animal model of muscular dystrophy and the biochemical evaluation of experimental exon skipping, as a possible suitable treatment for DMD (Doran et al., 2009).

The overall objectives of this study was to study MDX in severely affected cardiac muscle, to investigate the naturally protective phenotype of extraocular MDX tissue and to modify the current mass spectrometry-based proteomic workflow to include analysis of the dystrophin-glycoprotein complex and associated integral proteins.

Recent proteomic studies have demonstrated that mass spectrometry-based technologies can be used for studying a representative proportion of muscle proteins involved in contraction, regulation, metabolism, structure and cellular stress response (Doran et al., 2008; O'Connell et al., 2008; Lewis et al., 2010a). Proteomic profiling of muscle aims to quantitatively analyse the protein expression pattern of contractile fibres (Isfort, 2002) and then identifies the proteins of interest by high-throughput mass spectrometry. Mass spectrometry combined with fluorescence labelling methods can detect several thousand-muscle proteins in high-resolution 2D gel electrophoresis (2D-GE) (Doran et al., 2006a). However, there are limitations to this method with respect to studying the entire cellular proteome (Rabilloud et al., 2009). High molecular mass proteins, membrane proteins and low-abundance proteins can be difficult to detect in polyacrylamide gels due to pore size, hydrophobic nature and dynamic range

respectively. Removal of the gel step has been attempted in order to gain a wider insight into the protein complement. Lu and colleagues (2008) demonstrated a complementary gel-free approach with it own limitations, although being able to substantiate “one-hit wonders”, the storage of massive amounts of MS-data and access to high tech MS equipment may be inaccessible to many laboratories. Separation via liquid chromatography prior to MS-protein identification too has it limitations as complex samples may have at least nine orders of magnitude of a concentration range (Pieper et al., 2003) making low-abundance proteins difficult to detect. We attempted in this study to optimise the MS-based proteomic workflow by carrying out a gel-based study with two pH ranges to achieve further separation (Chapter 3) prior to MS identification. Furthermore, we modified the pore size of the polyacrylamide gel and ran sub-fractionated samples to show the inclusion of high-molecular mass integral proteins (Chapter 5).

The loss of dystrophin, its associated proteins and individual sarcolemmal proteins have shown to be responsible for many neuromuscular disorders but due to the limitations of 2D-GE full-length dystrophin has not been identified in recent MS-proteomic studies with many other novel biomarkers highlighted as changed in concentration. These markers are then secondary down-stream effects of the disease on muscle (Emery, 2002). Incorporating the on-membrane technique used in Chapter 5 made possible the mass spectrometric identification of the high-molecular mass protein dystrophin and many of its associated proteins. Low-abundance protein changes in dystrophic tissue usually under-represented in 2D-GE studies were subsequently identified by specific antibody detection (Chapter 4).

By studying two tissue types, one naturally protected against most neuromuscular dystrophies, we observed differences in the type of protein being expressed between a severely dystrophic phenotype and the naturally protected one. Figure 6-1 shows the flowchart of comparative proteomic analysis between these two tissue types. We found drastic changes in the expression of over 17 proteins plus an additional 55 moderate changes in cardiac tissue whereas we identified only seven moderate EOM changes in

a DIGE study. This relates directly to the severity of the disease. The majority of cardiac alterations were cytoskeletal proteins. It is interesting that an increase in intermediate filament proteins that provide membrane stability in the myofibre were drastically altered in cardiac tissue while only moderately increased in EOM. This suggests that EOM may be naturally protected by its physical property of small diameter fibres (Chapter 4). As seen in Chapter 3 though, a concomitant decrease in abundance in cardiac intermediate filament proteins displays the complexity of studying crude tissue and exhibiting the muscles ability to adapt to its changing surroundings. Additionally, it was observed that isoforms of the same protein display differential expression patterns, again displaying the complexity of the disease. These features demonstrate the benefits of 2D-GE in its ability to display crude soluble protein complement of muscle fibres. ATP production was badly affected in cardiac tissue whereas we saw only moderate changes in ATP production in the milder phenotype of the extraocular muscle. Both muscle types saw an increase in the stress response due to the lack of dystrophin, but a decrease in some small heat shock proteins and a similar change in larger stress proteins may contribute to the extra damage within the contracting myofibre as seen in the severely dystrophic cardiac tissue. While a drastic increased expression level of stress response proteins both large and small in EOM may protect the dystrophic tissue, explaining its milder phenotype. An alteration in the concentration of various cardiac cytoskeletal proteins is a likely cause of problems observed in the excitation-contraction coupling.

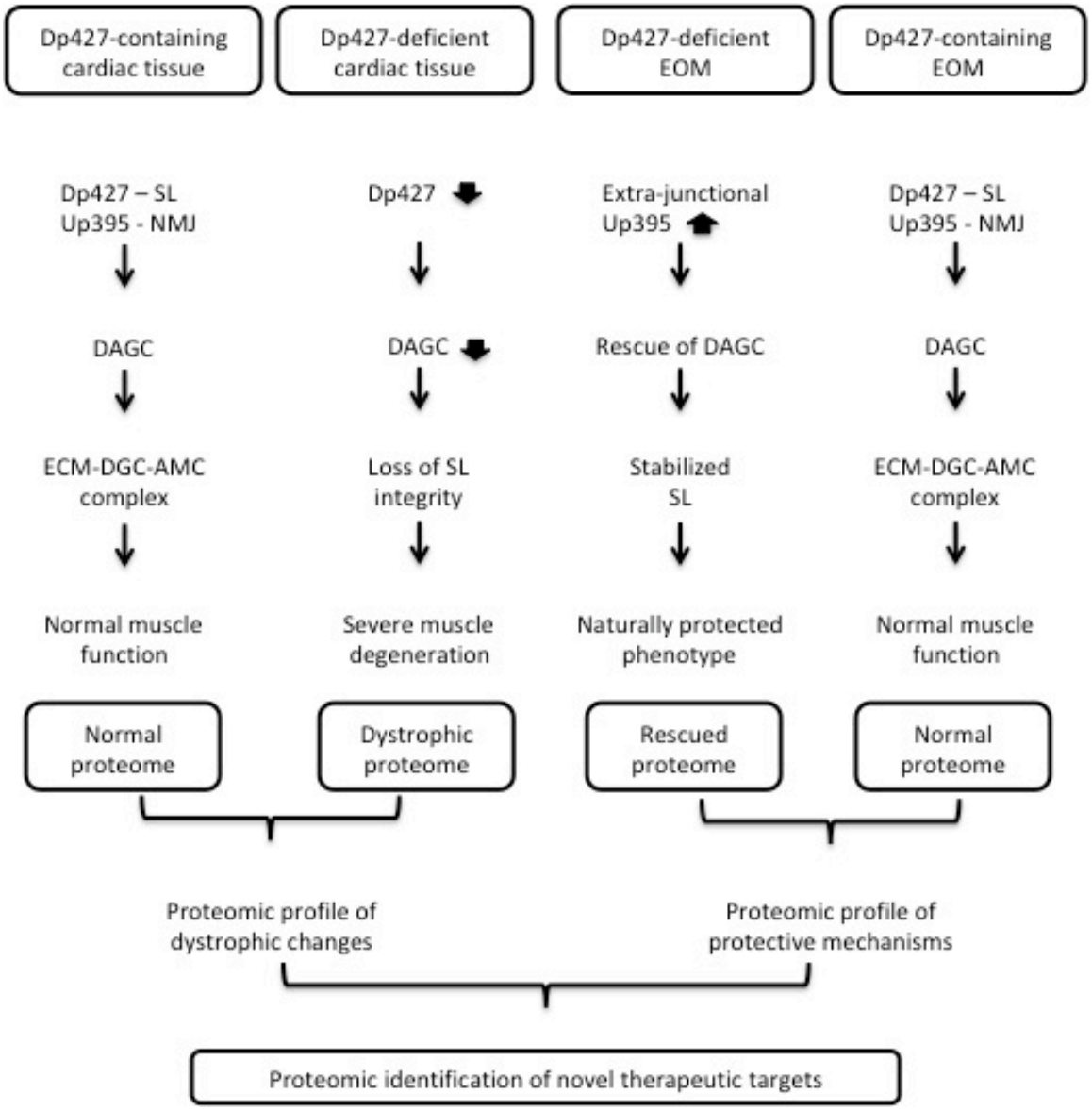

Figure 6-1. Flowchart of the comparative proteomic analysis of dystrophic cardiac tissue versus naturally protected extraocular muscle.

The proteomic profiling of extraocular muscle (EOM) from dystrophin-deficient organisms should reveal protective mechanisms that prevent severe muscle degeneration in this subtype of skeletal muscle. In contrast to the lack of full-length dystrophin (Dp427), EOM exhibit an extra-junctional expression of a dystrophin homologue named utrophin (Up395). In healthy fibres, Up395 is restricted to the neuromuscular junction (NMJ). The supramolecular dystrophin-glycoprotein (DGC) of the sarcolemmal (SL) links the actin membrane cytoskeleton (AMC) to the extracellular matrix (ECM). Reduced levels of the dystrophin-associated glycoprotein complex (DAGC) trigger severe cellular abnormalities and are characteristic for the dystrophic phenotype

Sarcolemma disruption is high in cardiomyofibres (Lohan and Ohlendieck, 2004). The loss of dystrophin, which anchors the extracellular component laminin through to the actin cytoskeleton leads to a drastic reduction in the dystrophin-glycoprotein complex. One of these glycoproteins, ßDG is rescued in EOM (Chapter 4). The rescue of this sarcolemmal protein reduces the contraction-induced micro-rupturing normally seen in dystrophic tissue. Whereas cardiac fibres are replaced by connective tissue and become weakened, the EOM appear naturally protected. Interestingly, Porter and colleagues (2003b) studied the individual fibre types of the eye and found that three of the six dystrophic fibres did not show an expression of the dystrophin homologue, utrophin. These fibres also display a reduction in sarcolemma proteins but do not display the calcium-related muscle fibre degeneration. Our immunoblotting results showing comparable levels of calcium handling proteins agrees with this previously reported resistance of dystrophic EOM fibres to calcium-induced damage, suggesting no sarcolemma disruption in dystrophic EOM tissues (Chapter 4).

From our studies we find that the EOM is under less stress than cardiac tissue. This is evident from the stress response possible due to the rescue of sarcolemma proteins and normal calcium handling abilities in EOM. The smaller diameter of the fibres may be more suitable to the replacement of utrophin and provide mechanical stability to the membrane. Although the eye muscle require vast ranges of movement they have a limited load bearing function, these may be critical factors that render this subtype of skeletal muscle resistant to fibre degeneration. A future MS-based proteomic study into the individual muscle subtypes within the eye may establish a novel mechanism to explain the spared dystrophic phenotype.

Since the discovery of dystrophin and its involvement in Duchenne muscular dystrophy, several experimental treatment strategies have emerged. These include gene replacement in utero, myoblast transfer treatment and stem cell therapy. Exon skipping therapy, which produces a truncated dystrophin molecule similar to the

dystrophin isoform of the milder Becker muscular dystrophy, suggests itself as a novel therapeutic approach. A comparative proteomic approach was applied to evaluate exon skipping and a restoration of key muscle proteins was seen after the dystrophic diaphragm cells were restored with the dystrophin isoform. Reversal of differential proteins involved in DGC, calcium handling, and energy production were significantly expressed. Although this therapy appears promising skipping over a single exon in such a large gene will only serve to treat a small number of suitable candidates and provide them with a milder form of the disease and tailored therapy would prove costly at this early stage of the development.

So many neuromuscular disorders are involved with this membrane-spanning complex that a detailed investigation into its assembly, maintenance and interactions in healthy fibres versus its dysfunction in muscular dystrophic tissue is warranted. A proteomic study inclusive of the high-molecular mass proteins unable to enter a traditional 2D polyacrylamide gel with subsequent mass spectrometric identification may give insight into the fate of proteins over the progression of muscular dystrophies. The detailed comparison into severely affected diaphragm, mildly dystrophic gastrocnemius, and spared extraocular, toe or laryngeal fibres may provide new insights into the protective mechanisms that counteract dystrophic abnormalities. An aging study of MDX tissues may produce interesting results to demonstrate whether irreversible alterations might occur in tissues that lack Dp427, which would be important for therapeutic value.

Through proteomic profiling, we observed changes in essential proteins that might be useful for the future improvement of differential diagnostic procedures. This makes these proteins potential pharmacological targets for the development of future therapies to treat DMD.

Bibliography

Adams, M. E., M. H. Butler, T. M. Dwyer, M. F. Peters, A. A. Murnane, and S. C. Froehner. 1993. Two forms of mouse syntrophin, a 58 kD dystrophin-associated protein, differ in primary structure and tissue distribution. *Neuron* 11 (3):531-40.

Aebersold, R. H., J. Leavitt, R. A. Saavedra, L. E. Hood, and S. B. Kent. 1987. Internal amino acid sequence analysis of proteins separated by one- or two-dimensional gel electrophoresis after *in situ* protease digestion on nitrocellulose. *Proc Natl Acad Sci U S A* 84 (20):6970-4.

Ahn, A. H., and L. M. Kunkel. 1993. The structural and functional diversity of dystrophin. *Nat Genet* 3 (4):283-91.

Ahn, A. H., M. Yoshida, M. S. Anderson, C. A. Feener, S. Selig, Y. Hagiwara, E. Ozawa, and L. M. Kunkel. 1994. Cloning of human basic A1, a distinct 59-kDa dystrophin-associated protein encoded on chromosome 8q23-24. *Proc Natl Acad Sci U S A* 91 (10):4446-50.

Ahn, A. H., C. A. Freener, E. Gussoni, M. Yoshida, E. Ozawa, and L. M. Kunkel. 1996. The three human syntrophin genes are expressed in diverse tissues, have distinct chromosomal locations, and each bind to dystrophin and its relatives. *J Biol Chem* 271 (5):2724-30.

Albrecht, D. E., and S. C. Froehner. 2002. Syntrophins and dystrobrevins: defining the dystrophin scaffold at synapses. *Neurosignals* 11 (3):123-9.

Anderson, L., and J. Seilhamer. 1997. A comparison of selected mRNA and protein abundances in human liver. *Electrophoresis* 18 (3-4):533-7.

Andrade, F. H., J. D. Porter, and H. J. Kaminski. 2000. Eye muscle sparing by the muscular dystrophies: lessons to be learned? *Microsc Res Tech* 48 (3-4):192-203.

Barresi, R., S. A. Moore, C. A. Stolle, J. R. Mendell, and K. P. Campbell. 2000. Expression of gamma -sarcoglycan in smooth muscle and its interaction with the smooth muscle sarcoglycan-sarcospan complex. *J Biol Chem* 275 (49):38554-60.

Bassani, J. W., R. A. Bassani, and D. M. Bers. 1994. Relaxation in rabbit and rat cardiac cells: species-dependent differences in cellular mechanisms. *J Physiol* 476 (2):279-93.

Bassingthwaighte, J. B., L. Noodleman, G. van der Vusse, and J. F. Glatz. 1989. Modeling of palmitate transport in the heart. *Mol Cell Biochem* 88 (1-2):51-8.

Benz, R., and D. Brdiczka. 1992. The cation-selective substate of the mitochondrial outer membrane pore: single-channel conductance and influence on intermembrane and peripheral kinases. *J Bioenerg Biomembr* 24 (1):33-9.

Bers, D. M. 2000. Calcium fluxes involved in control of cardiac myocyte contraction. *Circ Res* 87 (4):275-81.

Bia, B. L., P.J. Cassidy, and M.E Young. 1999. Decreased myocardial nNOS, increased iNOS and abnormal ECGs in mouse models of Duchenne muscular dystrophy. *J Mol Cell Cardiol* 31 (10):1857-1862.

Blake, D. J., R. Hawkes, M. A. Benson, and P. W. Beesley. 1999. Different dystrophin-like complexes are expressed in neurons and glia. *J Cell Biol* 147 (3):645-58.

Blake, D. J., A. Weir, S. E. Newey, and K. E. Davies. 2002. Function and genetics of dystrophin and dystrophin-related proteins in muscle. *Physiol Rev* 82 (2):291-329.

Boluyt, M. O., J. L. Brevick, D. S. Rogers, M. J. Randall, A. F. Scalia, and Z. B. Li. 2006. Changes in the rat heart proteome induced by exercise training: Increased abundance of heat shock protein hsp20. *Proteomics* 6 (10):3154-69.

Bonilla, E., C. E. Samitt, A. F. Miranda, A. P. Hays, G. Salviati, S. DiMauro, L. M. Kunkel, E. P. Hoffman, and L. P. Rowland. 1988. Duchenne muscular dystrophy: deficiency of dystrophin at the muscle cell surface. *Cell* 54 (4):447-52.

Boyce, F. M., A. H. Beggs, C. Feener, and L. M. Kunkel. 1991. Dystrophin is transcribed in brain from a distant upstream promoter. *Proc Natl Acad Sci U S A* 88 (4):1276-80.

Bradford, M.M 1976. A rapid and senstive method for the quantitation of microgram quantities of protein utilizing the principle of protein-dye binding. *Anal Biochem* 72:248-254.

Braun, U., K. Paju, M. Eimre, E. Seppet, E. Orlova, L. Kadaja, S. Trumbeckaite, F. N. Gellerich, S. Zierz, H. Jockusch, and E. K. Seppet. 2001. Lack of dystrophin is associated with altered integration of the mitochondria and ATPases in slow-twitch muscle cells of MDX mice. *Biochim Biophys Acta* 1505 (2-3):258-70.

Bridges, L. R. 1986. The association of cardiac muscle necrosis and inflammation with the degenerative and persistent myopathy of MDX mice. *J Neurol Sci* 72 (2-3):147-57.

Bulfield, G., W. G. Siller, P. A. Wight, and K. J. Moore. 1984. X chromosome-linked muscular dystrophy (mdx) in the mouse. *Proc Natl Acad Sci U S A* 81 (4):1189-92.

Byers, T. J., H. G. Lidov, and L. M. Kunkel. 1993. An alternative dystrophin transcript specific to peripheral nerve. *Nat Genet* 4 (1):77-81.

Campbell, K. P., and S. D. Kahl. 1989. Association of dystrophin and an integral membrane glycoprotein. *Nature London* 338 (6212):259-62.

Campbell, K. P. 1995. Three muscular dystrophies: loss of cytoskeleton-extracellular matrix linkage. *Cell* 80 (5):675-9.

Carlson, C. G., and R. V. Makiejus. 1990. A noninvasive procedure to detect muscle weakness in the mdx mouse. *Muscle Nerve* 13 (6):480-4.

Chazotte, B. 2009. Labeling mitochondria with fluorescent dyes for imaging. *Cold Spring Harb Protoc* 2009 (6):pdb prot4948.

Chen, J., L. Li, and L. S. Chin. 2010. Parkinson disease protein DJ-1 converts from a zymogen to a protease by carboxyl-terminal cleavage. *Hum Mol Genet*.

Colussi, C., C. Banfi, M. Brioschi, E. Tremoli, S. Straino, F. Spallotta, Antonello. Mai, Dante. Rotili, M. C. Capogrossi, and Carlo. Gaetano. 2010. Proteomic profile of differentially expressed plasma proteins from dystrophic mice and following suberoylanilide hydroxamic acid treatment. *Proteomics. Clinical applications* 4 (1):71-83.

Cooke, R. 1986. The mechanism of muscle contraction. *CRC Crit Rev Biochem* 21 (1):53-118.

Cox, G. A., S. F. Phelps, V. M. Chapman, and J. S. Chamberlain. 1993. New mdx mutation disrupts expression of muscle and nonmuscle isoforms of dystrophin. *Nat Genet* 4 (1):87-93.

Crosbie, R. H., J. Heighway, D. P. Venzke, J. C. Lee, and K. P. Campbell. 1997. Sarcospan, the 25-kDa transmembrane component of the dystrophin-glycoprotein complex. *J Biol Chem* 272 (50):31221-4.

Culligan, K., N. Banville, P. Dowling, and K. Ohlendieck. 2002. Drastic reduction of calsequestrin-like proteins and impaired calcium binding in dystrophic mdx muscle. *J Appl Physiol* 92 (2):435-45.

Culligan, K., and K. Ohlendieck. 2002. Diversity of the Brain Dystrophin-Glycoprotein Complex. *J Biomed Biotechnol* 2 (1):31-36.

D'Souza, V. N., T. M. Nguyen, G. E. Morris, W. Karges, D. A. Pillers, and P. N. Ray. 1995. A novel dystrophin isoform is required for normal retinal electrophysiology. *Hum Mol Genet* 4 (5):837-42.

de Hoog, C. L., and M. Mann. 2004. Proteomics. *Annu Rev Genomics Hum Genet* 5:267-93.

Deconinck, A. E., J. A. Rafael, J. A. Skinner, S. C. Brown, A. C. Potter, L. Metzinger, D. J. Watt, J. G. Dickson, J. M. Tinsley, and K. E. Davies. 1997. Utrophin-dystrophin-deficient mice as a model for Duchenne muscular dystrophy. *Cell* 90 (4):717-27.

Den Dunnen, J. T., P. M. Grootscholten, E. Bakker, L. A. Blonden, H. B. Ginjaar, M. C. Wapenaar, H. M. van Paassen, C. van Broeckhoven, P. L. Pearson, and G. J. van Ommen. 1989. Topography of the Duchenne muscular dystrophy (DMD) gene: FIGE and cDNA analysis of 194 cases reveals 115 deletions and 13 duplications. *Am J Hum Genet* 45 (6):835-47.

Donoghue, P., P. Doran, P. Dowling, and K. Ohlendieck. 2005. Differential expression of the fast skeletal muscle proteome following chronic low-frequency stimulation. *Biochim Biophys Acta* 1752 (2):166-76.

Doran, P., P. Dowling, J. Lohan, K. McDonnell, S. Poetsch, and K. Ohlendieck. 2004. Subproteomics analysis of Ca^{++}-binding proteins demonstrates

decreased calsequestrin expression in dystrophic mouse skeletal muscle. *Eur J Biochem* 271 (19):3943-52.

Doran, P., P. Dowling, P. Donoghue, M. Buffini, and K. Ohlendieck. 2006a. Reduced expression of regucalcin in young and aged mdx diaphragm indicates abnormal cytosolic calcium handling in dystrophin-deficient muscle. *Biochim Biophys Acta* 1764 (4):773-85.

Doran, P., G. Martin, P. Dowling, H. Jockusch, and K. Ohlendieck. 2006b. Proteome analysis of the dystrophin-deficient MDX diaphragm reveals a drastic increase in the heat shock protein cvHSP. *Proteomics* 6 (16):4610-21.

Doran, P., K. O'Connell, J. Gannon, M. Kavanagh, and K. Ohlendieck. 2008. Opposite pathobiochemical fate of pyruvate kinase and adenylate kinase in aged rat skeletal muscle as revealed by proteomic DIGE analysis. *Proteomics* 8 (2):364-77.

Doran, P., S. D. Wilton, S. Fletcher, and K. Ohlendieck. 2009. Proteomic profiling of antisense-induced exon skipping reveals reversal of pathobiochemical abnormalities in dystrophic mdx diaphragm. *Proteomics* 9 (3):671-85.

Dowling, P., K. Culligan, and K. Ohlendieck. 2002. Distal mdx muscle groups exhibiting up-regulation of utrophin and rescue of dystrophin-associated glycoproteins exemplify a protected phenotype in muscular dystrophy. *Naturwissenschaften* 89 (2):75-8.

Dowling, P., J. Lohan, and K. Ohlendieck. 2003. Comparative analysis of Dp427-deficient mdx tissues shows that the milder dystrophic phenotype of extraocular and toe muscle fibres is associated with a persistent expression of beta-dystroglycan. *Eur J Cell Biol* 82 (5):222-30.

Dowling, P., P. Doran, J. Lohan, K. Culligan, and K. Ohlendieck. 2004a. Naturally protected muscle phenotypes: Development of Novel Treatment Stragegies for Duchenne Muscular Dystrophy. *Basic Appl Myol* 14 (3):169-177.

Dowling, P., P. Doran, and K. Ohlendieck. 2004b. Drastic reduction of sarcalumenin in Dp427 (dystrophin of 427 kDa)-deficient fibres indicates that abnormal calcium handling plays a key role in muscular dystrophy. *Biochem J* 379 (Pt 2):479-88.

Duclos, F., V. Straub, S. A. Moore, D. P. Venzke, R. F. Hrstka, R. H. Crosbie, M. Durbeej, C. S. Lebakken, A. J. Ettinger, J. van der Meulen, K. H. Holt, L. E. Lim, J. R. Sanes, B. L. Davidson, J. A. Faulkner, R. Williamson, and K. P. Campbell. 1998. Progressive muscular dystrophy in alpha-sarcoglycan-deficient mice. *J Cell Biol* 142 (6):1461-71.

Dunn, J. F., I. Tracey, and G. K. Radda. 1993. Exercise metabolism in Duchenne muscular dystrophy: a biochemical and [31P]-nuclear magnetic resonance study of mdx mice. *Proc Biol Sci* 251 (1332):201-6.

Dupont-Versteegden, E. E., R. A. Baldwin, R. J. McCarter, and M. G. Vonlanthen. 1994. Does muscular dystrophy affect metabolic rate? A study in mdx mice. *J Neurol Sci* 121 (2):203-7.

Durbeej, M., and K. P. Campbell. 2002. Muscular dystrophies involving the dystrophin-glycoprotein complex: an overview of current mouse models. *Curr Opin Genet Dev* 12 (3):349-61.

Emery, A. E. 2002. The muscular dystrophies. *Lancet* 359 (9307):687-95.

Ervasti, J. M., K. Ohlendieck, S. D. Kahl, M. G. Gaver, and K. P. Campbell. 1990. Deficiency of a glycoprotein component of the dystrophin complex in dystrophic muscle. *Nature London* 345 (6273):315-9.

Ervasti, J. M., and K. P. Campbell. 1993. A role for the dystrophin-glycoprotein complex as a transmembrane linker between laminin and actin. *J Cell Biol* 122 (4):809-23.

Farley, J. M., and P. R. Miles. 1977. Role of depolarization in acetylcholine-induced contractions of dog trachealis muscle. *J Pharmacol Exp Ther* 201 (1):199-205.

Fenn, J. B., M. Mann, C. K. Meng, S. F. Wong, and C. M. Whitehouse. 1989. Electrospray ionization for mass spectrometry of large biomolecules. *Science* 246 (4926):64-71.

Finsterer, J., and C. Stollberger. 2003. The heart in human dystrophinopathies. *Cardiology* 99 (1):1-19.

Fischer, M. D., J. R. Gorospe, E. Felder, S. Bogdanovich, F. Pedrosa-Domellof, R. S. Ahima, N. A. Rubinstein, E. P. Hoffman, and T. S. Khurana. 2002.

Expression profiling reveals metabolic and structural components of extraocular muscles. *Physiol Genomics* 9 (2):71-84.

Forner, F., L. J. Foster, S. Campanaro, G. Valle, and M. Mann. 2006. Quantitative proteomic comparison of rat mitochondria from muscle, heart, and liver. *Mol Cell Proteomics* 5 (4):608-19.

Gannon, J., L. Staunton, K. O'Connell, P. Doran, and K. Ohlendieck. 2008. Phosphoproteomic analysis of aged skeletal muscle. *Int J Mol Med* 22 (1):33-42.

Ge, Y., M. P. Molloy, J. S. Chamberlain, and P. C. Andrews. 2003. Proteomic analysis of mdx skeletal muscle: Great reduction of adenylate kinase 1 expression and enzymatic activity. *Proteomics* 3 (10):1895-903.

Gorecki, D. C., A. P. Monaco, J. M. Derry, A. P. Walker, E. A. Barnard, and P. J. Barnard. 1992. Expression of four alternative dystrophin transcripts in brain regions regulated by different promoters. *Hum Mol Genet* 1 (7):505-10.

Gulston, M. K., D. V. Rubtsov, H. J. Atherton, K. Clarke, K. E. Davies, K. S. Lilley, and J. L. Griffin. 2008. A combined metabolomic and proteomic investigation of the effects of a failure to express dystrophin in the mouse heart. *J Proteome Res* 7 (5):2069-77.

Herrmann, H., and U. Aebi. 2004. Intermediate filaments: molecular structure, assembly mechanism, and integration into functionally distinct intracellular Scaffolds. *Annu Rev Biochem* 73:749-89.

Hoffman, E. P., R. H. Brown, Jr., and L. M. Kunkel. 1987. Dystrophin: the protein product of the Duchenne muscular dystrophy locus. *Cell* 51 (6):919-28.

Hohenester, E., D. Tisi, J. F. Talts, and R. Timpl. 1999. The crystal structure of a laminin G-like module reveals the molecular basis of alpha-dystroglycan binding to laminins, perlecan and agrin. *Mol Cell* 4 (5):783-92.

Huxley, A. F., and R. Niedergerke. 1954. Structural changes in muscle during contraction; interference microscopy of living muscle fibres. *Nature London* 173 (4412):971-3.

Huxley, H. E. 2004. Fifty years of muscle and the sliding filament hypothesis. *Eur J Biochem* 271 (8):1403-15.

Ibraghimov-Beskrovnaya, O., J. M. Ervasti, C. J. Leveille, C. A. Slaughter, S. W. Sernett, and K. P. Campbell. 1992. Primary structure of dystrophin-associated glycoproteins linking dystrophin to the extracellular matrix. *Nature London* 355 (6362):696-702.

Isfort, R. J. 2002. Proteomic analysis of striated muscle. *J Chromatogr B Analyt Technol Biomed Life Sci* 771 (1-2):155-65.

Jung, C., A. S. Martins, E. Niggli, and N. Shirokova. 2008. Dystrophic cardiomyopathy: amplification of cellular damage by Ca^{2+} signalling and reactive oxygen species-generating pathways. *Cardiovasc Res* 77 (4):766-73.

Jung, D., B. Yang, J. Meyer, J. S. Chamberlain, and K. P. Campbell. 1995. Identification and characterization of the dystrophin anchoring site on beta-dystroglycan. *J Biol Chem* 270 (45):27305-10.

Jung, D., F. Duclos, B. Apostol, V. Straub, J. C. Lee, V. Allamand, D. P. Venzke, Y. Sunada, C. R. Moomaw, C. J. Leveille, C. A. Slaughter, T. O. Crawford, J. D. McPherson, and K. P. Campbell. 1996. Characterization of delta-sarcoglycan, a novel component of the oligomeric sarcoglycan complex involved in limb-girdle muscular dystrophy. *J Biol Chem* 271 (50):32321-9.

Karp, N. A., and K. S. Lilley. 2005. Maximising sensitivity for detecting changes in protein expression: experimental design using minimal CyDyes. *Proteomics* 5 (12):3105-15.

Karp, N. A., and K. S. Lilley. 2007. Design and analysis issues in quantitative proteomics studies. *Proteomics* 7 Suppl 1:42-50.

Khurana, T. S., R. A. Prendergast, H. S. Alameddine, F. M. Tome, M. Fardeau, K. Arahata, H. Sugita, and L. M. Kunkel. 1995. Absence of extraocular muscle pathology in Duchenne's muscular dystrophy: role for calcium homeostasis in extraocular muscle sparing. *J Exp Med* 182 (2):467-75.

Kimura, N., N. Shimada, M. Fukuda, Y. Ishijima, H. Miyazaki, A. Ishii, Y. Takagi, and N. Ishikawa. 2000. Regulation of cellular functions by nucleoside diphosphate kinases in mammals. *J Bioenerg Biomembr* 32 (3):309-15.

Knudson, C. M., E. P. Hoffman, S. D. Kahl, L. M. Kunkel, and K. P. Campbell. 1988. Evidence for the association of dystrophin with the transverse tubular system in skeletal muscle. *J Biol Chem* 263 (17):8480-4.

Koenig, M., E. P. Hoffman, C. J. Bertelson, A. P. Monaco, C. Feener, and L. M. Kunkel. 1987. Complete cloning of the Duchenne muscular dystrophy (DMD) cDNA and preliminary genomic organization of the DMD gene in normal and affected individuals. *Cell* 50 (3):509-17.

Koenig, M., A. P. Monaco, and L. M. Kunkel. 1988. The complete sequence of dystrophin predicts a rod-shaped cytoskeletal protein. *Cell* 53 (2):219-28.

Koenig, M., and L. M. Kunkel. 1990. Detailed analysis of the repeat domain of dystrophin reveals four potential hinge segments that may confer flexibility. *J Biol Chem* 265 (8):4560-6.

Koukourakis, M. I., A. Giatromanolaki, E. Sivridis, K. C. Gatter, and A. L. Harris. 2005. Pyruvate dehydrogenase and pyruvate dehydrogenase kinase expression in non small cell lung cancer and tumor-associated stroma. *Neoplasia* 7 (1):1-6.

Laemmli, U. K. 1970. Cleavage of structural proteins during the assembly of the head of bacteriophage T4. *Nature London* 227 (5259):680-5.

Lebakken, C. S., D. P. Venzke, R. F. Hrstka, C. M. Consolino, J. A. Faulkner, R. A. Williamson, and K. P. Campbell. 2000. Sarcospan-deficient mice maintain normal muscle function. *Mol Cell Biol* 20 (5):1669-77.

Leferovich, J. M., K. Bedelbaeva, S. Samulewicz, X. M. Zhang, D. Zwas, E. B. Lankford, and E. Heber-Katz. 2001. Heart regeneration in adult MRL mice. *Proc Natl Acad Sci U S A* 98 (17):9830-5.

Lemieux, H., and C. L. Hoppel. 2009. Mitochondria in the human heart. *J Bioenerg Biomembr* 41 (2):99-106.

Lewis, C., S. Carberry, and K. Ohlendieck. 2010a. Proteomic profiling of X-linked muscular dystrophy. *J Muscle Res Cell Motil*.

Lewis, C., H. Jockusch, and K. Ohlendieck. 2010b. Proteomic profiling of the dystrophin-deficient MDX heart reveals drastically altered levels of key metabolic and contractile proteins. *J Biomed Biotechnol*.

Li, D., C. Long, Y. Yue, and D. Duan. 2009. Sub-physiological sarcoglycan expression contributes to compensatory muscle protection in mdx mice. *Hum Mol Genet* 18 (7):1209-20.

Liao, R., L. Nascimben, J. Friedrich, J. K. Gwathmey, and J. S. Ingwall. 1996. Decreased energy reserve in an animal model of dilated cardiomyopathy. Relationship to contractile performance. *Circ Res* 78 (5):893-902.

Lidov, H. G., S. Selig, and L. M. Kunkel. 1995. Dp140: a novel 140 kDa CNS transcript from the dystrophin locus. *Hum Mol Genet* 4 (3):329-35.

Lim, L. E., F. Duclos, O. Broux, N. Bourg, Y. Sunada, V. Allamand, J. Meyer, I. Richard, C. Moomaw, C. Slaughter, Fernando M.S. Tomé, Michel. Fardeau, Charles E. Jackson, Jacques S. Beckmann, and Kevin P. Campbell. 1995. Beta-sarcoglycan: characterization and role in limb-girdle muscular dystrophy linked to 4q12. *Nat Genet* 11 (3):257-65.

Lim, L. E., and K. P. Campbell. 1998. The sarcoglycan complex in limb-girdle muscular dystrophy. *Curr Opin Neurol* 11 (5):443-52.

Loh, N. Y., S. E. Newey, K. E. Davies, and D. J. Blake. 2000. Assembly of multiple dystrobrevin-containing complexes in the kidney. *J Cell Sci* 113 (Pt 15):2715-24.

Lohan, J., and K. Ohlendieck. 2004. Drastic reduction in the luminal Ca^{2+} -binding proteins calsequestrin and sarcalumenin in dystrophin-deficient cardiac muscle. *Biochim Biophys Acta* 1689 (3):252-8.

Lohan, J., K. Culligan, and K. Ohlendieck. 2005. Deficiency in Cardiac Dystrophin Affects the Abundance of the α/βDystroglycan Complex. *J Biomed Biotechnol* 2005 (1):28-36.

Lovering, R. M., and P. G. De Deyne. 2004. Contractile function, sarcolemma integrity, and the loss of dystrophin after skeletal muscle eccentric contraction-induced injury. *Am J Physiol Cell Physiol* 286 (2):C230-8.

Lu, B., A. Motoyama, C. Ruse, J. Venable, and J. R. Yates, 3rd. 2008. Improving protein identification sensitivity by combining MS and MS/MS information for shotgun proteomics using LTQ-Orbitrap high mass accuracy data. *Anal Chem* 80 (6):2018-25.

Luque-Garcia, J. L., G. Zhou, T. T. Sun, and T. A. Neubert. 2006. Use of nitrocellulose membranes for protein characterization by matrix-assisted laser desorption/ionization mass spectrometry. *Anal Chem* 78 (14):5102-8.

Luque-Garcia, J. L., G. Zhou, D. S. Spellman, T. T. Sun, and T. A. Neubert. 2008. Analysis of electroblotted proteins by mass spectrometry: protein identification after Western blotting. *Mol Cell Proteomics* 7 (2):308-14.

Marques, M. J., R. Ferretti, V. U. Vomero, E. Minatel, and H. S. Neto. 2007. Intrinsic laryngeal muscles are spared from myonecrosis in the mdx mouse model of Duchenne muscular dystrophy. *Muscle Nerve* 35 (3):349-53.

Meissner, G., and X. Lu. 1995. Dihydropyridine receptor-ryanodine receptor interactions in skeletal muscle excitation-contraction coupling. *Biosci Rep* 15 (5):399-408.

Menke, A., and H. Jockusch. 1991. Decreased osmotic stability of dystrophin-less muscle cells from the mdx mouse. *Nature* 349 (6304):69-71.

Minetti, C., M. Bado, G. Morreale, M. Pedemonte, and G. Cordone. 1996. Disruption of muscle basal lamina in congenital muscular dystrophy with merosin deficiency. *Neurology* 46 (5):1354-8.

Monaco, A. P., C. J. Bertelson, S. Liechti-Gallati, H. Moser, and L. M. Kunkel. 1988. An explanation for the phenotypic differences between patients bearing partial deletions of the DMD locus. *Genomics* 2 (1):90-5.

Moser, H. 1984. Duchenne muscular dystrophy: pathogenetic aspects and genetic prevention. *Hum Genet* 66 (1):17-40.

Neuhoff, V, R Stamm, and H Eibl. 1985. Clear background and highly sensitive protein staining with Coomassie Blue dyes in polyacrylamide gels: A systemic analysis. *Electrophoresis* 6:427-448.

Newey, S. E., M. A. Benson, C. P. Ponting, K. E. Davies, and D. J. Blake. 2000. Alternative splicing of dystrobrevin regulates the stoichiometry of syntrophin binding to the dystrophin protein complex. *Curr Biol* 10 (20):1295-8.

Nicholl, I. D., and R. A. Quinlan. 1994. Chaperone activity of alpha-crystallins modulates intermediate filament assembly. *EMBO J* 13 (4):945-53.

O'Connell, K., J. Gannon, P. Doran, and K. Ohlendieck. 2007. Proteomic profiling reveals a severely perturbed protein expression pattern in aged skeletal muscle. *Int J Mol Med* 20 (2):145-53.

O'Connell, K., J. Gannon, P. Doran, and K. Ohlendieck. 2008. Reduced expression of sarcalumenin and related Ca2+ -regulatory proteins in aged rat skeletal muscle. *Exp Gerontol* 43 (10):958-61.

O'Farrell, P. H. 1975. High resolution two-dimensional electrophoresis of proteins. *J Biol Chem* 250 (10):4007-21.

Ohlendieck, K., J. M. Ervasti, J. B. Snook, and K. P. Campbell. 1991. Dystrophin-glycoprotein complex is highly enriched in isolated skeletal muscle sarcolemma. *J Cell Biol* 112 (1):135-48.

Ohlendieck, K., K. Matsumura, V. V. Ionasescu, J. A. Towbin, E. P. Bosch, S. L. Weinstein, S. W. Sernett, and K. P. Campbell. 1993. Duchenne muscular dystrophy: deficiency of dystrophin-associated proteins in the sarcolemma. *Neurology* 43 (4):795-800.

Ohlendieck, K. 2010. Proteomics of skeletal muscle differentiation, neuromuscular disorders and fiber aging. *Expert Rev Proteomics* 7 (2):283-96.

Osio, A., L. Tan, S. N. Chen, R. Lombardi, S. F. Nagueh, S. Shete, R. Roberts, J. T. Willerson, and A. J. Marian. 2007. Myozenin 2 is a novel gene for human hypertrophic cardiomyopathy. *Circ Res* 100 (6):766-8.

Pendergrass, W., N. Wolf, and M. Poot. 2004. Efficacy of MitoTracker Green and CMXrosamine to measure changes in mitochondrial membrane potentials in living cells and tissues. *Cytometry A* 61 (2):162-9.

Pertille, A., C. L. de Carvalho, C. Y. Matsumura, H. S. Neto, and M. J. Marques. 2010. Calcium-binding proteins in skeletal muscles of the mdx mice: potential role in the pathogenesis of Duchenne muscular dystrophy. *Int J Exp Pathol* 91 (1):63-71.

Phillips, D., M. Ten Hove, J. E. Schneider, C. O. Wu, L. Sebag-Montefiore, A. M. Aponte, C. A. Lygate, J. Wallis, K. Clarke, H. Watkins, R. S. Balaban, and S. Neubauer. 2010. Mice over-expressing the myocardial creatine transporter develop progressive heart failure and show decreased glycolytic capacity. *J Mol Cell Cardiol* 48 (4):582-90.

Pieper, R., C. L. Gatlin, A. J. Makusky, P. S. Russo, C. R. Schatz, S. S. Miller, Q. Su, A. M. McGrath, M. A. Estock, P. P. Parmar, M. Zhao, S. T. Huang, J. Zhou, F. Wang, R. Esquer-Blasco, N. L. Anderson, J. Taylor, and S.

Steiner. 2003. The human serum proteome: display of nearly 3700 chromatographically separated protein spots on two-dimensional electrophoresis gels and identification of 325 distinct proteins. *Proteomics* 3 (7):1345-64.

Piluso, G., M. Mirabella, E. Ricci, A. Belsito, C. Abbondanza, S. Servidei, A. A. Puca, P. Tonali, G. A. Puca, and V. Nigro. 2000. Gamma1- and gamma2-syntrophins, two novel dystrophin-binding proteins localized in neuronal cells. *J Biol Chem* 275 (21):15851-60.

Poot, M., Y. Z. Zhang, J. A. Kramer, K. S. Wells, L. J. Jones, D. K. Hanzel, A. G. Lugade, V. L. Singer, and R. P. Haugland. 1996. Analysis of mitochondrial morphology and function with novel fixable fluorescent stains. *J Histochem Cytochem* 44 (12):1363-72.

Porter, J. D., J. A. Rafael, R. J. Ragusa, J. K. Brueckner, J. I. Trickett, and K. E. Davies. 1998. The sparing of extraocular muscle in dystrophinopathy is lost in mice lacking utrophin and dystrophin. *J Cell Sci* 111 (Pt 13):1801-11.

Porter, J. D., A. P. Merriam, B. Gong, S. Kasturi, X. Zhou, K. F. Hauser, F. H. Andrade, and G. Cheng. 2003a. Postnatal suppression of myomesin, muscle creatine kinase and the M-line in rat extraocular muscle. *J Exp Biol* 206 (Pt 17):3101-12.

Porter, J. D., A. P. Merriam, S. Khanna, F. H. Andrade, C. R. Richmonds, P. Leahy, G. Cheng, P. Karathanasis, X. Zhou, L. L. Kusner, M. E. Adams, M. Willem, U. Mayer, and H. J. Kaminski. 2003b. Constitutive properties, not molecular adaptations, mediate extraocular muscle sparing in dystrophic mdx mice. *FASEB J* 17 (8):893-5.

Quinlan, J. G., H. S. Hahn, B. L. Wong, J. N. Lorenz, A. S. Wenisch, and L. S. Levin. 2004. Evolution of the mdx mouse cardiomyopathy: physiological and morphological findings. *Neuromuscul Disord* 14 (8-9):491-6.

Rabilloud, T., L. Vuillard, C. Gilly, and J. J. Lawrence. 1994. Silver-staining of proteins in polyacrylamide gels: a general overview. *Cell Mol Biol (Noisy-le-grand)* 40 (1):57-75.

Rabilloud, T. 1996. Solubilization of proteins for electrophoretic analyses. *Electrophoresis* 17 (5):813-29.

Rabilloud, T. 1998. Use of thiourea to increase the solubility of membrane proteins in two-dimensional electrophoresis. *Electrophoresis* 19 (5):758-760.

Rabilloud, T., A. R. Vaezzadeh, N. Potier, C. Lelong, E. Leize-Wagner, and M. Chevallet. 2009. Power and limitations of electrophoretic separations in proteomics strategies. *Mass Spectrom Rev* 28 (5):816-43.

Rafael, J. A., J. I. Trickett, A. C. Potter, and K. E. Davies. 1999. Dystrophin and utrophin do not play crucial roles in nonmuscle tissues in mice. *Muscle Nerve* 22 (4):517-9.

Rayment, I., H. M. Holden, M. Whittaker, C. B. Yohn, M. Lorenz, K. C. Holmes, and R. A. Milligan. 1993. Structure of the actin-myosin complex and its implications for muscle contraction. *Science* 261 (5117):58-65.

Reedy, M. C. 2000. Visualizing myosin's power stroke in muscle contraction. *J Cell Sci* 113 (Pt 20):3551-62.

Rentschler, S., H. Linn, K. Deininger, M. T. Bedford, X. Espanel, and M. Sudol. 1999. The WW domain of dystrophin requires EF-hands region to interact with beta-dystroglycan. *Biol Chem* 380 (4):431-42.

Rosenfeld, J., J. Capdevielle, J. C. Guillemot, and P. Ferrara. 1992. In-gel digestion of proteins for internal sequence analysis after one- or two-dimensional gel electrophoresis. *Anal Biochem* 203 (1):173-9.

Rouslin, W. 1983. Mitochondrial complexes I, II, III, IV, and V in myocardial ischemia and autolysis. *Am J Physiol* 244 (6):H743-8.

Sanchez, J. C., D. Chiappe, V. Converset, C. Hoogland, P. A. Binz, S. Paesano, R. D. Appel, S. Wang, M. Sennitt, A. Nolan, M. A. Cawthorne, and D. F. Hochstrasser. 2001. The mouse SWISS-2D PAGE database: a tool for proteomics study of diabetes and obesity. *Proteomics* 1 (1):136-63.

Seow, T. K., S. E. Ong, R. C. Liang, E. C. Ren, L. Chan, K. Ou, and M. C. Chung. 2000. Two-dimensional electrophoresis map of the human hepatocellular carcinoma cell line, HCC-M, and identification of the separated proteins by mass spectrometry. *Electrophoresis* 21 (9):1787-813.

Shevchenko, A., M. Wilm, O. Vorm, and M. Mann. 1996. Mass spectrometric sequencing of proteins silver-stained polyacrylamide gels. *Anal Chem* 68 (5):850-8.

Shevchenko, A., H. Tomas, J. Havlis, J. V. Olsen, and M. Mann. 2006. In-gel digestion for mass spectrometric characterization of proteins and proteomes. *Nat Protoc* 1 (6):2856-60.

Shih, H. T. 1994. Anatomy of the action potential in the heart. *Tex Heart Inst J* 21 (1):30-41.

Sicinski, P., Y. Geng, A. S. Ryder-Cook, E. A. Barnard, M. G. Darlison, and P. J. Barnard. 1989. The molecular basis of muscular dystrophy in the mdx mouse: a point mutation. *Science* 244 (4912):1578-80.

Sjostrom, M., and J. M. Squire. 1977. Fine structure of the A-band in cryo-sections. The structure of the A-band of human skeletal muscle fibres from ultra-thin cryo-sections negatively stained. *J Mol Biol* 109 (1):49-68.

Sotgia, F., J. K. Lee, K. Das, M. Bedford, T. C. Petrucci, P. Macioce, M. Sargiacomo, F. D. Bricarelli, C. Minetti, M. Sudol, and M. P. Lisanti. 2000. Caveolin-3 directly interacts with the C-terminal tail of beta -dystroglycan. Identification of a central WW-like domain within caveolin family members. *J Biol Chem* 275 (48):38048-58.

Southern, E. M. 1975. Detection of specific sequences among DNA fragments separated by gel electrophoresis. *J Mol Biol* 98 (3):503-17.

Spurney, C. F., S. Knoblach, E. E. Pistilli, K. Nagaraju, G. R. Martin, and E. P. Hoffman. 2008. Dystrophin-deficient cardiomyopathy in mouse: expression of Nox4 and Lox are associated with fibrosis and altered functional parameters in the heart. *Neuromuscul Disord* 18 (5):371-81.

Stedman, H. H., H. L. Sweeney, J. B. Shrager, H. C. Maguire, R. A. Panettieri, B. Petrof, M. Narusawa, J. M. Leferovich, J. T. Sladky, and A. M. Kelly. 1991. The mdx mouse diaphragm reproduces the degenerative changes of Duchenne muscular dystrophy. *Nature London* 352 (6335):536-9.

Stirn Kranjc, B., V. Smerdu, and I. Erzen. 2009. Histochemical and immunohistochemical profile of human and rat ocular medial rectus muscles. *Graefes Arch Clin Exp Ophthalmol* 247 (11):1505-15.

Swanson, M. A., R. J. Usselman, F. E. Frerman, G. R. Eaton, and S. S. Eaton. 2008. The iron-sulfur cluster of electron transfer flavoprotein-ubiquinone oxidoreductase is the electron acceptor for electron transfer flavoprotein. *Biochemistry* 47 (34):8894-901.

Szczesna, D. 2003. Regulatory light chains of striated muscle myosin. Structure, function and malfunction. *Curr Drug Targets Cardiovasc Haematol Disord* 3 (2):187-97.

Tanabe, T., K. G. Beam, B. A. Adams, T. Niidome, and S. Numa. 1990. Regions of the skeletal muscle dihydropyridine receptor critical for excitation-contraction coupling. *Nature London* 346 (6284):567-9.

Tinsley, J. M., D. J. Blake, A. Roche, U. Fairbrother, J. Riss, B. C. Byth, A. E. Knight, J. Kendrick-Jones, G. K. Suthers, D. R. Love, Y. H. Edwards, and K. E. Davies. 1992. Primary structure of dystrophin-related protein. *Nature* 360 (6404):591-3.

Tonge, R., J. Shaw, B. Middleton, R. Rowlinson, S. Rayner, J. Young, F. Pognan, E. Hawkins, I. Currie, and M. Davison. 2001. Validation and development of fluorescence two-dimensional differential gel electrophoresis proteomics technology. *Proteomics* 1 (3):377-96.

Towbin, H., T. Staehelin, and J. Gordon. 1979. Electrophoretic transfer of proteins from polyacrylamide gels to nitrocellulose sheets: procedure and some applications. *Proc Natl Acad Sci U S A* 76 (9):4350-4.

Towbin, J. A., J. F. Hejtmancik, P. Brink, B. Gelb, X. M. Zhu, J. S. Chamberlain, E. R. McCabe, and M. Swift. 1993. X-linked dilated cardiomyopathy. Molecular genetic evidence of linkage to the Duchenne muscular dystrophy (dystrophin) gene at the Xp21 locus. *Circulation* 87 (6):1854-65.

Unlu, M., M. E. Morgan, and J. S. Minden. 1997. Difference gel electrophoresis: a single gel method for detecting changes in protein extracts. *Electrophoresis* 18 (11):2071-7.

Veigel, C., L. M. Coluccio, J. D. Jontes, J. C. Sparrow, R. A. Milligan, and J. E. Molloy. 1999. The motor protein myosin-I produces its working stroke in two steps. *Nature London* 398 (6727):530-3.

Viswanathan, S., M. Unlu, and J. S. Minden. 2006. Two-dimensional difference gel electrophoresis. *Nat Protoc* 1 (3):1351-8.

Wagner, K. R., J. B. Cohen, and R. L. Huganir. 1993. The 87K postsynaptic membrane protein from Torpedo is a protein-tyrosine kinase substrate homologous to dystrophin. *Neuron* 10 (3):511-22.

Wasserstrom, J. A. 1998. New evidence for similarities in excitation-contraction coupling in skeletal and cardiac muscle. *Acta Physiol Scand* 162 (3):247-52.

Weller, B., G. Karpati, and S. Carpenter. 1990. Dystrophin-deficient mdx muscle fibers are preferentially vulnerable to necrosis induced by experimental lengthening contractions. *J Neurol Sci* 100 (1-2):9-13.

Williams, M. W., and R. J. Bloch. 1999. Extensive but coordinated reorganization of the membrane skeleton in myofibers of dystrophic (mdx) mice. *J Cell Biol* 144 (6):1259-70.

Wittmann-Liebold, B., H. R. Graack, and T. Pohl. 2006. Two-dimensional gel electrophoresis as tool for proteomics studies in combination with protein identification by mass spectrometry. *Proteomics* 6 (17):4688-703.

Yaffe, D., A. Makover, D. Lederfein, D. Rapaport, S. Bar, E. Barnea, and U. Nudel. 1992. Multiple products of the Duchenne muscular dystrophy gene. *Symp Soc Exp Biol* 46:179-88.

Yamashita, M, and J.B Fenn. 1984. Electrospray Ion Source. Another Variation on the Free-Jet Theme. *J Phys Chem* 88 (20):4451-4459.

Yan, J. X., R. A. Harry, R. Wait, S. Y. Welson, P. W. Emery, V. R. Preedy, and M. J. Dunn. 2001. Separation and identification of rat skeletal muscle proteins using two-dimensional gel electrophoresis and mass spectrometry. *Proteomics* 1 (3):424-34.

Zhang, W., M. ten Hove, J. E. Schneider, D. J. Stuckey, L. Sebag-Montefiore, B. L. Bia, G. K. Radda, K. E. Davies, S. Neubauer, and K. Clarke. 2008. Abnormal cardiac morphology, function and energy metabolism in the dystrophic mdx mouse: an MRI and MRS study. *J Mol Cell Cardiol* 45 (6):754-60.

Zubrzycka-Gaarn, E. E., D. E. Bulman, G. Karpati, A. H. Burghes, B. Belfall, H. J. Klamut, J. Talbot, R. S. Hodges, P. N. Ray, and R. G. Worton. 1988. The Duchenne muscular dystrophy gene product is localized in sarcolemma of human skeletal muscle. *Nature London* 333 (6172):466-9.